

University of Kentucky

UKnowledge

Theses and Dissertations--Nutritional Sciences

Nutritional Sciences

2014

THE ROLE OF ANGIOTENSINOGEN IN ATHEROSCLEROSIS AND OBESITY

Congqing Wu

University of Kentucky, push2wu@yahoo.com

[Right click to open a feedback form in a new tab to let us know how this document benefits you.](#)

Recommended Citation

Wu, Congqing, "THE ROLE OF ANGIOTENSINOGEN IN ATHEROSCLEROSIS AND OBESITY" (2014). *Theses and Dissertations--Nutritional Sciences*. 16.

https://uknowledge.uky.edu/nutrisci_etds/16

This Doctoral Dissertation is brought to you for free and open access by the Nutritional Sciences at UKnowledge. It has been accepted for inclusion in Theses and Dissertations--Nutritional Sciences by an authorized administrator of UKnowledge. For more information, please contact UKnowledge@lsv.uky.edu.

STUDENT AGREEMENT:

I represent that my thesis or dissertation and abstract are my original work. Proper attribution has been given to all outside sources. I understand that I am solely responsible for obtaining any needed copyright permissions. I have obtained needed written permission statement(s) from the owner(s) of each third-party copyrighted matter to be included in my work, allowing electronic distribution (if such use is not permitted by the fair use doctrine) which will be submitted to UKnowledge as Additional File.

I hereby grant to The University of Kentucky and its agents the irrevocable, non-exclusive, and royalty-free license to archive and make accessible my work in whole or in part in all forms of media, now or hereafter known. I agree that the document mentioned above may be made available immediately for worldwide access unless an embargo applies.

I retain all other ownership rights to the copyright of my work. I also retain the right to use in future works (such as articles or books) all or part of my work. I understand that I am free to register the copyright to my work.

REVIEW, APPROVAL AND ACCEPTANCE

The document mentioned above has been reviewed and accepted by the student's advisor, on behalf of the advisory committee, and by the Director of Graduate Studies (DGS), on behalf of the program; we verify that this is the final, approved version of the student's thesis including all changes required by the advisory committee. The undersigned agree to abide by the statements above.

Congqing Wu, Student

Dr. Alan Daugherty, Major Professor

Dr. Howard P. Glauert, Director of Graduate Studies

THE ROLE OF ANGIOTENSINOGEN IN ATHEROSCLEROSIS AND OBESITY

DISSERTATION

A dissertation submitted in partial fulfillment of the requirements for the degree of
Doctor of Philosophy in Nutritional Sciences in the College of Medicine
at the University of Kentucky

By

CONGQING WU

Lexington, Kentucky

Director: Dr. Alan Daugherty, Professor of Medicine and Physiology

Lexington, Kentucky

2014

Copyright © CONGQING WU 2014

ABSTRACT OF DISSERTATION

THE ROLE OF ANGIOTENSINOGEN IN ATHEROSCLEROSIS AND OBESITY

Angiotensinogen is the only known precursor in the renin-angiotensin system, a hormonal system best known as an essential regulator of blood pressure and fluid homeostasis. Angiotensinogen is sequentially cleaved by renin and angiotensin-converting enzyme to generate angiotensin II. As the major effector peptide, angiotensin II mainly function through angiotensin type 1 receptor.

Angiotensin-converting enzyme inhibitors, angiotensin receptor blockers, and more recently renin inhibitors are widely known as the 3 classic renin-angiotensin system inhibitory drugs against hypertension and atherosclerosis. Here, we developed an array of regents to explore the effects of angiotensinogen inhibition. First, we demonstrated that genetic deficiency of angiotensinogen not only protected against hypercholesterolemia-induced atherosclerosis but also prevented diet-induced obesity. Then we found weekly intraperitoneal injection of antisense oligonucleotides against angiotensinogen remarkably suppressed body weight gain in mice fed a western diet, which was absent from classic renin-angiotensin system inhibition. The suppressed body weight gain was attributable to diminished body fat mass gain and enhanced energy expenditure. More excitingly, angiotensinogen antisense oligonucleotides regressed body weight gain on obese mice. Together, our findings revealed a unique feature of angiotensinogen inhibition beyond classic renin angiotensin inhibition and demonstrated therapeutic potentials of angiotensinogen antisense oligonucleotides against hypertension, atherosclerosis, and obesity.

We also developed an in vivo system to explore the functional consequences of disrupting a conserved Cys18-Cys137 disulfide bridge in angiotensinogen. The formation of this disulfide bridge could trigger conformational changes in angiotensinogen, thereby facilitating renin cleavage of angiotensinogen. It was predicted that the redox-sensitive disulfide bridge might change the efficiency of angiotensinogen/renin reaction to release angiotensin II, thus modulate angiotensin II-dependent functions. We determined effects of the presence and absence of the disulfide bridge on angiotensin II concentrations and responses in mice expressing either native angiotensinogen or Cys18Ser, Cys137Ser mutated angiotensinogen in liver via adeno-associated viral vectors. Contrary to the prediction, disruption of Cys18-Cys137 disulfide bridge in angiotensinogen had no discernible effects on angiotensin II production and angiotensin II-dependent functions in mice.

KEYWORDS: Angiotensinogen, atherosclerosis, obesity, disulfide bridge

CONGQING WU

June 25, 2014

THE ROLE OF ANGIOTENSINOGEN IN ATHEROSCLEROSIS AND OBESITY

By

CONGQING WU

Dr. Alan Daugherty
Director of Dissertation

Dr. Howard P. Glauert
Director of Graduate Studies

June 25, 2014

TABLE OF CONTENTS

List of Tables.....	vii
List of Figures.....	viii
Chapter One: Literature Review	1
Introduction.....	1
Molecular characteristics of AGT	2
Gene structure of AGT	2
Protein characteristics of AGT	2
Regulation of AGT	4
Tissue and cellular distribution of AGT	5
Enzymes using AGT as a substrate.....	6
Plasma concentrations of AGT	7
Plasma and tissue catabolism of AGT	7
Pathophysiological features of AGT	8
Genetic manipulation of AGT in mice	8
Genetic manipulation of AGT in experimental atherosclerosis and obesity.....	9
Genetic association of AGT with atherosclerosis and obesity in humans.....	10
Conclusions and perspectives	12
Specific aims	12
Chapter Two: Angiotensinogen Inhibition Protects Against Atherosclerosis and Obesity in Mice	19
Synopsis	19
Introduction.....	20
Methods.....	22
Ethics statement	22

Mouse housing condition and diet.....	22
Development of hypomorphic AGT mice	22
Development of hepatocyte-specific AGT deficient mice	23
RNA isolation and real-time PCR.....	23
Measurement of plasma components.....	24
Drug administration	24
Antisense oligonucleotide administration.....	25
Irradiation and bone marrow repopulation	25
Quantification of atherosclerosis	25
Body composition	25
Systolic blood pressure measurements	26
Intestinal fat absorption	26
Metabolic cages.....	26
Metabolome analysis.....	27
Microarray analysis.....	28
Statistical analysis	28
Results.....	29
Mice with global AGT reduction were protected from atherosclerosis	29
AGT deficiency in hepatocytes was responsible for protection against atherosclerosis.....	30
AGT ASO reduced atherosclerosis	31
AGT ASO prevented diet-induced obesity	31
AGT deficiency tipped energy balance by increasing energy expenditure	32
AGT ASO regressed diet-induced obesity	33
AGT deficiency decreased lipid metabolites in both liver and plasma	34
AGT deficiency resulted in broad alteration in gene expression in brown fat	34

Chapter Three: The Role of Cys18-Cys137 Disulfide Bridge in Angiotensinogen	66
Synopsis	66
Introduction	67
Methods	69
Ethics statement	69
Mouse housing conditions and diets	69
Development of hepatocyte-specific AGT deficient mice	69
Production and injection of AAV vectors	70
Systolic blood pressure measurements	70
Measurement of plasma components	71
Western blotting of oxidized versus reduced forms of mouse AGT	72
Quantification of atherosclerosis	72
Statistical analysis	73
Results	73
AAV expression of native AGT raised plasma AGT concentrations in a dose- dependent manner	73
AAV expression of native or mutated (C18S, C137S) AGT restored plasma AGT concentrations	74
Predominance of oxidized AGT in mouse plasma	75
Replenishment of native versus mutated AGT had equivalent effects on plasma renin and AngII concentrations	76
Replenishment of native versus mutated AGT had equivalent effects on systolic blood pressure and atherosclerosis	76
Chapter Four: General Discussion	86
The role of angiotensinogen in atherosclerosis	87

The role of AGT in obesity	88
Systemic AGT versus local AGT	91
The role of Cys18-Cys137 disulfide bridge.....	92
Conclusions	95
References.....	97

LIST OF TABLES

Table 1.1 Characteristics of mice with genetic manipulations of AGT.	17
Table 2.1 Primers for gene expression profiling by qPCR.....	65

LIST OF FIGURES

Figure 1.1 Schematic Representation of Human AGT Gene and Protein.....	14
Figure 1.2 Structure of AGT and its complex with renin	15
Figure 2.1 Construct map of hypoAGT mice.....	35
Figure 2.2 AGT mRNA abundance was dramatically reduced in hypoAGT mice.....	36
Figure 2.3 Plasma AGT concentrations were dramatically lower in hypoAGT mice.....	37
Figure 2.4 Systolic blood pressure was lower in hypoAGT mice.....	37
Figure 2.5 Plasma Total Cholesterol was lower in hypoAGT mice.....	38
Figure 2.6 Atherosclerosis was greatly reduced in the arch of hypoAGT mice.....	38
Figure 2.7 Atherosclerosis in arch of chimeric Ldlr ^{-/-} mice repopulated with bone marrow cell from Agt ^{+/+} or Agt ^{-/-} mice was not different, regardless of genotype of donors.	39
Figure 2.8 Breeding strategy of hepatocyte-specific AGT deficient mice (hepAGT ^{-/-}). ...	39
Figure 2.9 AGT mRNA abundance was specifically reduced in the liver of hepAGT ^{-/-} mice.....	40
Figure 2.10 Plasma AGT concentrations were greatly reduced in hepAGT ^{-/-} mice.	41
Figure 2.11 Systolic blood pressure was lower in hepAGT ^{-/-} mice.....	41
Figure 2.12 Plasma total cholesterol was not different in hepAGT ^{-/-} and hepAGT ^{+/+} mice.....	42
Figure 2.13 Atherosclerosis was greatly reduced in the arch of hepAGT ^{-/-} mice.	42
Figure 2.14 AGT mRNA abundance was greatly reduced in mice administered AGT ASO.....	43
Figure 2.15 Plasma AGT concentrations were greatly reduced in Ldlr ^{-/-} mice 9 weeks post initial AGT ASO injection	44
Figure 2.16 Systolic BP was lowered in Ldlr ^{-/-} mice 4 weeks post initial AGT ASO injection.	44

Figure 2.17 Atherosclerosis was greatly reduced in the arch of <i>Ldlr</i> ^{-/-} mice administered AGT ASO.	45
Figure 2.18 Plasma total cholesterol in <i>Ldlr</i> ^{-/-} mice fed the western diet for 12 weeks. .	45
Figure 2.19 Diet-induced weight gain was suppressed in hypoAGT and hepAGT ^{-/-} mice.	47
Figure 2.20 Fat mass, not lean mass, was suppressed in hypoAGT and hepAGT ^{-/-} mice.	48
Figure 2.21 Diet-induced weight gain was suppressed in mice administered AGT ASO.	49
Figure 2.22 Diet-induced body weight gain was not affected in mice administered Aliskiren, Enalapril, or Losartan.	51
Figure 2.23 Representative images of <i>Ldlr</i> ^{-/-} mice administered CON ASO (CON) or AGT ASO (AGT) fed the western diet for 12 weeks.	52
Figure 2.24 Fat mass, not lean mass, was suppressed in mice administered AGT ASO.	52
Figure 2.25 H&E staining of epididymal fat from mice administered control ASO (CON) or AGT ASO (AGT).	53
Figure 2.26 Intestinal fat absorption was not affected in hypoAGT, hepAGT ^{-/-} , or AGT ASO administered mice.	53
Figure 2.27 Food intake was higher in hypoAGT mice, but not different in hepAGT ^{-/-} and AGT ASO administered mice, compared with their wild type controls, respectively.	54
Figure 2.28 Physical activity was higher in hypoAGT mice, but not different in hepAGT ^{-/-} and AGT ASO administered mice, compared with their wild type controls, respectively.	54

Figure 2.29 O ₂ consumption, in a 24-h period, was higher in hypoAGT, hepAGT ^{-/-} , and AGT ASO administered mice, compared with their wild type controls, respectively.	55
Figure 2.30 CO ₂ production, in a 24-h period, was higher in hypoAGT, hepAGT ^{-/-} , and AGT ASO administered mice, compared with their wild type controls, respectively.	57
Figure 2.31 Gene expression profiling using qPCR in hepAGT ^{-/-} mice and hepAGT ^{+/+} mice fed the western diet for 12 weeks.	59
Figure 2.32 AGT inhibition protects against liver steatosis.	60
Figure 2.33 AGT ASO, but not aliskiren, regresses diet-induced obesity.	61
Figure 2.34 Global metabolite profiling in liver and plasma of hypoAGT mice.	63
Figure 2.35 Clustered heat map of genes with 1.3 folds or larger change in expression of hepAGT ^{-/-} mice.	64
Figure 3.1 Plasma AGT concentrations were restored by AAV-mediated AGT expression at a dose-dependent manner.	78
Figure 3.2 Plasma AGT concentrations were not different between hepAGT ^{+/+} and hepAGT ^{-/-} receiving either WT AGT or C18-137 AGT AAV.	79
Figure 3.3 Only oxidized AGT was detected in mouse plasma.	80
Figure 3.4 Plasma renin concentrations were not different between hepAGT ^{-/-} receiving native or C18-137S AGT AAV.	81
Figure 3.5 Plasma AngII concentrations were not different between hepAGT ^{-/-} receiving native or C18-137S AGT AAV.	82
Figure 3.6 Systolic blood pressure was not different between hepAGT ^{-/-} receiving native or C18-137S AGT AAV.	83
Figure 3.7 Plasma cholesterol concentrations were not different between hepAGT ^{-/-} receiving native or C18-137S AGT AAV.	84

Figure 3.8 Atherosclerotic lesion areas were not different between hepAGT ^{-/-} receiving native or C18-137S AGT AAV.	85
---	----

Chapter One: Literature Review

This chapter is based on a review published in “N Am J Med Sci (Boston). 2011 October 1; 4(4): 183–190”, with Congqing Wu as the first author.

Introduction

The renin-angiotensin system (RAS) is essential for the regulation of blood pressure and fluid homeostasis. Angiotensinogen (AGT) is the only known precursor of all angiotensin peptides. Through sequential cleavages by the classic enzymes, renin and angiotensin-converting enzyme (ACE), or enzymes of alternative pathways, AGT gives rise to a spectrum of angiotensin peptides, with angiotensin (Ang) II being the major effector peptide that regulates blood pressure and sodium/water homeostasis. Many components of the renin-angiotensin system including renin and ACE, as well as ang II and its receptors are well characterized and have been comprehensively studied in animal models. While much of the basic understanding of AGT has come from research efforts to define its role in blood pressure regulation, novel pathophysiological functions of AGT have been discovered in the last two decades, including kidney developmental abnormalities, atherosclerosis, and obesity. Despite advances in the understanding of AGT gene and protein functions, some fundamental questions remain unanswered. This is partially due to the traditional view of AGT as a passive substrate and lack of pharmacological inhibitors that directly target the protein. Development of many state-of-the-art techniques including the successful creation of cell-specific deficient mice is providing new insights into this substrate of the RAS. In this chapter, I summarize the literature on molecular characteristics of AGT and its pathophysiological features. In light

of the recent progress, I emphasize some newly recognized functional features of AGT other than its regulation on blood pressure. Specifically, I highlight effects of AGT on atherosclerosis and obesity.

Molecular characteristics of AGT

Gene structure of AGT

The AGT gene in humans and rodents was cloned, mapped and characterized throughout the 1980s (1-7). It is well conserved among vertebrates (8). Human AGT gene is a single-copy gene, locating within 20 Mb to the end of the long arm (1q42.2) on chromosome 1. With 5 exons and 4 introns, it spans 12,063 bp (nucleotide 230,838,274 - 230,850,336) and encodes 485 amino acids. The first exon contains 500 bp of the 5'-untranslated region. The second exon codes the 33- amino-acid signal peptide and more than half of the mature protein. Exon 5 encompasses the C-terminus of the protein as well as over 600 bp of the 3'-untranslated region (Figure 1.1).

The AGT gene in mice is similar to that of humans in terms of genomic size, gene structure, and coding exons (encoding 477 amino acids in mice versus 485 amino acids in humans). It is located on chromosome 8 within only 4.6 Mb to the telomere, which makes genetic manipulations of the AGT gene in mice an arduous task.

Protein characteristics of AGT

Human AGT is a heterogeneous plasma glycoprotein, mainly synthesized in hepatocytes. After removal of the 33-amino-acid signal peptide, the 452-amino-acid mature protein, with the first 10 amino acids corresponding to AngI is secreted into

plasma. The heterogeneity of plasma AGT is primarily due to variable glycosylation (9). Human AGT protein contains four putative sites for N-linked glycosylation (Asn-X-Ser/Thr): Asn14, Asn137, Asn271 and Asn295. An *in vitro* site-mutagenesis study demonstrates that all four sites can be glycosylated, with preference at Asn14 and Asn271 (9). Asn14 is close to the renin cleavage site (Leu10-Val11), and its glycosylation has been demonstrated to lower the affinity of AGT for renin (9). Asn14 glycosylation is also present in mice, but not in rats. These glycosylation sites appear to have no critical roles on folding, intracellular trafficking, or secretion of the AGT protein (9).

Human AGT protein contains four cysteines. Only two of these forming Cys18-Cys138 linkage (Figure 1.1) are conserved across species (9, 10). The crystal structure of human AGT shows that the formation of Cys18-Cys138 disulfide bridge confers a conformational change that allows access of renin to its cleavage site of AGT (Figure 1.2). It has been demonstrated that oxidative status of AGT has an impact on the rate of AGT-renin reaction *in vitro* (11), which may contribute to preeclampsia. It is unknown whether this disulfide bridge has similar properties in mouse AGT.

Another noteworthy feature is the species specificity of AGT-renin reaction. For example, human AGT is not cleaved by mouse renin efficiently (12, 13). While this may be influenced by an amino acid substitution at the renin cleavage site, Leu10-Val11 bond in humans versus Leu10-Leu11 bond in mice (13), the mechanism of this unique property has not been completely unraveled.

The cleavage of intact AGT by renin leads to generation of both AngI and des(AngI)-AGT, the remaining residues after removal of AngI that accounts for more than 95% of

the AGT protein sequence and maintains a typical serpin folding. The relative abundance of intact versus des(AngI)-AGT has not been characterized. There is some evidence that des(AngI)-AGT itself has biological properties that may relate to the serpin characteristics of the protein (14, 15).

Regulation of AGT

AGT gene expression is under developmental and hormonal controls in a cell type-specific manner (16). It is generally accepted that the predominant regulation of AGT occurs at the transcriptional level, although some post-transcriptional regulation also exists (17). AngII has been consistently shown to enhance mRNA stability of AGT and exert positive feedback on AGT protein production (17-21). AngII upregulates AGT mRNA in hepatocytes through nuclear factor-kappaB activation (NF-kB) (22), and increases plasma AGT protein through signal transducer and activator of transcription 3 (STAT3) induced interleukin-6 (IL-6) (21, 23). In our laboratory, we have consistently observed over 2-fold increase of plasma AGT concentrations in mice with exogenous AngII infusion (unpublished data). The positive feedback of AngII on AGT is balanced by its negative feedback on renin, the rate-limiting enzyme in the synthesis of angiotensin peptides.

Multiple putative cis-acting DNA regulatory elements, including glucocorticoids, estrogen, and acute phase responsive elements, are located within a region of 1 kb that is immediately upstream of human AGT gene (2, 6). Dexamethasone administration leads to striking increases of AGT mRNA abundance in liver and modest increases in brain (24, 25). However, increases of the AGT protein are much less than the mRNA increases (25). Estrogen is another positive regulator of AGT synthesis. Plasma AGT concentrations increase in parallel with estrogen during pregnancy. Synthetic estrogen in

oral contraceptive pills also increases plasma AGT concentrations in a dose-dependent manner (25). In contrast to the direct interactions of glucocorticoids and estrogen on the 5'-region of the AGT gene through their corresponding receptors, thyroid hormones seem to affect AGT mRNA abundance dependent on a secondary gene or protein, since their effects can be blocked by cycloheximide, an inhibitor of protein synthesis (25). In addition, for these 3 hormonal regulations, there are many confounding factors, such as a malignantly high dose above the physiological concentrations, a certain approach of administration, or interactions with a secondary gene or protein that complicate the interpretation of the reported findings (25). Therefore, their roles as primary regulators of AGT require further examination.

Tissue and cellular distribution of AGT

AGT is promptly secreted from cells into extracellular compartments (26). Therefore, the distribution of AGT synthesis is more commonly determined by mRNA rather than protein abundance. AGT mRNA has been consistently detected in many tissues such as liver, adipose, brain, heart, kidneys, and vessels (27-30). It has also been identified in spinal cord, lungs, adrenal glands, large intestine, stomach, spleen, and ovaries with low or variable abundances (24, 30). While most AGT mRNA is found in adult liver, it may be present mainly in adipose tissues, brain, and kidneys at embryonic stage. AGT production rises remarkably after birth and reaches adult level within 24 hours (31).

At cellular level, besides hepatocytes, it is widely accepted that adipocytes, proximal tubule epithelial cells, and astrocytes are AGT synthesizing cells (29, 32, 33). Among all extra-hepatic tissues synthesizing AGT, only adipose tissue has been shown to have an impact on plasma AGT concentrations using an adipocyte-specific AGT deficient mouse model (34). On the other hand, liver-specific deletion of a floxed human AGT transgene

using adenoviral delivery of Cre recombinase largely diminishes plasma human AGT concentrations (35). It infers that circulating AGT cannot be compensated by extra-hepatic tissues in the absence of hepatocyte-derived AGT. Indeed, liver is not only the source for plasma AGT but also for AGT in tissues like kidney (36).

Enzymes using AGT as a substrate

While AGT is the only known substrate of all angiotensin peptides, there are many enzymes that have been identified to use AGT as a substrate (37-40). Renin, a plasma aspartyl protease, is best known for cleaving AGT into AngI. Indeed, AGT is the only defined substrate for renin (41). As AGT is the only precursor and AGT-renin reaction is the rate-limiting step, renin becomes the most effective enzymatic target to inhibit the renin-angiotensin cascade (42). There is compelling evidence that renal renin is secreted into plasma to cleave AGT released from liver (38, 43-45). Therefore, this is considered a systemic pathway to generate angiotensin peptides. There are controversial findings regarding the local production of renin outside kidneys. While some studies have reported that kidney-derived renin is the only source to catalyze AGT locally (45, 46), there is growing evidence that renin can also be synthesized in tissues other than kidneys or non- juxtaglomerular cells (47-50). In addition to renin, many other enzymes such as cathepsin D, cathepsin G, kallikrein, pepsin, tissue-plasminogen activator, tonin, and trypsin have been demonstrated to convert AGT into either AngI or AngII (39, 40, 51, 52). These enzymes are abundant in tissues or some cell types, which has led to speculation that these enzymes may impact local generation of angiotensin peptides. However, most enzymes require an acidic environment (pH range 4–7) to actively catalyze AGT (40). Currently, the physiological significance of these enzymes using AGT as a substrate in vivo has not been established.

Plasma concentrations of AGT

AGT concentrations in human plasma are approximately 1 μM or 60 $\mu\text{g/ml}$ (28 - 71 $\mu\text{g/ml}$) (53). This is close to the Michaelis-Menton constant (K_M) of human renin (1.25 μM) (54). This indicates both AGT and renin concentrations are important for the rate of AngII generation, thus control the tonic activity of the RAS. Mice have much lower plasma AGT concentrations ($\approx 20 - 30 \text{ nM}$ or $1216 \pm 101 \text{ ng/ml}$ in C57BL/6 strain), which are similar in rats (55). It is not clear why plasma AGT concentrations could differ by over one order of magnitude between humans and rodents.

There is no standard method for measuring AGT protein concentration. Two approaches, indirect enzymatic assays and direct radioimmunoassay or ELISA, are currently used by many investigators. Indirect assays measure intact AGT through equivalent AngI released from the cleavage of AGT by renin in a given amount of time. Direct assay measures total AGT, which consists of both intact AGT and des(AngI)-AGT. Recently, a simple and sensitive sandwich ELISA kit has been developed to measure AGT concentrations in both humans and rodents (53, 55). However, this kit does not distinguish intact AGT from des(AngI)-AGT, which is important when changes in plasma concentrations of intact AGT are not correlated with that of total AGT. For instance, neither sodium depletion nor pharmacological inhibition of the RAS affects plasma total AGT concentrations, although both intact AGT concentrations and des(AngI)-AGT have significant changes (37, 56).

Plasma and tissue catabolism of AGT

The cleavage of AGT by renin is well known. However, there is a relative paucity of information of plasma clearance of either intact AGT or des(AngI)-AGT. Using radioiodinated tracer studies of AGT, the half-life of the protein has been estimated to be

5 hours in rats and rabbits (57-59). It is unknown whether intact and des(AngI)-AGT have similar rates of clearance from plasma.

There is also sparse evidence of tissues responsible for the catabolism of AGT. A single line of evidence displays that the protein is predominantly accumulated in kidney (59). However, this study was performed with directly radioiodinated proteins in which the label may not accumulate at the loci of catabolism. More meaningful analysis may be obtained by the conjugation of radioiodinated residualizing labels to track tissue sites of AGT catabolism (60).

Pathophysiological features of AGT

Genetic manipulation of AGT in mice

It has been reported that mice overexpressing either rat (61, 62) or human (63, 64) AGT gene alone do not exhibit any significant phenotype. In contrast, mice carrying both human AGT and renin genes display pronounced phenotypes including increased blood pressure, cardiac hypertrophy, and kidney abnormalities (63, 64), providing *in vivo* evidences for the species specificity of AGT-renin reaction.

AGT deficient mice have been developed by two laboratories (65, 66). Besides expected profound reductions in blood pressure, AGT deficient mice also have renal and cardiac dysfunction. However, pathologies in these two organs are distinct between transgenic AGT overexpressing mice and AGT deficient mice. While mice with human AGT and renin transgenes develop nephrosclerosis and cardiac hypertrophy (67), AGT deficient mice exhibit hydronephrosis and dilated cardiomyopathy (68, 69). These distinct

pathologies strongly indicate that tight regulation of AGT production is important to maintain normal blood pressure as well as normal renal and cardiac structures and functions.

Characteristics of mice with genetic manipulations of AGT are summarized in Table 1.1. It is speculated that the phenotypic changes in these mouse models are directly related to the changes of AngII production since the phenotypes in AGT deficient mice are also observed equivalently in renin, ACE, and combined AT1a and AT1b receptor deficient mice (70-73). However, exogenous AngII or tissue-specific enhancement of AngII cannot fully recover the phenotypes in AGT deficient mice (74-76), indicating that AGT may have both AngII-dependent and AngII-independent functions. In addition, phenotypes in AGT deficient mice can only be partially rescued by restoring AGT in circulation or one to multiple tissues (75-80), supporting a theme that this glycoprotein produced in both systemic and cell-specific manners synergistically contribute to its pathophysiological functions.

Recently, AGT floxed mice have been developed by two independent research groups (34, 36). These mice have normal neonatal survival rate and display no gross kidney abnormalities. Using Cre recombinase transgenic approach under the control of a specific promoter, AGT floxed mice will provide an optimal approach to understanding the relationship between AGT and many pathophysiological features as well as the underlying mechanisms in a cell-specific mode.

Genetic manipulation of AGT in experimental atherosclerosis and obesity

There is compelling evidence that the RAS plays a critical role in the development of atherosclerosis (81, 82). While many atherosclerosis studies in mice have directly

targeted AngII type 1 receptors or either of the two critical enzymes (renin and ACE) (50, 56, 83-87), no study has addressed the role of AGT in atherosclerosis. We have detected AGT protein in mouse atherosclerotic lesions using immunostaining (85). One study has reported that mice with human AGT and human renin transgenes in C57BL/6 background had augmented atherosclerosis, compared to the wild type controls, when fed a high-fat diet for 14 weeks (88). There is no study that has determined the role of AGT deficiency in atherosclerosis in mice. This is possibly due to their low neonatal survival rate and severe phenotypes that hamper the breeding of AGT deficient mice to hypercholesterolemic apolipoprotein E (apoE) or low density lipoprotein (LDL) receptor deficient mice (68).

Potential associations of AGT with obesity and adipocyte metabolism have been noted in animal models and *in vitro* studies. AGT mRNA abundance is increased in adipose tissues of obese rodents (89-91). Whole body deficiency of AGT leads to a lean phenotype that is manifested with impaired high fat diet-induced body weight gain, reduced fat mass, and increased locomotor activity in mice (92, 93). However, these mice have severe phenotypes that strongly impact the normal development and growth (64). The unhealthy condition may confound the interpretation of the observed metabolic phenotypes. In comparison with AGT deficient mice, mice with human AGT and renin transgenes also exhibit reduced body weight gain compared to their wild type controls, although these mice have increased tissue and plasma AGT abundance (94). The paradoxical observations require systematic research on the effects of this gene in obesity.

Genetic association of AGT with atherosclerosis and obesity in humans

The correlation of AGT gene with human diseases has been investigated primarily

through screening single nucleotide polymorphisms (SNPs). The first compelling genetic evidence of M235T polymorphism implicating a causal relationship between the AGT gene and essential hypertension in humans was published in 1992 (95). Since this initial report, M235T has become the most frequently studied SNP in AGT for hypertension. It has also been investigated frequently in patients with atherosclerotic diseases. While a few studies failed to define an association of M235T with atherosclerosis (96), most studies demonstrated that this polymorphism was associated with atherosclerosis in different populations (97-100). In addition to M235T, a few studies have also reported that T174M, another polymorphism in exon 2 of the AGT gene, is related with risk factors or prevalence of coronary artery disease (101, 102).

Although there is no direct evidence, animal studies and *in vitro* experiments indicate that AGT may also play an important role in obesity in humans. Investigations of the common AGT polymorphisms have shown a significant association of M235T with obesity in female hypertensive patients in different populations (103-105), although it failed to display any correlation in males (106).

Currently, genetic polymorphism analyses of the AGT gene are a cardinal approach to defining an association of this gene with human diseases. Many studies have reported potential links between SNPs in AGT and atherosclerosis or obesity, although their causal relationships remain to be established. For both atherosclerosis and obesity, the reported associations are either modest or only significant in a specific disease state, either of the two genders, or certain age group within one study. Confounding factors including small sample size, population heterogeneity, environmental and culture/ethnic differences, multiple disease states, and complex interactions within the gene or with many other genes, may complicate the interpretation of these polymorphism studies.

Therefore, it is important to control for the confounding factors in order to define a clear link between the AGT gene and atherosclerosis or obesity.

Conclusions and perspectives

The unique position of AGT in the RAS and its distinct features may make this protein an attractive target in developing effective therapeutic strategies in many human diseases such as atherosclerosis and obesity. However, despite great efforts in discovering the molecular mechanisms and clinical relevance of AGT gene and protein functions, some fundamental questions remain unanswered. These include: (i) Are the effects of AGT on its pathophysiological phenotypes, in part or in whole, dependent on AngII? (ii) What is the correlation of AGT produced in local tissues with the circulating pool? And what is the relative contribution of local versus circulating AGT to its pathophysiological functions? (iii) What is the fate of des(AngI)- AGT? Is it degraded rapidly after the release of AngI, or is it biologically functional, independent of the classic RAS? (iv) As demonstrated by the crystal structure of AGT, Cys18-Cys138 linkage determines the accessibility of its cleavage site to renin. Is the modulation of this disulfide bond relevant to the development or progress of its pathophysiological functions? These unanswered questions provide both challenges and opportunities to explore the mechanisms and effects of AGT in human diseases. Current advancement of many state-of-the-art techniques, including reconstructing AGT protein and the availability of cell-specific AGT deficient mice, provides excellent tools to answer these questions.

Specific aims

To address some of the fundamental questions discussed above, I propose three specific aims:

Aim 1: To investigate the role of AGT inhibition in atherosclerosis and obesity (Chapter two)

Aim 2: To determine the contributions of systemic and local AGT to atherosclerosis and obesity (Chapter two)

Aim 3: To analyze the structure-function relationship of Cys18-C138 linkage in AGT (Chapter three)

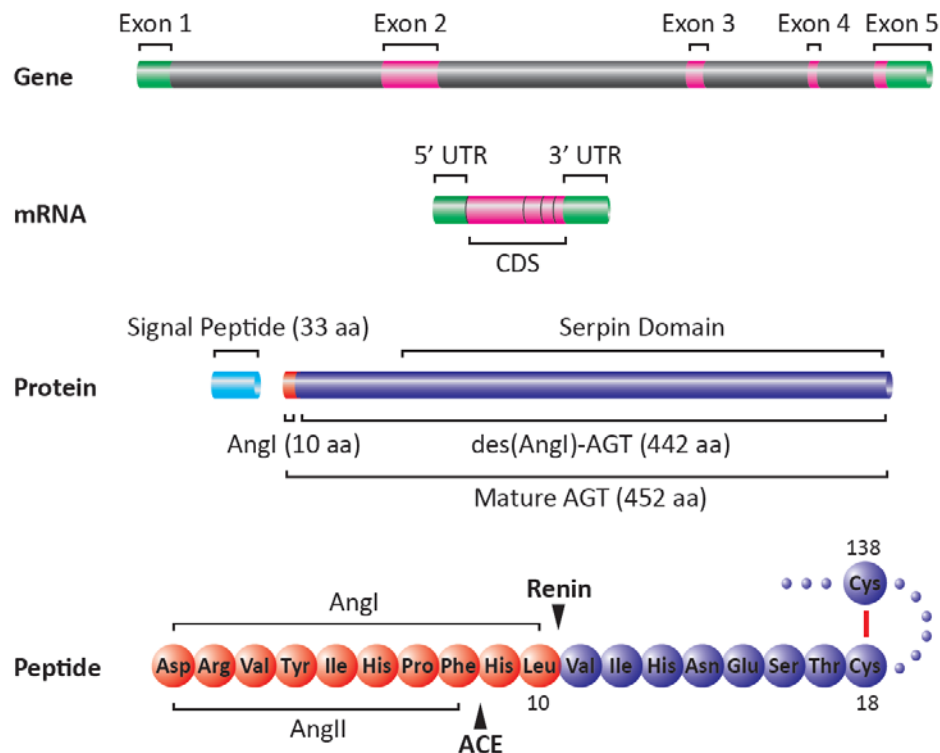


Figure 1.1 Schematic Representation of Human AGT Gene and Protein. Human AGT gene contains 5 exons. Exon 2 encodes the majority of the protein. After removal of the 33 aa signal peptide, the 452 aa mature AGT is secreted. Cleavage of mature AGT by renin gives a decapeptide, AngI, and the 442 aa des(AngI)-AGT. AngI is further cleaved by ACE into AngII. Two cysteines at 18 and 138 form a disulfide bridge (Cys18-Cys138) that confers a conformational change allowing access of renin to the AngI cleavage site of AGT. Diagrams were drawn proportional to actual gene and protein size based on the University of California Santa Cruz Human Genome Browser Feb 2009 Assembly. UTR: untranslated region; CDS: coding sequences.

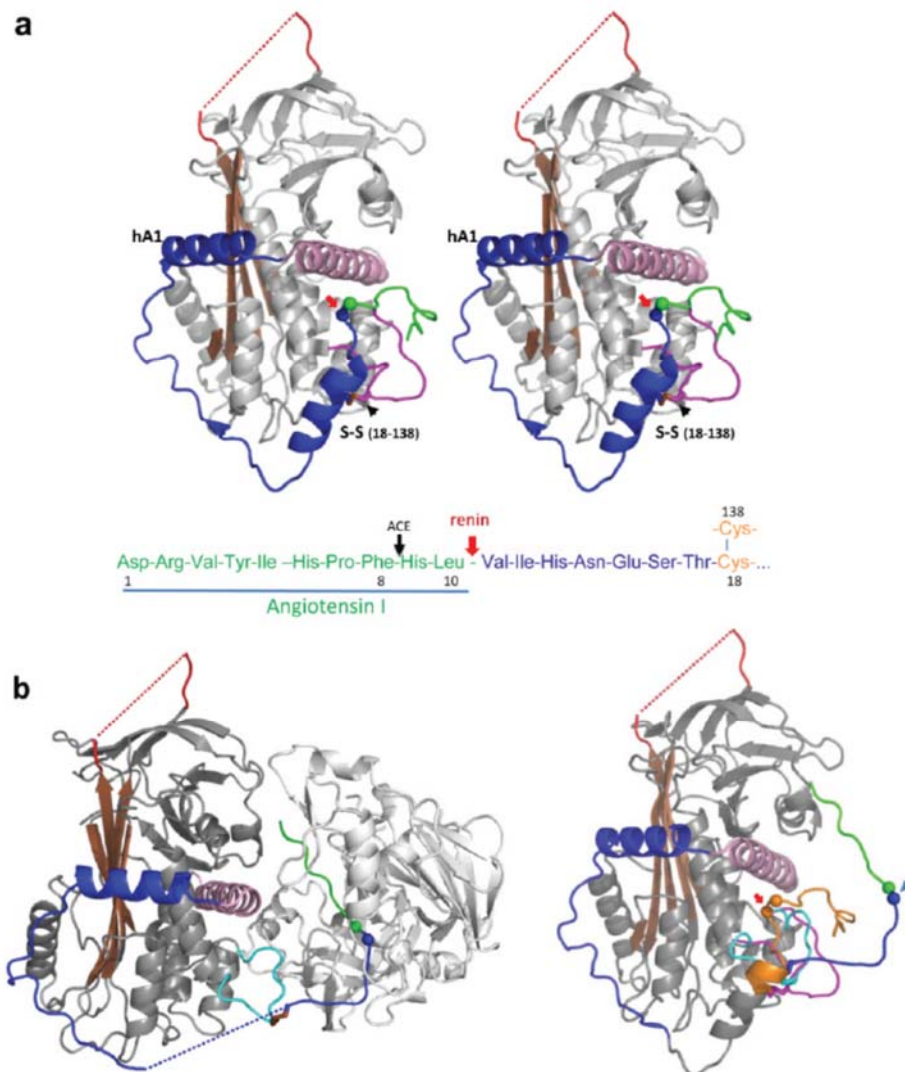


Figure 1.2 Structure of AGT and its complex with renin (adapted from figure 1 of “A redox switch in angiotensinogen modulates angiotensin release” (11)) a. Stereo image of human AGT: serpin template in grey and helix A in purple with the A-sheet in brown, the unresolved reactive loop in dark red, and in dark purple the CD loop containing Cys 138. The amino-tail is in blue with the new helix A1 and a second helix A2 containing Cys18 (linked in brown to Cys 138); the terminal AngI segment is in green with the renin-cleavage site shown as green and blue balls. The sequence below (same color coding) also indicates the subsequent cleavage by ACE releasing AngII. b. the initiating complex formed by AGT with inactivated (Asp292Ala) renin (left), and on right superimposed on

the unreacted form (brown) showing the displacement of the CD loop and the movement of the aminoterminal peptide (visible to Cys 18), into the active cleft of renin.

Table 1.1 Characteristics of mice with genetic manipulations of AGT.

Manipulation	Strategy	Pathophysiological Features				References
		BP	kidney	heart	Others	
rat <i>Agt</i> overexpression	rat <i>Agt</i> transgene under the control of the mouse metallothionein I promoter	↔	ND	ND	ND	(61)
	rat <i>Agt</i> transgene under the control of the rat <i>Agt</i> promoter	↑	nephro-sclerosis	hyper-trophy	ND	(62, 76)
human <i>Agt</i> overexpression	human <i>Agt</i> transgene under the control of the human <i>Agt</i> promoter	↔	↔	↔	↔	(63)
rat <i>Agt</i> and <i>Ren</i> overexpression	breeding of rat <i>Agt</i> transgenic mice with rat <i>Ren</i> transgenic mice	↑	ND	ND	ND	(61)
human <i>Agt</i> and <i>Ren</i> overexpression	breeding of human <i>Agt</i> transgenic mice with human <i>Ren</i> transgenic mice	↑	nephro-sclerosis	hyper-trophy	↓ body weight	(64, 94)
whole body <i>Agt</i> deficiency (<i>Agt</i> ^{-/-})	insertion of a neo cassette to the exon 2 prior to the start codon of the mouse <i>Agt</i>	↓	hydro-nephrosis	cardio-myopathy	↓ body weight, fat mass & locomoter activity	(65, 66)

Table 1.1 Characteristics of mice with genetic manipulations of AGT (cont'd).

rat <i>Agt</i> overexpression in adipocytes	rat <i>Agt</i> transgene under the control of aP2 promoter in wild type mice	↑	ND	ND	↑ body weight & fat mass, ↓ energy expenditure	(79)
rat <i>Agt</i> adipocyte-specific expression	rat <i>Agt</i> transgene under the control of aP2 promoter in <i>Agt</i> ^{-/-} mice	↔	↔	ND		
<i>Agt</i> adipocyte-specific deficiency	breeding of <i>Agt</i> floxed mice with transgenic mice expressing Cre recombinase under the control of aP2 promoter	↓ in aged mice	ND	ND	↔ body weight & fat mass	(34)

Notes: *Agt* = angiotensinogen gene ; *Ren* = renin gene; BP = blood pressure; ↔ = no change; ↑ = increase; ↓ = decrease; ND = not determined. Pathophysiological changes were determined in comparison with their relative wild type littermates.

Chapter Two: Angiotensinogen Inhibition Protects Against Atherosclerosis and Obesity in Mice

This chapter is based on a manuscript in preparation, titled “Angiotensinogen inhibition prevents and regresses diet-induced obesity in mice”, with Congqing Wu as the first author.

Figures based on experiments conducted by others are listed here: figure 2.5, 2.6, 2.7, 2.22, 2.33E,F from Hong Lu, figure 2.15 from ISIS, figure 2.16, 2.17, 2.18, 2.21, 2.23, 2.24, 2.33A-D from Deborah A. Howatt and Anju Balakrishnan.

Synopsis

In the renin-angiotensin system, angiotensinogen is sequentially cleaved by renin and angiotensin-converting enzyme to generate angiotensin II. As the major effector peptide, angiotensin II mainly function through angiotensin type 1 receptor. Inhibition of the renin-angiotensin system using enzyme inhibitors or receptor blockers of the renin-angiotensin system, such as angiotensin-converting enzyme inhibitors, angiotensin receptor blockers, and more recently renin inhibitors, are known to reduce blood pressure and atherosclerosis. As expected, we demonstrated that angiotensinogen inhibition by antisense oligonucleotides had similar protective effects on blood pressure and atherosclerosis comparable with these classic inhibitory drugs. Unexpectedly, weekly injection of antisense oligonucleotides against angiotensinogen remarkably slowed body weight gain in mice fed a western diet. This body weight effect was not observed in same mouse strain fed same western diet that were administered any of the 3 classic

renin-angiotensin system inhibitors. The suppressed body weight gain was attributable to diminished body fat mass gain and enhanced energy expenditure. Genetic deletion of angiotensinogen, globally or specifically in hepatocytes, recapitulated phenotypes observed in mice administered angiotensinogen antisense oligonucleotides. More excitingly, injection of angiotensinogen antisense oligonucleotides regressed body weight gain on obese mice. Together, our findings revealed a unique feature of angiotensinogen inhibition beyond classic renin angiotensin inhibition and demonstrated therapeutic potentials of angiotensinogen antisense oligonucleotides against hypertension, atherosclerosis, and obesity.

Introduction

The renin-angiotensin system (RAS) regulates blood pressure and fluid homeostasis. Angiotensinogen (AGT) is the only precursor of this peptide hormone system (107). In the classic cascade, AGT is cleaved by renin, the rate-limiting enzyme, to release the inactive AngI. AngI is cleaved by angiotensin-converting enzyme (ACE) to generate AngII. As the major effector peptide of the RAS, AngII functions predominantly through AngII type 1 (AT1) receptors.

With the advent of pharmacological agents targeting ACE, AT1 receptors, or renin, RAS inhibition has become a prominent strategy for hypertension management. The landmark HOPE trial (108) is the first to demonstrate cardiac benefits of the ACE inhibitor independent of lowering blood pressure, followed by ONTARGET trial showing comparable benefits of angiotensin receptor blocker (ARB) (109). Numerous animal studies have consistently demonstrated anti-atherosclerotic effects of RAS inhibition

(81). In addition, RAS inhibition has been reported to profoundly improve obesity-related diseases such as diabetic nephropathy (110). There is no evidence that these 3 classes of drugs affect body weight in humans. In our recent side-by-side comparison study in mice, these 3 classes of drugs, inhibiting either enzymes (renin and ACE) or AT1 receptors, equivalently reduces atherosclerosis through AngII-dependent mechanisms (56). However, none of them has significant effects on body weight (56).

In contrast to extensive studies on the enzymes and receptors of the RAS, effects of AGT inhibition have not been directly explored due to the lack of pharmacological agents targeting the AGT protein as well as severe health problems associated with global AGT deficient mice. AGT gene and protein are well conserved among vertebrates. Human AGT is mainly synthesized in hepatocytes and secreted into blood, where it is cleaved by plasma renin or taken up by peripheral tissues. While the first ten amino acids of secreted AGT correspond to AngI, the remaining residues after the removal of AngI, des(AngI)-AGT, accounts for nearly 98% of the AGT protein sequence and maintains a typical serpin folding, suggesting alternative functions other than being a passive substrate of the RAS. Indeed, a previous study implicates that des(AngI)-AGT has functions independent of AngII (14).

We have developed both pharmacological and genetic tools to modulate AGT expression, and demonstrated that AGT inhibition, not only reduces blood pressure and atherosclerosis, but also increases energy expenditure and confers resistance to diet-induced obesity, which is beyond the classic RAS inhibition.

Methods

Ethics statement

All animal experiments reported in this part were performed with approval of the University of Kentucky Institutional Animal Care and Use Committee (University of Kentucky IACUC protocol number: 2006-0009).

Mouse housing condition and diet

All mice were maintained in individually vented cages (maximally 5 mice per cage) in a barrier facility (14:10 hour light-dark cycles, ambient temperature of 22°C). Cage bedding was Teklad Sani-Chip bedding (Cat # 7090A, Harlan Teklad, Madison, WI, USA). Mice were fed a normal rodent laboratory diet (Diet # 2918, Harlan Teklad) and provided with drinking water ad libitum from a reverse osmosis system. To induce hypercholesterolemia or obesity, mice were fed a saturated fat enriched diet (milk fat 21% wt/wt and cholesterol 0.2% wt/wt; Diet# TD.88137; Harlan Teklad). This diet was developed in 1988 by collaboration between Harlan Teklad and researchers at Rockefeller University to mimic the nutrient content of fast food in a typical western food chain (111). It is referred to as western diet. Indirect calorimetry was carried out on a subset of mice due to equipment capacity.

Development of hypomorphic AGT mice

AGT floxed mice (Figure 2.1) were developed under a contract with InGenious Targeting Laboratory (Stony Brook, NY, USA) using a construct containing mouse AGT gene with insertions of 3 loxP sites and 2 FRT sites, and 1 neo cassette as described previously (34, 112). This construct was electroporated into embryonic stem cells of mouse strain 129 that were subsequently bred in C57BL/6 mice. With the presence of the neo

cassette, the resulted AGT floxed mice showed reduced AGT expression globally. They were bred to *Ldlr*^{-/-} mice to generate hypomorphic AGT mice (hypoAGT) and AGT wild type mice (AGT^{+/+}) with LDL receptor ^{-/-} background.

Development of hepatocyte-specific AGT deficient mice

The breeding strategy to develop mice with hepatocyte-specific deficiency of AGT (Figure 2.8) included 4 steps: (1) AGT floxed mice were bred to FLPe mice (B6;SJL-Tg(ACTFLPe)9205Dym/J, Stock # 003800, N2 to C57BL/6 strain, The Jackson Laboratory, Bar Harbor, ME) to remove the neo cassette inserted in intron 2 of mouse AGT gene. (2) After removal of the neo cassette, these mice were bred to *Ldlr*^{-/-} mice (B6.129S7-Ldlrtm1Her/J, Stock # 002207, N13 to C57BL/6 strain, The Jackson Laboratory) to generate *Agt*^{fl/fl} x *Ldlr*^{-/-} mice. (3) Male mice expressing Cre recombinase under the control of a hepatocyte-specific albumin promoter (B6.Cg-Tg(Alb-cre)21Mgn/J, Stock # 003574, N7 to C57BL/6 strain, The Jackson laboratory) were bred to female *Ldlr*^{-/-} mice to generate male *Alb-cre*^{1/0} mice in the LDL receptor^{-/-} background. (4) *Alb-cre*^{0/0} x *Agt*^{fl/fl} x *Ldlr*^{-/-} females were bred with *Alb-cre*^{1/0} x *Agt*^{fl/fl} x *Ldlr*^{-/-} males to generate hepatocyte-specific AGT deficient mice hepAGT^{-/-}, and their wild type littermates hepAGT^{+/+}.

RNA isolation and real-time PCR

Total RNA in liver, kidney, adipose tissue, and brain was extracted with RNeasy Mini Kit (Qiagen), and then reversely transcribed with an iScript™ cDNA Synthesis Kit (Cat#170-8891; Bio-Rad, Hercules, CA). Real time PCR was performed to quantify mRNA abundance using a SsoFast™ EvaGreen® Supermix kit (Cat# 172-5203; Bio-Rad) on a Bio-Rad CFX96 cycler. Data were analyzed using $\Delta\Delta C_t$ method, normalized to β -actin abundance. Primers for real-time PCR are listed in table 2.1.

Measurement of plasma components

Blood samples were collected with EDTA (final concentration at 1.8 mg/ml) and centrifuged at 400 g for 20 minutes, 4 °C to separate plasma. Before termination, blood samples were collected using retro-orbital bleeding on conscious mice. At termination, blood samples were collected using right ventricular puncture after anesthesia (a mixture of ketamine 100 mg/kg and xylazine 10 mg/kg).

Plasma AGT concentrations were determined using an ELISA kit, as described previously (55) (Cat # 27413, Immuno-Biological Laboratories Co., Ltd, Takasaki-Shi, Gunma, Japan).

Plasma total cholesterol concentrations were measured using an enzymatic kit (Cat # 439-17501; Wako Chemicals USA, Richmond, VA).

Drug administration

Alzet mini-osmotic pumps (model 2004; Durect Corporation, Cupertino, CA, USA) were implanted into LDL receptor *-/-* male mice at the age of 8 weeks, and replaced every 4 weeks to continuously deliver drugs for a total of 12 weeks (83, 113). Drug doses were listed as follows: vehicle (PBS); aliskiren 2.5, 12.5 or 25 mg/kg/day; enalapril 0.25, 1.25 or 2.5 mg/kg/day; and losartan 2.5, 12.5 or 25 mg/kg/day. Doses of each drug were chosen based on estimates that would encompass a range of partial to complete inhibition of their respective targets (50, 114, 115). Aliskiren was provided by Novartis. Enalapril (Cat# E6888) and losartan (Cat# 61188) were purchased from Sigma-Aldrich (St. Louis, MO, USA).

Antisense oligonucleotide administration

All antisense oligonucleotides were provided by ISIS Pharmaceuticals (Carlsbad, CA). Two AGT ASOs with different targeting sequences, ISIS #261333 (5' TCTTCCACCCTGTCACAGCC 3') and ISIS #487022 (5' TCATCATTTATTCTCGGTCA 3'), are 20-mer phosphorothioate oligonucleotides perfectly complementary to mouse AGT mRNA. They were composed of three 2'-O-methoxyethyl-modified ribonucleosides at the 3' and 5' ends with 2'-deoxynucleosides in between. A control ASO, ISIS #141923 (5' CCTTCCCTGAAGGTTCTCC 3') was designed not to target any transcript, including AGT. Animals were injected intraperitoneally with either control ASO or AGT ASO diluted in PBS at different doses (12.5, 25 and 50 mg/kg/day), once a week until termination.

Irradiation and bone marrow repopulation

This procedure was performed as described previously (116). Bone marrow was harvested from *Agt*^{-/-} (B6.129P2.Agt tm1Unc/J; stock # 002681, The Jackson laboratory) or *Agt*^{+/+} mice and injected (1 x 10⁷ cells/mouse) into age-matched male *Ldlr*^{-/-} recipient mice that had been lethally irradiated. Four weeks after bone marrow repopulation, recipient mice were placed on western diet for the next 12 weeks.

Quantification of atherosclerosis

Atherosclerosis was quantified on the intima of the ascending region, aortic arch and 3 mm of the descending region using an *en face* method with ImagePro software as described previously (117, 118).

Body composition

Body composition was measured on conscious mice in a constrained tube using

EchoMRI-100™ (Echo Medical Systems, Houston, TX) that reads whole body fat mass, lean mass, and water content within 2 minutes.

Systolic blood pressure measurements

Systolic blood pressure was measured on conscious mice using a non-invasive tail-cuff system (Kent Scientific Corporation, Torrington, CT, USA) following a standardized protocol described previously (119).

Intestinal fat absorption

We use sucrose polybehenate (SPB) as a marker for noninvasive measurement of intestinal fat absorption. SPB is part of olestra (Olean; P&G, Cincinnati, OH), a commercially used long-chain fatty acid ester blend. Although virtually identical to triglycerides in physical properties (120), olestra is not hydrolyzed by pancreatic lipase and not absorbed through the intestine (121). In addition, olestra does not interfere with normal dietary triglycerides absorption (122). As described previously (123), mice were individually caged and fed test diet containing 5% SPB for 2 or 3 days. A few fecal pellets were collected for each mouse, and approximately 10 mg (a single fecal pellet) were assayed. Intestinal fat absorption was calculated from the ratios of behenic acid to other fatty acids in diet and feces as analyzed by gas chromatography of fatty acid methyl esters.

Metabolic cages

Metabolic parameters were measured by indirect calorimetry with a TSE Labmaster Platform (TSE System). Mice were individually placed in metabolic chambers and measured for 5 days after 2 days of acclimation. Mice were fed the same western diet in the chambers as in their home cages.

Metabolome analysis

Unbiased global metabolite profiling were conducted in liver and serum, comparing between hypoAGT mice and wild type controls, under contract with Metabolon, Inc.(Durham, NC). A total of 12 liver and 18 serum samples were extracted and prepared for analysis using a proprietary series of organic and aqueous extractions to remove the protein fraction while allowing maximum recovery of small molecules. The extracted samples were split into equal parts for analysis on the GC/MS and LC/MS/MS platforms. Also included were several technical replicate samples created from a homogeneous pool containing a small amount of all study samples. Recovery standards were added prior to the first step in the extraction process for QC purposes.

Compounds were identified by comparison to library entries of purified standards or recurrent unknown entities. Identification of known chemical entities was based on comparison to metabolomic library entries of purified standards. As of this writing, more than 1000 commercially available purified standard compounds had been acquired registered into LIMS for distribution to both the LC and GC platforms for determination of their analytical characteristics. The combination of chromatographic properties and mass spectra gave an indication of a match to the specific compound or an isobaric entity. Additional entities could be identified by virtue of their recurrent nature (both chromatographic and mass spectral). These compounds have the potential to be identified by future acquisition of a matching purified standard or by classical structural analysis.

For this experiment, two types of statistical analysis were performed, significance tests and classification analysis. For pair-wise comparisons, Welch's t-tests and/or Wilcoxon's rank sum tests was performed. For other statistical designs, various ANOVA procedures

(e.g., repeated measures ANOVA) were performed. For classification, random forest analyses were used. Random forests give an estimate of how well individuals in a new data set are classified into each group, in contrast to a t-test, which tests whether the unknown means for two populations are different or not. Random forests create a set of classification trees based on continual sampling of the experimental units and compounds. Then each observation is classified based on the majority votes from all the classification trees. Statistical analyses are performed with the program “R”.

Microarray analysis

Global differential gene expression induced by hepatic AGT deficiency was determined in liver, white adipose tissue (epididymal fat), and brown adipose tissue using Affymetrix GeneChip Mouse Gene 2.0 ST. Total RNA (100 ng) for each sample was extracted using RNeasy Mini Kit (Qiagen). RNA integrity, measured by 28S/18S ratio, was determined with Bioanalyzer 2100 (Agilent). Microarray hybridization was performed in London Regional Genomics Centre (London, ON, Canada). Data were analyzed with Partek Genomics Suite (Partek Incorporated; St. Louis, MO).

Statistical analysis

Data are represented as means \pm standard error of means. SigmaPlot version 12.0 (SYSTAT Software Inc., Chicago, IL) was used for statistical analyses. To compare continuous response variables between two groups, an unpaired two-tailed Student's t test was used for normally distributed variables and Mann-Whitney U test was performed for non-normally distributed variables. To compare more than two groups of a study, we used one-way ANOVA for normally distributed variables and Kruskal-Wallis one way ANOVA on Ranks for non-normally distributed variables, respectively. $P < 0.05$ was considered statistically significant.

Results

Mice with global AGT reduction were protected from atherosclerosis

To examine the role of AGT in atherosclerosis, we started to generate *Agt/Ldlr* double knockout mice. Global AGT deficient mice were generated nearly two decades ago (65, 66). However, these mice are not suitable for our study because of their poor neonatal survival rate and severe developmental problems. To develop tissue-specific AGT deficient mice, we floxed exon 2 of the mouse AGT gene with a neo cassette immediately after exon 2 as described previously (34) (Figure 2.1). These AGT floxed mice were then crossed with *Ldlr*^{-/-} mice. Unexpectedly, the resulting mice had greatly reduced AGT mRNA abundance in all examined tissues, including liver, kidney, adipose tissue, and brain (Figure 2.2). We designated them as hypomorphic AGT (hypoAGT) mice. Unlike global AGT deficient mice, hypoAGT mice had normal neonatal survival rates, and were grossly healthy with a normal life span. With suppressed AGT mRNA expression, hypoAGT mice have barely detectable plasma AGT (Figure 2.3) and lower systolic BP (Figure 2.4).

To assess the effects of AGT global reduction on atherosclerosis, 8-10 week old hypoAGT mice and their wild type controls were fed a western diet (0.2% cholesterol, 42% calories from fat) to induce hypercholesterolemia. Plasma AGT concentrations remained unchanged in both groups fed the western diet (Figure 2.3). After 12 weeks, all mice developed severe hypercholesterolemia, although plasma total cholesterol concentrations were slightly lower in hypoAGT mice (Figure 2.5). HypoAGT mice developed minimal atherosclerotic lesions with only 1.9% intimal area in the arch covered by lesions, while wild type controls showed a nearly 9-fold increase at 17.4% (Figure 2.6).

AGT deficiency in hepatocytes was responsible for protection against atherosclerosis

Given that global AGT reduction protects against atherosclerosis, we sought to examine whether circulating or local (lesion) AGT contributes to these effects. On the basis of the critical roles of macrophage RAS in atherosclerosis (50, 115, 124), we performed a bone marrow transplantation study, in which recipient *Ldlr*^{-/-} mice were irradiated and replenished with bone marrow cells from either *Agt*^{-/-} or *Agt*^{+/+} donor mice. These chimeric mice were placed on western diet for 12 weeks. We found that the AGT genotype of donors had no effects on atherosclerosis in recipients (Figure 2.7), suggesting AGT deficiency in cells of hematopoietic lineage does not decrease atherosclerosis.

As hepatocytes are the source for circulating AGT (36), we determined whether hepatocyte-specific deletion of AGT would recapitulate the phenotypes in hypoAGT mice. After removal of the neo cassette, AGT floxed mice (with normal plasma AGT) in LDL receptor ^{-/-} background were bred to albumin promoter-driven Cre transgenic mice to generate hepatocyte-specific AGT deficient mice, designated as hepAGT^{-/-} mice (Figure 2.8). We confirmed that AGT deficiency was specific to liver in hepAGT^{-/-} mice by examining AGT mRNA abundance in major AGT expressing tissues, including liver, adipose tissue, kidney, and brain (Figure 2.9). Consistent with a previous report (36), hepatic AGT deficiency depleted plasma AGT concentrations to a similar extent as in hypoAGT mice as well as lowering systolic BP (Figure 2.10, 2.11).

Following the same experimental procedures as hypoAGT mice, we evaluated atherosclerosis in hepAGT^{-/-} mice and their wild type littermates. While hepatic AGT deficiency had no effects on plasma total cholesterol concentrations (Figure 2.12), hepAGT^{-/-} mice reduced atherosclerosis to a similar extent observed in hypoAGT mice

(Figure 2.13). Together, hepatic AGT is responsible for the protection against hypercholesterolemia-induced atherosclerosis.

AGT ASO reduced atherosclerosis

As hepatic AGT is a potential target against atherosclerosis and AGT expression is mainly regulated at the transcriptional level, we developed antisense oligonucleotides (ASO) to inhibit AGT. To evaluate the effect of AGT ASO on atherosclerosis, 8-10 week-old *Ldlr*^{-/-} mice received either control ASO or one of the two AGT ASOs with different targeting sequences weekly, starting 1 week prior to western diet feeding. Intraperitoneal injection of AGT ASO efficiently reduced AGT mRNA abundance in liver as well as in kidney and adipose tissues (Figure 2.14). Accordingly, plasma AGT concentrations showed nearly a 90% reduction in AGT ASO administered mice compared with those receiving control ASO (Figure 2.15). Consistent with blood pressure lowering and anti-atherogenic effects of the classic RAS inhibition (56), AGT ASO administered mice had lower systolic blood pressure and profoundly reduced atherosclerotic lesions, compared with mice administered control ASO (Figure 2.16, 2.17). One of the AGT ASO (AGT-2) had effects on plasma total cholesterol, thus only AGT ASO (AGT-1) was used in most of the following study (Figure 2.18).

AGT ASO prevented diet-induced obesity

For all study mice, we measured body weight weekly to monitor their general health. We noticed that both hypoAGT mice and hepAGT^{-/-} mice gained less body weight compared with their wild type controls, respectively (Figure 2.19). Based on body composition analysis by EchoMRI, the body weight difference was attributable to diminished fat mass gain (Figure 2.20). We were aware of previous reports that global deletion of major components of the RAS, including AGT, ACE, renin, and AT1 receptors, resulted in

lower body weight (92, 125, 126). In addition, all these knockout mice suffered from severe development problems and health issues. Given that all 3 classes of inhibitory drugs against the RAS have no effect on body weight in humans, it is reasonable to conclude that the lean phenotypes resulted from global deficiency of the RAS components were attributed to developmental problems and classic RAS inhibition has minimal effect on body weight. Therefore, we were surprised that age-matched *Ldlr*^{-/-} mice administered AGT ASO had impaired body weight gain (Figure 2.21) when fed the same western diet, which was not observed on any of the three classic modes of RAS inhibition (Figure 2.22). AGT ASO administered mice were apparently leaner without any health issues compared with control ASO administered mice (Figure 2.23). While lean mass was not different between AGT ASO and control ASO administered mice, fat mass growth was diminished in AGT ASO administered mice (Figure 2.24), which was confirmed by measuring tissue weight of epididymal, retroperitoneal, and inguinal fat (data not shown). Consistently, AGT ASO administered mice had much smaller adipocytes, as shown by the H&E staining of epididymal fat (Figure 2.25).

AGT deficiency tipped energy balance by increasing energy expenditure

To investigate the changes in energy balance induced by pharmacological or genetic AGT inhibition, we performed an intestinal fat absorption assay and indirect calorimetry studies on AGT ASO administered mice as well as hypoAGT mice and hepAGT^{-/-} mice. AGT inhibition did not affect intestinal fat absorption (Figure 2.26) and food intake (Figure 2.27), except that hypoAGT mice had increased food intake compared with their wild type controls. AGT ASO administered or hepAGT^{-/-} mice showed no difference in physical activity compared with their corresponding controls (Figure 2.28). Consistent with previous report (92), hypoAGT mice exhibited increased physical activity (Figure

2.28). AGT inhibition led to increased oxygen consumption (Figure 2.29) and carbon dioxide production (Figure 2.30) during both light and dark cycles.

Consistently, AGT inhibition increased uncoupling protein 1 (*Ucp1*) gene expression by 2 folds in brown adipose tissue (Figure 2.31A). We did not find changes in genes involved in lipid catabolism in liver, such as carnitine palmitoyltransferase 1 (*Cpt1*) and hepatic lipase (*Lip*c) (Figure 2.31B, C), but found downregulation in genes involved in fatty acid synthesis and lipogenesis in liver, such as fatty acid synthase (*Fasn*), stearoyl-CoA desaturase (*Scd1*), and peroxisome proliferator-activated receptor gamma (*PPAR*γ) (Figure 2.31D, E and, F). Indeed, both hypoAGT mice and hepAGT^{-/-} were protected from liver steatosis with lower liver mass and liver triglycerides content (Figure 2.32A-E).

AGT ASO regressed diet-induced obesity

To assess whether the energy expenditure elevated by AGT ASO is sufficient to regress established obesity, we fed 8-10 week-old *Ldlr*^{-/-} mice the western diet for 12 weeks to induce body weight gain, then randomized them into two groups receiving weekly injection of either control or AGT ASO with continuous western diet feeding. AGT ASO administration lowered systolic blood pressure in obese *Ldlr*^{-/-} mice by 20 mmHg (Figure 2.33A). In contrast to continuous body weight gain in mice receiving control ASO, AGT ASO administered mice stopped body weight gain 2 weeks after initial AGT ASO injection, then started losing weight at a constant rate for 6 weeks, and maintained body weight afterwards (Figure 2.33B). Weight loss in AGT ASO administered mice was due to decline in fat mass, as lean mass remained the same (Figure 2.33C,D). In contrast, following similar experimental protocol, mice infused with aliskiren, a renin inhibitor, had lower systolic blood pressure (Figure 2.33E), but comparable body weight gain to mice infused with PBS (Figure 2.33F).

AGT deficiency decreased lipid metabolites in both liver and plasma

To examine global metabolic changes resulting from AGT deficiency, unbiased biochemical profiles were determined in liver and plasma. Comparison of global biochemical profiles revealed altered metabolism in all nutrient categories, amino acids, carbohydrates, lipids, and nucleotides, in hypoAGT mice, compared with AGT^{+/+} mice. Overall, we observed more decrease in lipid metabolites, and more increase in other categories, in both liver and serum (Figure 2.34).

AGT deficiency resulted in broad alteration in gene expression in brown fat

To investigate AGT deficiency induced differential gene expression, we performed global gene profiling, using whole genome gene chips, on three tissue types including liver, white adipose tissue (epididymal fat), and brown adipose tissue, comparing hepAGT^{-/-} mice with hepAGT^{+/+} mice. We screened a total of 35,000 RefSeq transcripts for differences in gene expression. For better visualization, we generated a clustered heat map with a criterion of 1.3 folds or larger change in gene expression. Interestingly, AGT deficiency had much more extensive impact on gene expression of brown adipose tissue than both liver and white adipose tissue (Figure 2.35), suggesting a role of brown adipose tissue in AGT deficiency-induced lean phenotype.



Figure 2.1 Construct map of hypoAGT mice. The presence of the neo cassette in intron 2 unexpectedly suppressed AGT gene expression globally, possibly by interfering with normal RNA splicing of AGT.

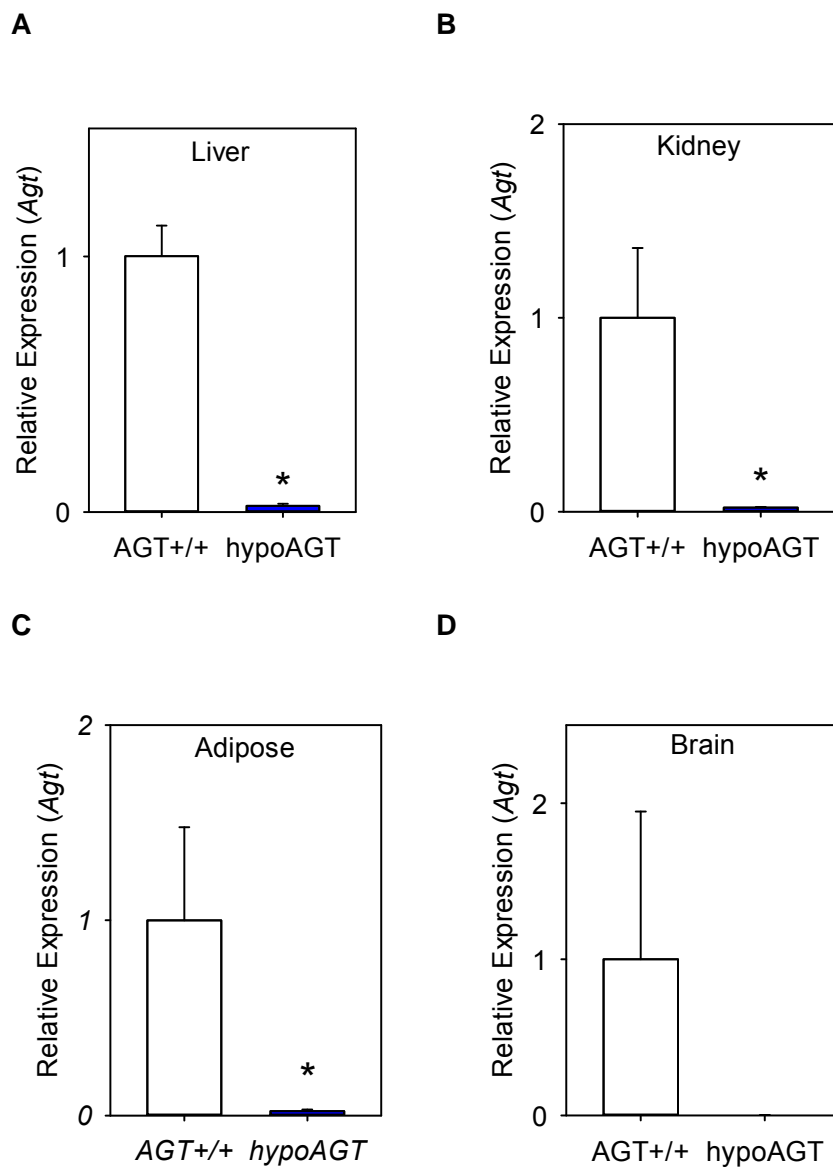


Figure 2.2 AGT mRNA abundance was dramatically reduced in hypoAGT mice. n = 2-3 per group. All data are the mean \pm SEM. * p < 0.05, Student's *t* test.

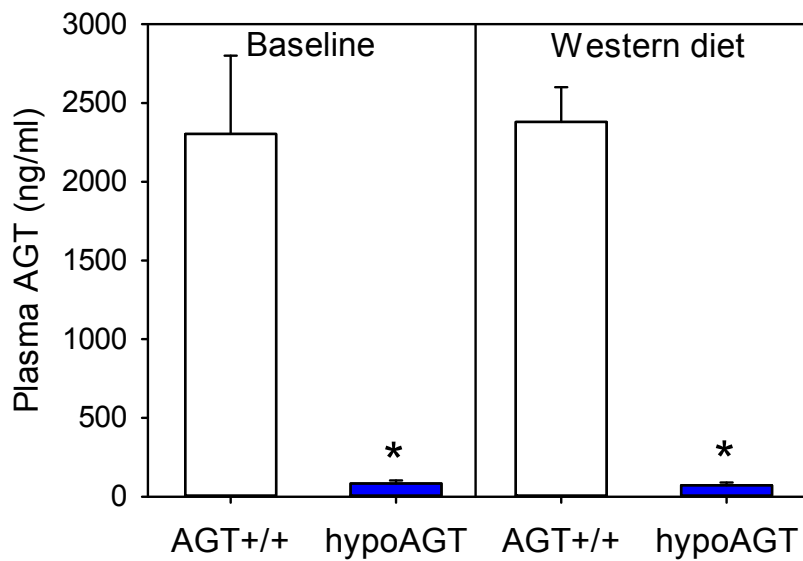


Figure 2.3 Plasma AGT concentrations were dramatically lower in hypoAGT mice.

n = 7-9 per group. All data are the mean \pm SEM. * p < 0.001 versus AGT+/+, two way ANOVA.

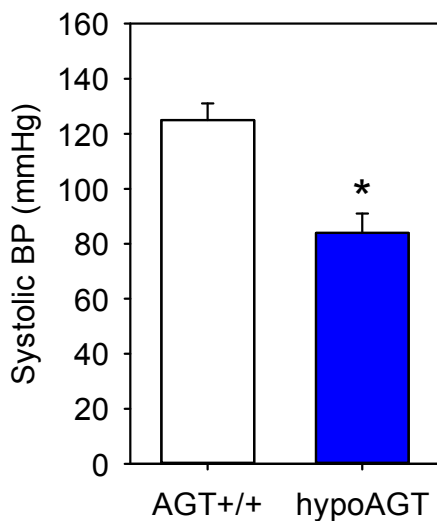


Figure 2.4 Systolic blood pressure was lower in hypoAGT mice. Mice were fed the western diet. n = 16-17 per group. All data are the mean \pm SEM. * p < 0.001, Student's *t* test.

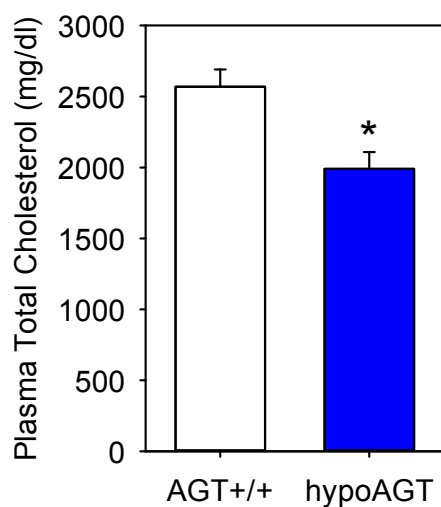


Figure 2.5 Plasma Total Cholesterol was lower in hypoAGT mice. Mice were fed the western diet for 12 weeks. n = 16-17 per group. All data are the mean \pm SEM. * p < 0.01, Student's *t* test.

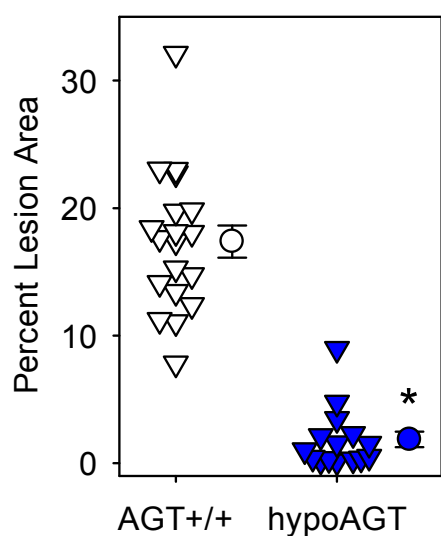


Figure 2.6 Atherosclerosis was greatly reduced in the arch of hypoAGT mice. It was quantified as percent area covered by lesions. n = 16-17 per group. Triangles represent individual mice, circles with error bars are the mean \pm SEM. * p < 0.001, Student's *t* test.

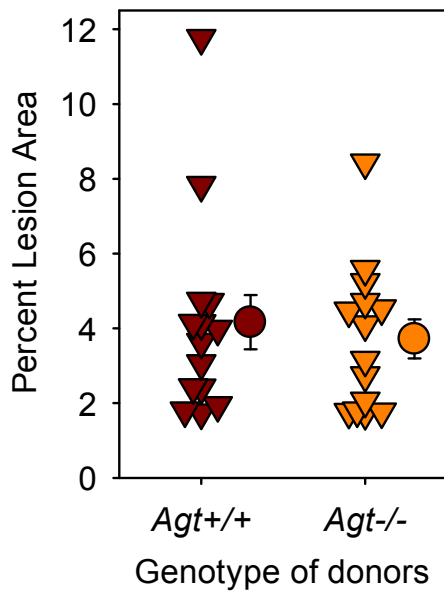


Figure 2.7 Atherosclerosis in arch of chimeric *Ldlr*^{-/-} mice repopulated with bone marrow cell from *Agt*^{+/+} or *Agt*^{-/-} mice was not different, regardless of genotype of donors. It was quantified as percent area covered by lesions. *n* = 14 per group. Triangles represent individual mice, circles with error bars are the mean ± SEM. Student's *t* test.

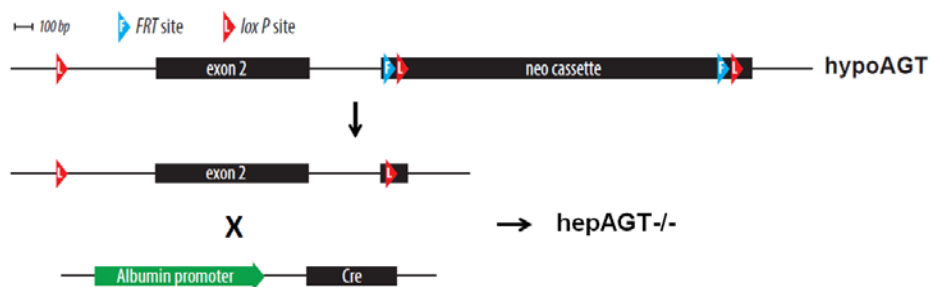


Figure 2.8 Breeding strategy of hepatocyte-specific AGT deficient mice (hepAGT^{-/-}). *Alb-cre*^{0/0} x *Agt*^{fl/fl} x *Ldlr*^{-/-} females were bred with *Alb-cre*^{1/0} x *Agt*^{fl/fl} x *Ldlr*^{-/-} males to generate hepAGT^{-/-} and their wild type littermates hepAGT^{+/+}.

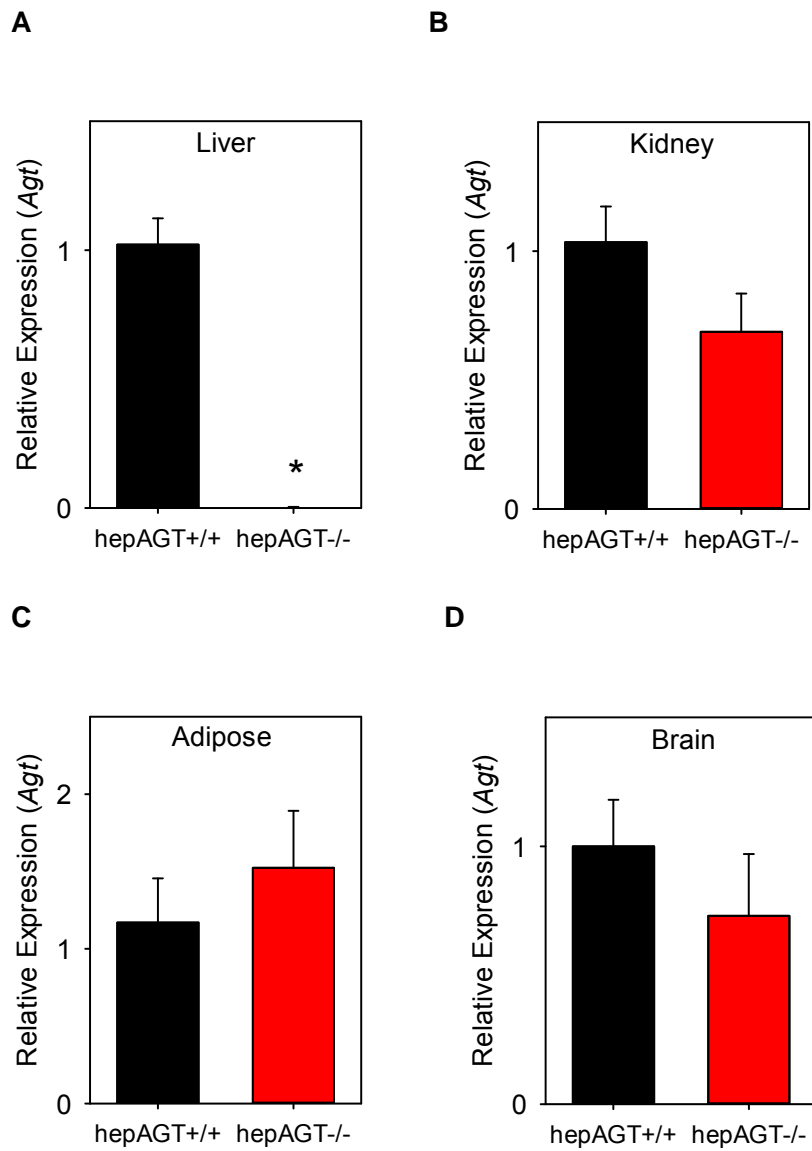


Figure 2.9 AGT mRNA abundance was specifically reduced in the liver of hepAGT-/- mice. n = 4-7 per group. All data are the mean \pm SEM. * p < 0.05, Student's *t* test.

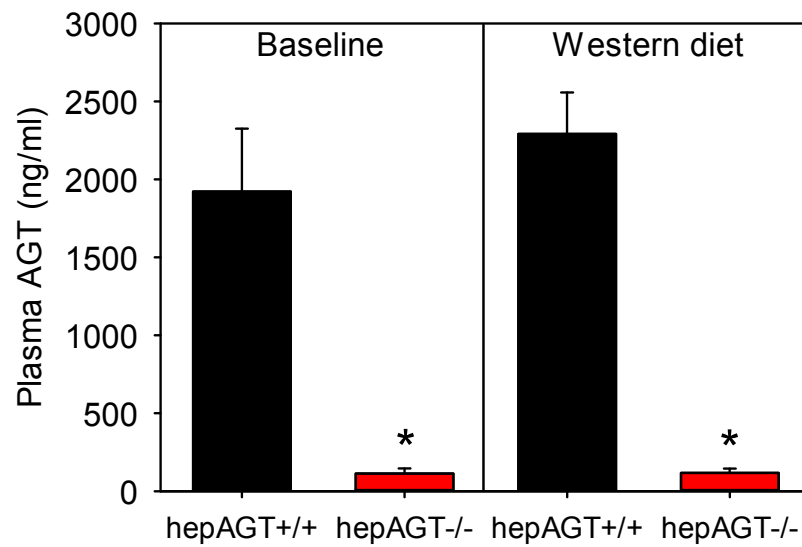


Figure 2.10 Plasma AGT concentrations were greatly reduced in hepAGT-/- mice. n = 6-7 per group. All data are the mean \pm SEM. * $p < 0.001$ versus AGT+/+, two way ANOVA.

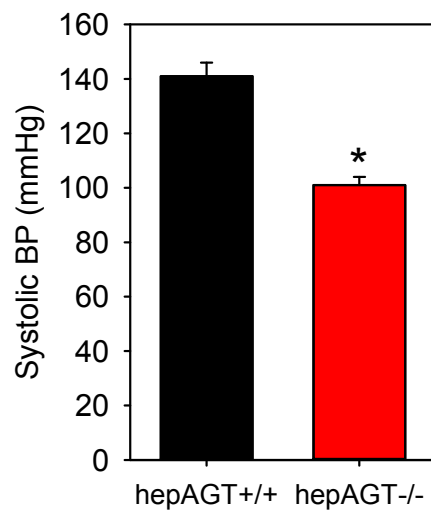


Figure 2.11 Systolic blood pressure was lower in hepAGT-/- mice. n = 10 per group.

All data are the mean \pm SEM. * $p < 0.01$, Student's *t* test.

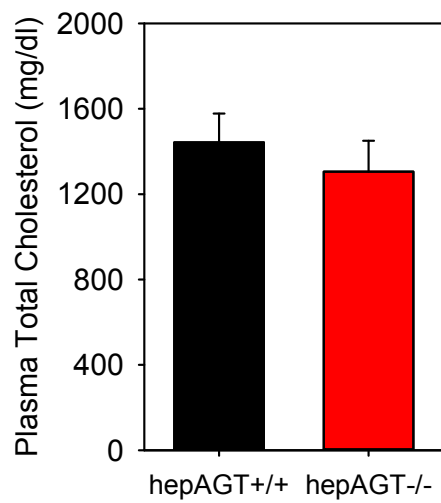


Figure 2.12 Plasma total cholesterol was not different in hepAGT^{-/-} and hepAGT^{+/+} mice. Mice were fed the western diet for 12 weeks. n = 6-7 per group. All data are the mean \pm SEM. Student's *t* test.

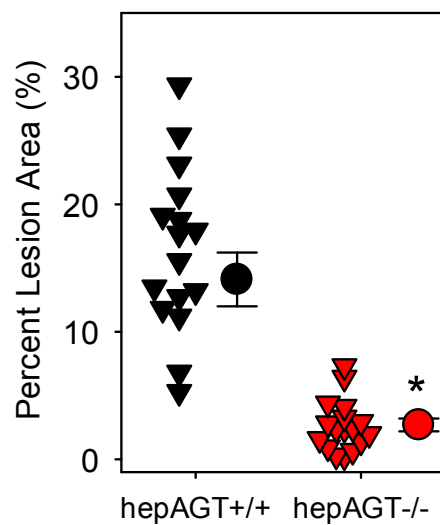


Figure 2.13 Atherosclerosis was greatly reduced in the arch of hepAGT^{-/-} mice. It was quantified as percent area covered by lesions. n = 16-18 per group. Triangles represent individual mice, circles with error bars are the mean \pm SEM. * *p* < 0.001, Student's *t* test.

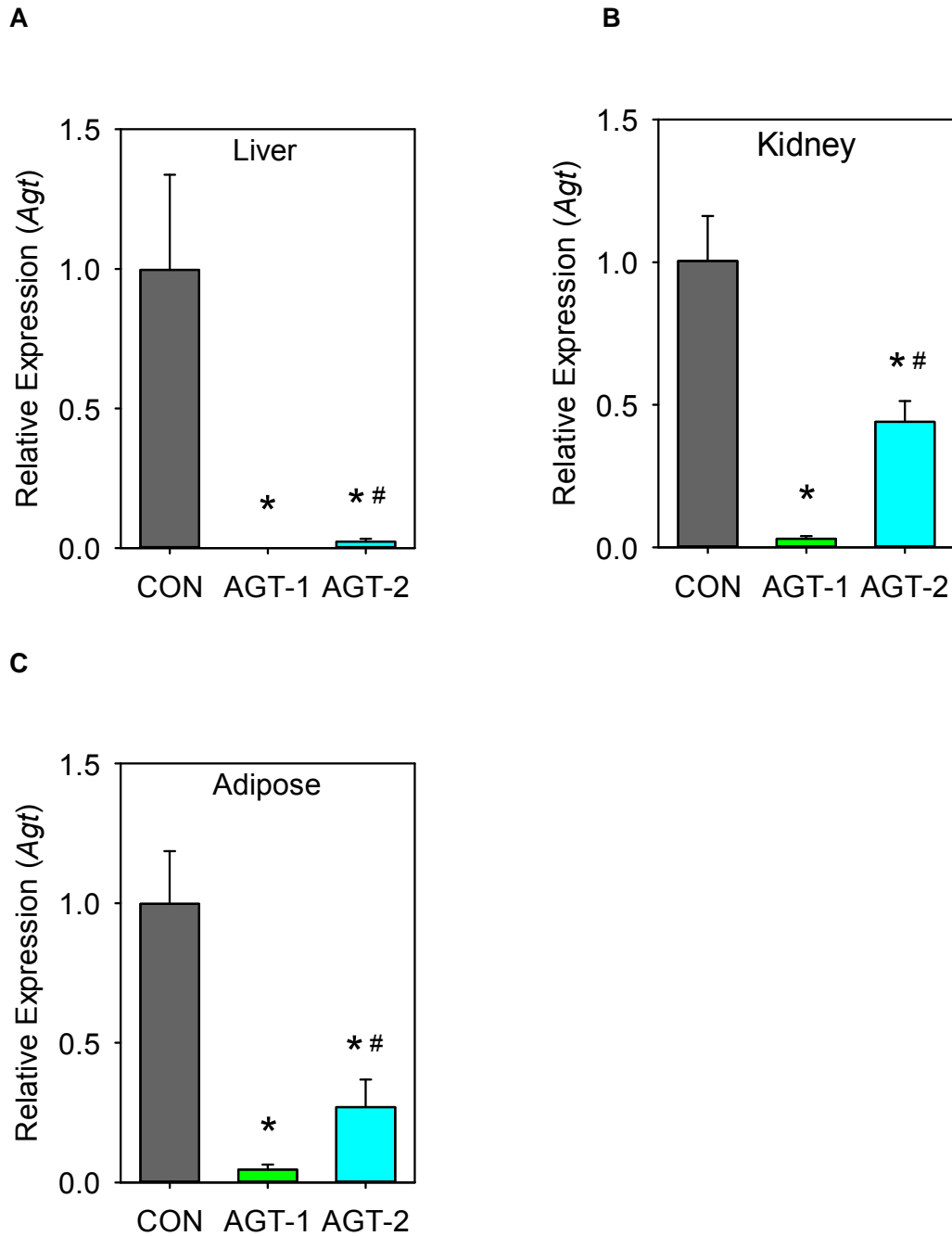


Figure 2.14 AGT mRNA abundance was greatly reduced in mice administered AGT ASO. Mice were administered control ASO (CON), AGT ASO #261333 (AGT-1), or AGT ASO #487022 (AGT-2), at a dose of 50 mg/kg. n = 5-6 per group. All data are the mean \pm SEM. * p < 0.01 versus CON, # p < 0.05 versus AGT-1, one way ANOVA.

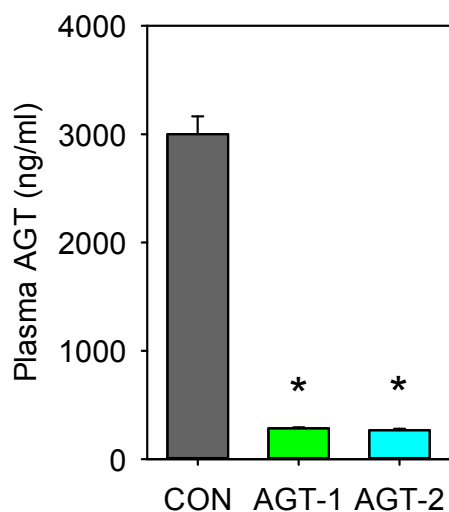


Figure 2.15 Plasma AGT concentrations were greatly reduced in Ldlr^{-/-} mice 9 weeks post initial AGT ASO injection. Mice were administered control ASO (CON), AGT ASO #261333 (AGT-1), or AGT ASO #487022 (AGT-2), at a dose of 50 mg/kg. n = 10 per group. All data are the mean \pm SEM. * $p < 0.001$ versus CON, one way ANOVA.

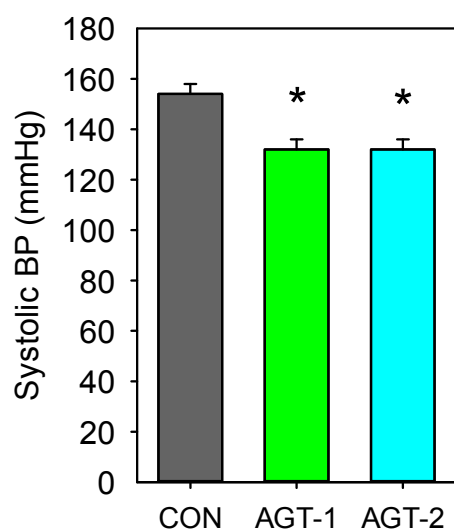


Figure 2.16 Systolic BP was lowered in Ldlr^{-/-} mice 4 weeks post initial AGT ASO injection. Mice were administered control ASO (CON), AGT ASO #261333 (AGT-1), or AGT ASO #487022 (AGT-2), at a dose of 50 mg/kg. n = 10 per group. All data are the mean \pm SEM. * $p < 0.01$ versus CON, one way ANOVA.

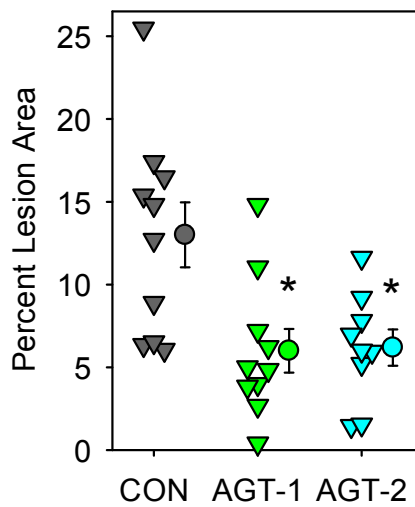


Figure 2.17 Atherosclerosis was greatly reduced in the arch of Ldlr^{-/-} mice administered AGT ASO. It was quantified as percent area covered by lesions. Mice were administered control ASO (CON), AGT ASO #261333 (AGT-1), or AGT ASO #487022 (AGT-2), at a dose of 50 mg/kg. n = 9-10 per group. Triangles represent individual mice, circles with error bars are the mean ± SEM. * p < 0.01 versus CON, one way ANOVA.

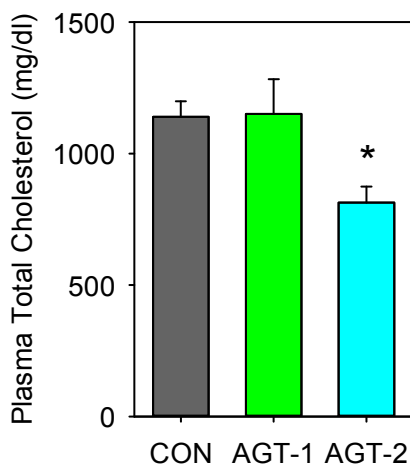
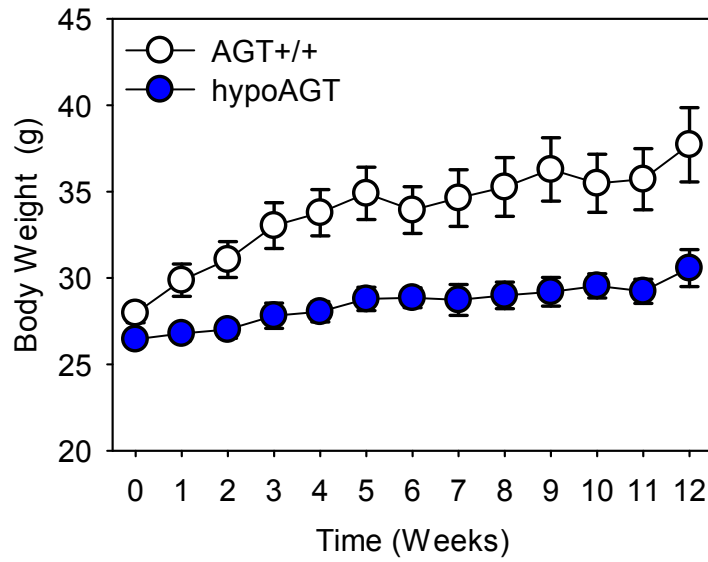


Figure 2.18 Plasma total cholesterol in Ldlr^{-/-} mice fed the western diet for 12 weeks. Mice were administered control ASO (CON), AGT ASO #261333 (AGT-1), or

AGT ASO #487022 (AGT-2), at a dose of 50 mg/kg. n = 10 per group. All data are the mean \pm SEM. * p < 0.05 versus CON, one way ANOVA.

A



B

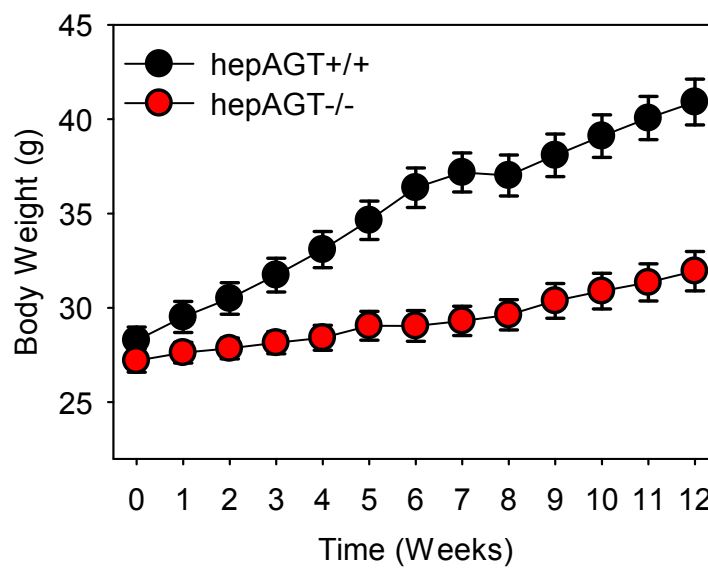
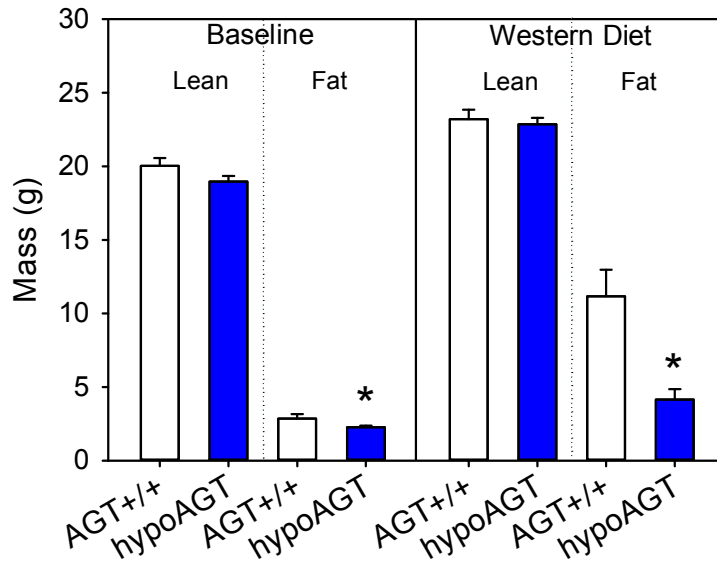


Figure 2.19 Diet-induced weight gain was suppressed in hypoAGT and hepAGT-/- mice. Mice were fed the western diet for 12 weeks. n = 10-12 per group. All data are the mean \pm SEM. $P < 0.001$ between groups, two way repeated measures ANOVA.

A



B

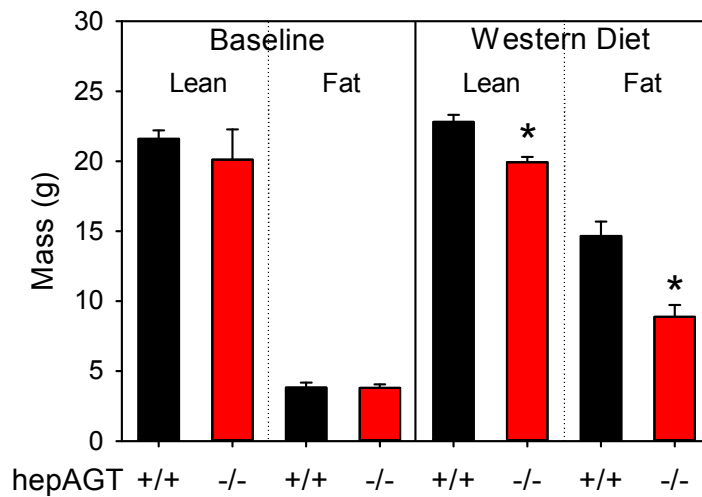


Figure 2.20 Fat mass, not lean mass, was suppressed in hypoAGT and hepAGT-/- mice. Body composition is determined by EchoMRI at week 0 (baseline) and week 12 of the western diet feeding. n = 10-12 per group. All data are the mean \pm SEM. * p < 0.01 versus wild type control, two way ANOVA.

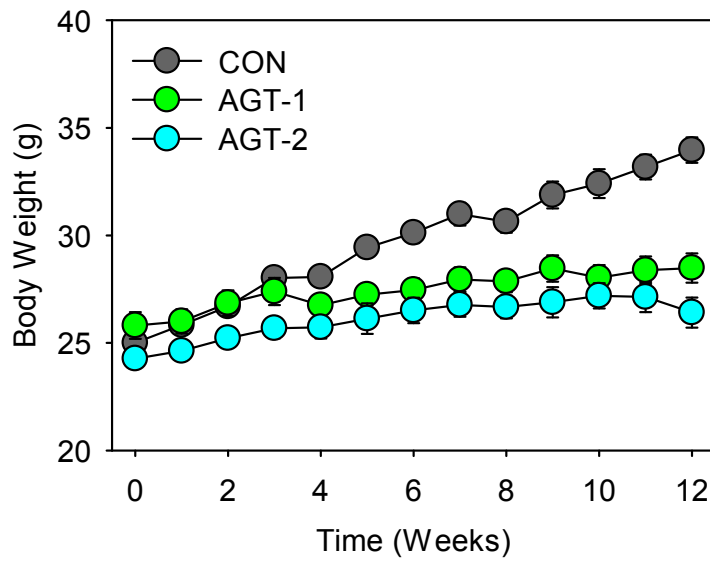
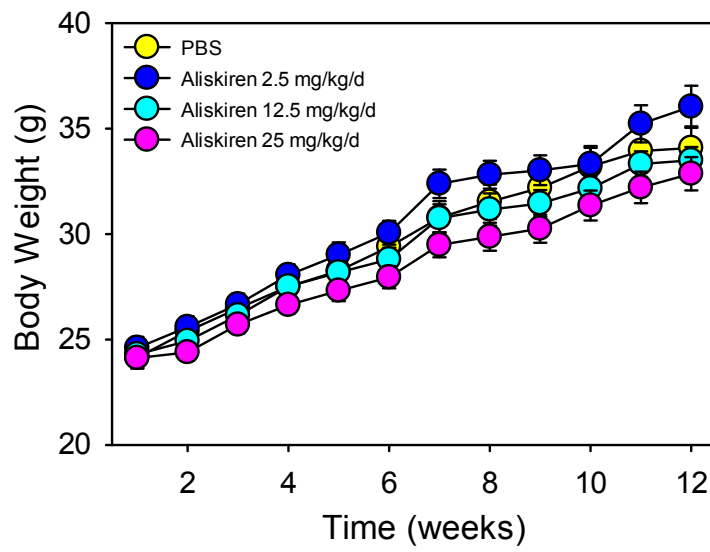
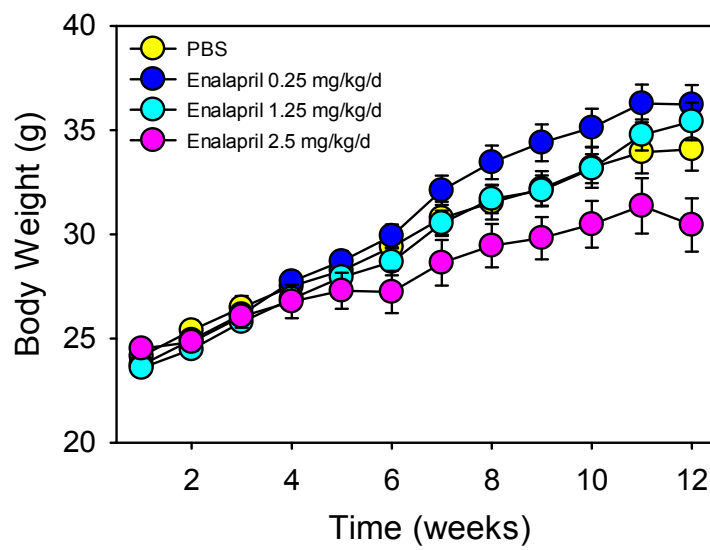


Figure 2.21 Diet-induced weight gain was suppressed in mice administered AGT ASO. Mice were administered control ASO (CON), AGT ASO #261333 (AGT-1), or AGT ASO #487022 (AGT-2), at a dose of 50 mg/kg. ASOs were injected initially one week prior to 12 weeks of the western diet feeding, and once a week until termination. n = 10 per group. All data are the mean \pm SEM. $p < 0.001$ between CON ASO and either of AGT ASO group, two way repeated measures ANOVA.

A



B



c

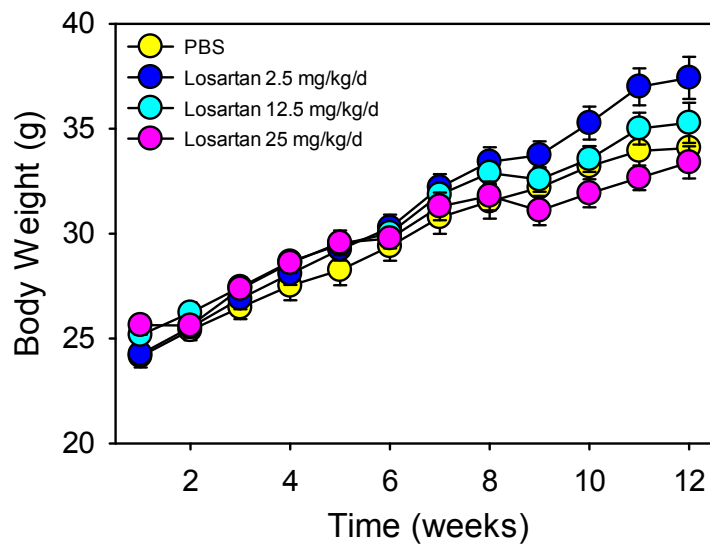


Figure 2.22 Diet-induced body weight gain was not affected in mice administered Aliskiren, Enalapril, or Losartan. Mice were fed the western diet for 12 weeks. n = 10 per group. All data are the mean \pm SEM.

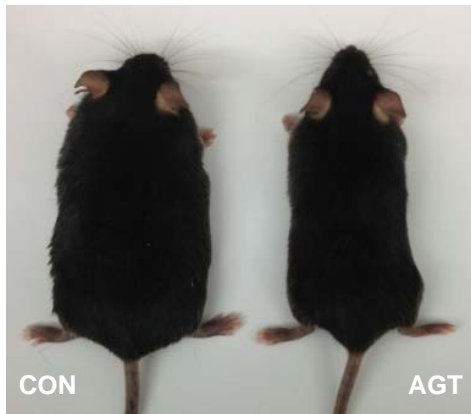


Figure 2.23 Representative images of *Ldlr*^{-/-} mice administered CON ASO (CON) or AGT ASO (AGT) fed the western diet for 12 weeks.

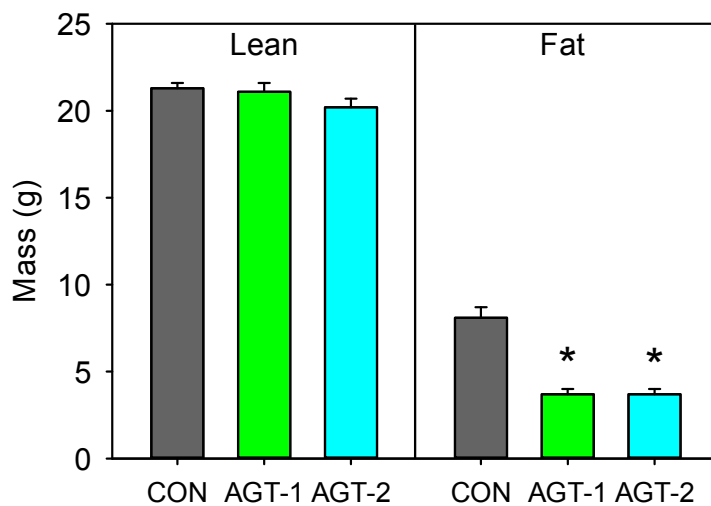


Figure 2.24 Fat mass, not lean mass, was suppressed in mice administered AGT ASO. Body composition was determined by EchoMRI post 12 weeks of the western diet feeding. Mice were administered control ASO (CON), AGT ASO #261333 (AGT-1), or AGT ASO #487022 (AGT-2), n = 10 per group. All data are the mean \pm SEM. * p < 0.01 versus CON, one way ANOVA.

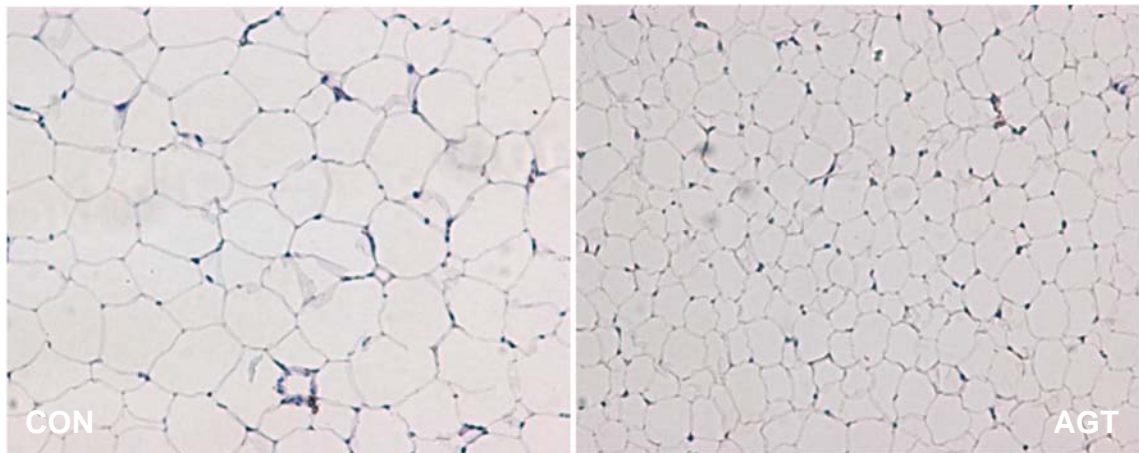


Figure 2.25 H&E staining of epididymal fat from mice administered control ASO (CON) or AGT ASO (AGT).

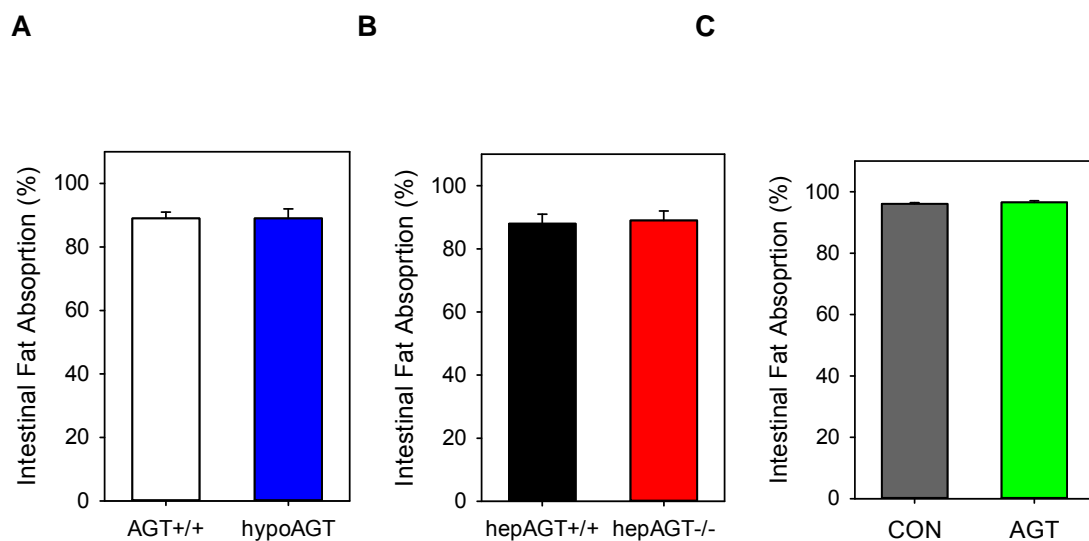


Figure 2.26 Intestinal fat absorption was not affected in hypoAGT, hepAGT^{-/-}, or AGT ASO administered mice. Mice were fed diet supplemented with 5% sucrose polybehenate. n = 6 per group. All data are the mean \pm SEM. Student's *t* test.

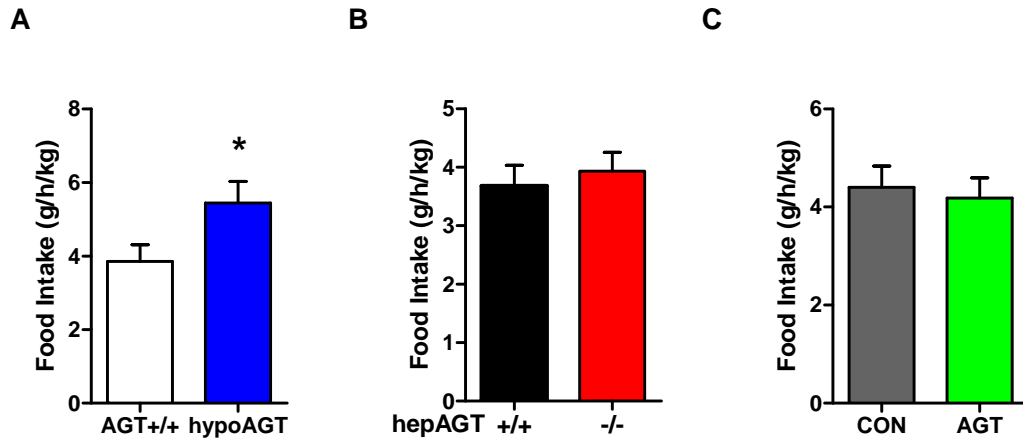


Figure 2.27 Food intake was higher in hypoAGT mice, but not different in hepAGT-/- and AGT ASO administered mice, compared with their wild type controls, respectively. Mice were fed the western diet. n = 6 per group. All data are the mean \pm SEM. * $p < 0.01$ vs AGT+/+, Student's *t* test.

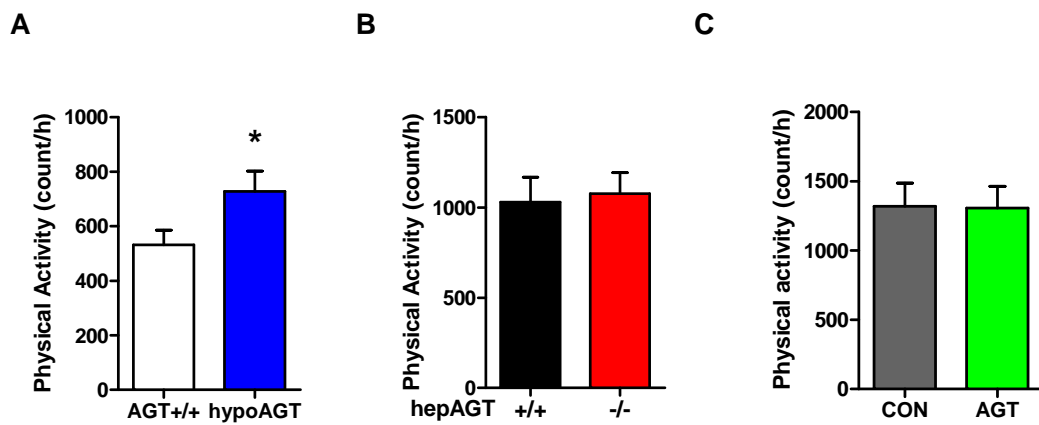
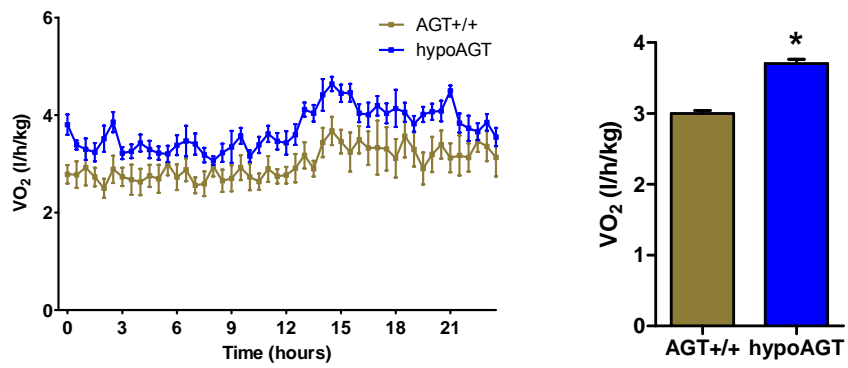
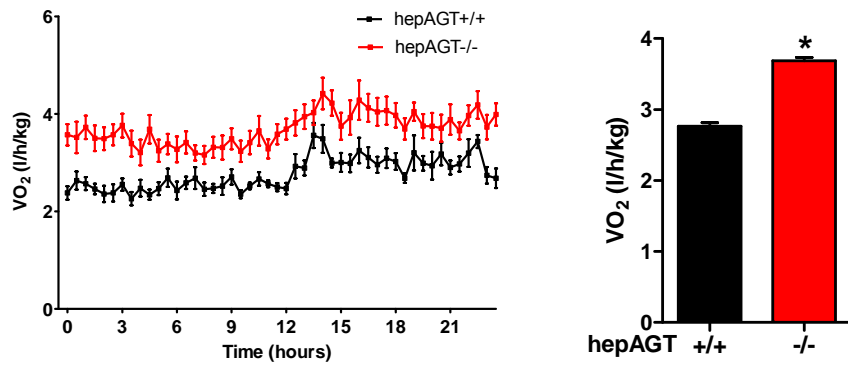


Figure 2.28 Physical activity was higher in hypoAGT mice, but not different in hepAGT-/- and AGT ASO administered mice, compared with their wild type controls, respectively. It was quantified as movement counts per hour. n = 6 per group. All data are the mean \pm SEM. * $p < 0.01$ vs AGT+/+, Student's *t* test.

A



B



C

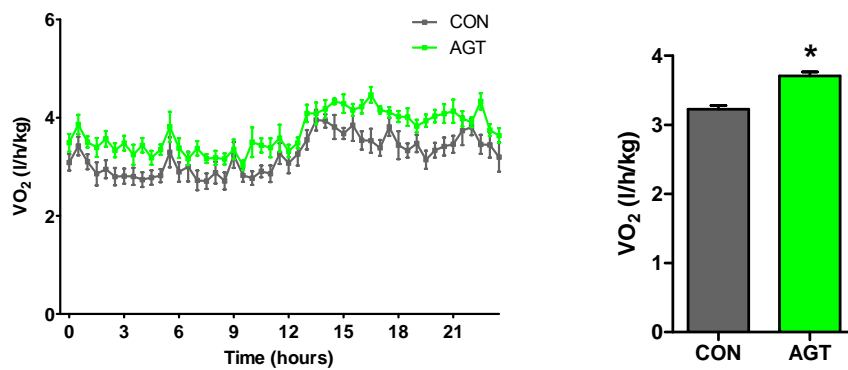
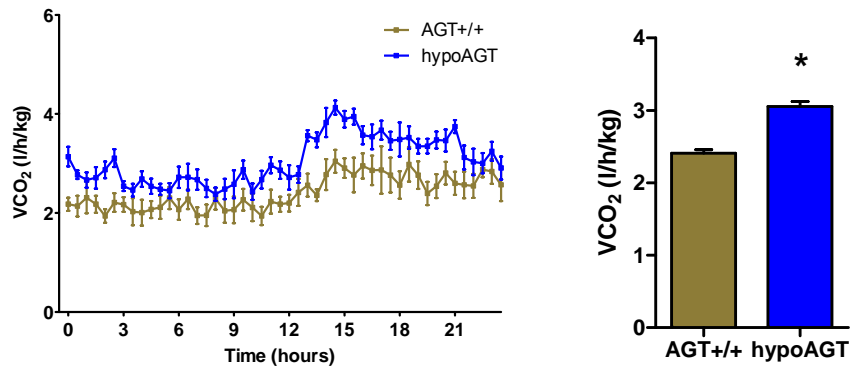


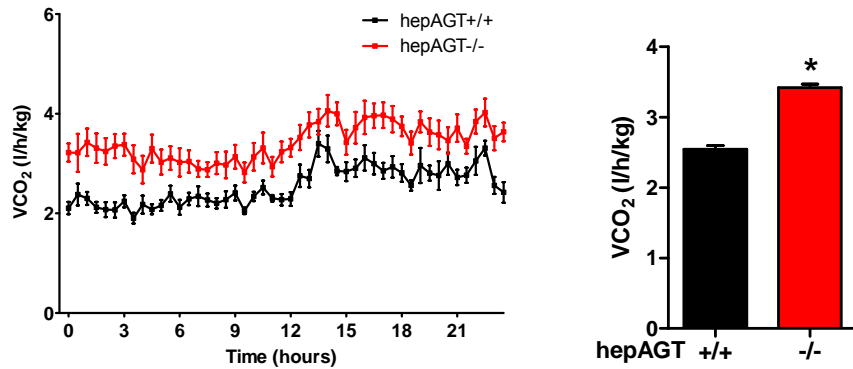
Figure 2.29 O₂ consumption, in a 24-h period, was higher in hypoAGT, hepAGT^{-/-}, and AGT ASO administered mice, compared with their wild type controls,

respectively. Mice were fed the western diet. $n = 6$ per group. All data are the mean \pm SEM. $p < 0.05$ versus CON, Student t test.

A



B



C

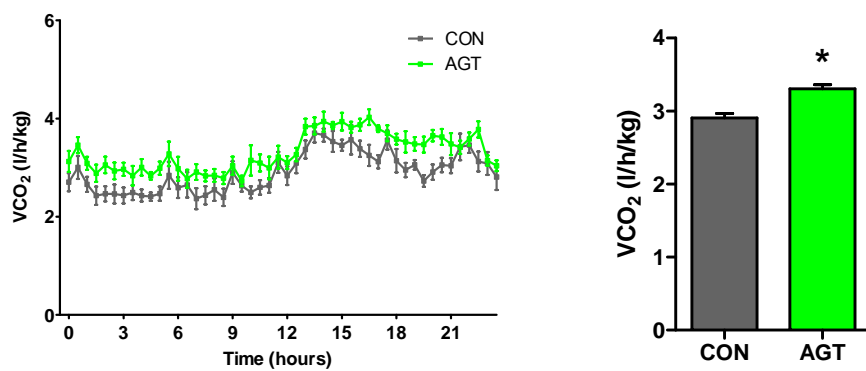


Figure 2.30 CO₂ production, in a 24-h period, was higher in hypoAGT, hepAGT^{-/-}, and AGT ASO administered mice, compared with their wild type controls,

respectively. Mice were fed the western diet. n = 6 per group. Data were collected every 30 minutes, represented as the mean \pm SEM. $p < 0.05$ versus CON, Student *t* test.

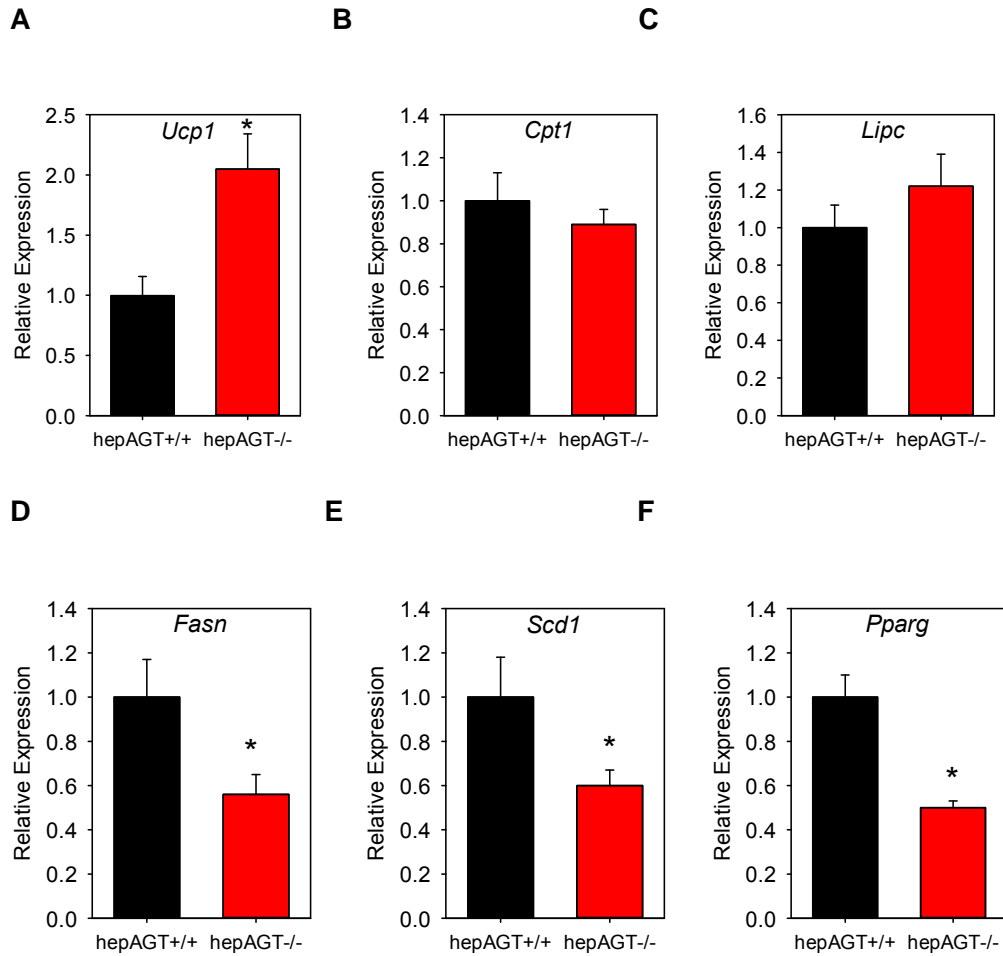


Figure 2.31 Gene expression profiling using qPCR in hepAGT^{-/-} mice and hepAGT^{+/+} mice fed the western diet for 12 weeks. Relative expression is normalized to β -actin abundance. **(A)** *Ucp1*: uncoupling protein 1 in brown adipose tissue; **(B)** *Cpt1*: carnitine palmitoyltransferase I in liver; **(C)** *Lipc*: hepatic lipase in liver; **(D)** *Fasn*: fatty acid synthase in liver; **(E)** *Scd1*: stearoyl-CoA desaturase in liver; **(F)** *Pparg*: peroxisome proliferator-activated receptor gamma in liver. n = 5 - 6 per group. All data are the mean \pm SEM. * p < 0.01 versus hepAGT^{+/+}, Student's *t* test. (Note: Mann-Whitney Rank Sum Test was used for *Pparg* data as it failed Equal Variance Test.)

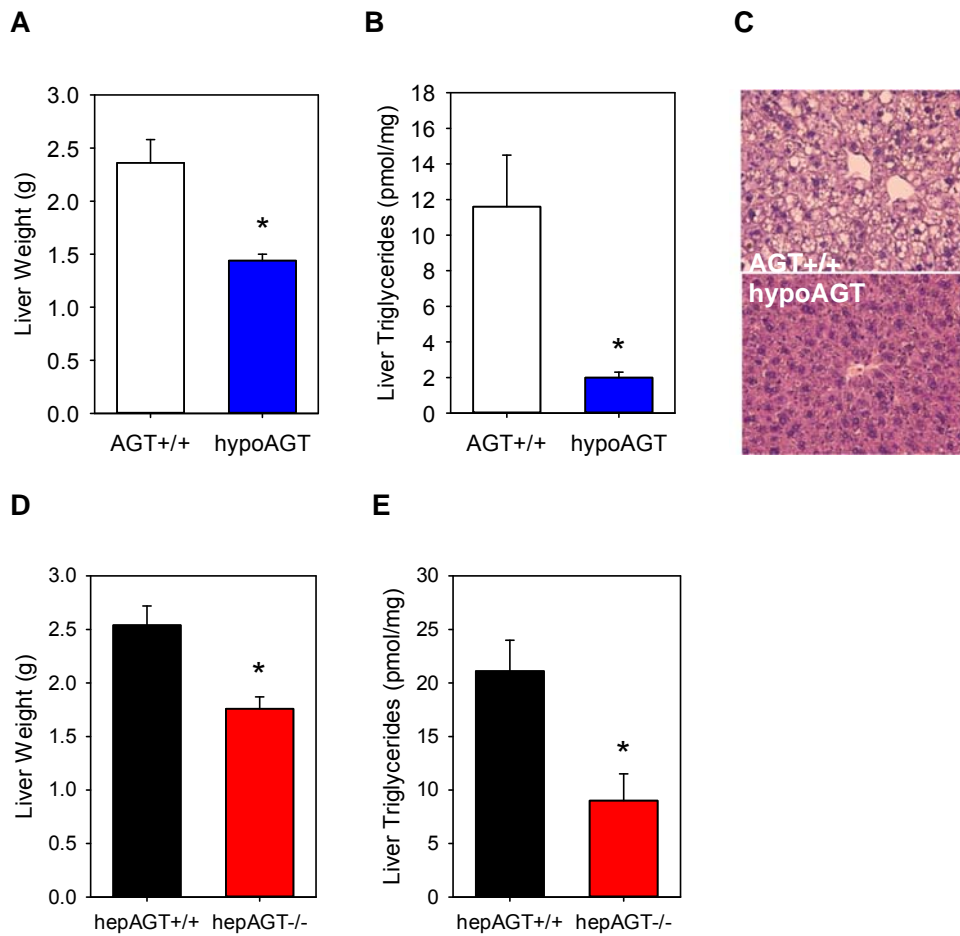


Figure 2.32 AGT inhibition protects against liver steatosis. Liver weight (**A**) and liver triglyceride (**B**) of the western diet-fed hypoAGT and AGT+/+ mice; n = 6-7 per group. All data are the mean \pm SEM. * $p < 0.01$ versus AGT+/+, Student's *t* test. (**C**) H&E staining of liver of hypoAGT and AGT+/+ mice. Liver weight (**D**) and liver triglycerides content (**E**) of the western diet-fed hepAGT-/- and hepAGT+/+ mice. n = 6-7 per group. All data are the mean \pm SEM. * $p < 0.01$ versus hepAGT+/+, Student's *t* test.

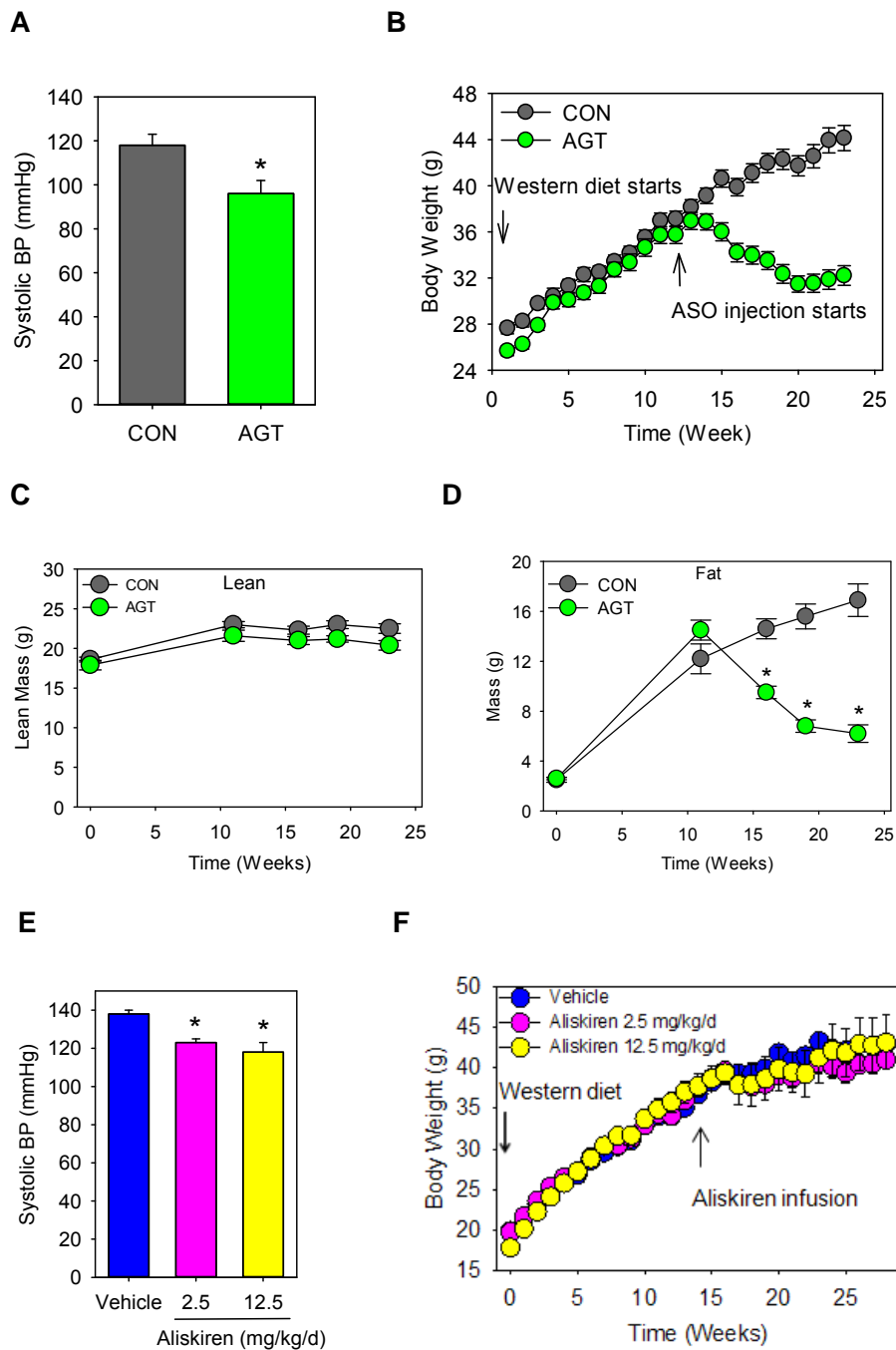


Figure 2.33 AGT ASO, but not aliskiren, regresses diet-induced obesity. Systolic blood pressure (**A**), weekly body weight (**B**), lean mass (**C**), and fat mass (**D**) of mice with established obesity administered control ASO (CON) and AGT ASO (AGT). Systolic blood pressure (**E**) and weekly body weight (**F**) of mice with established obesity

administered aliskiren and vehicle (PBS). n = 10 per group. All data are the mean \pm SEM. * $p < 0.01$ versus CON or Vehicle, Student's t test or one way ANOVA.

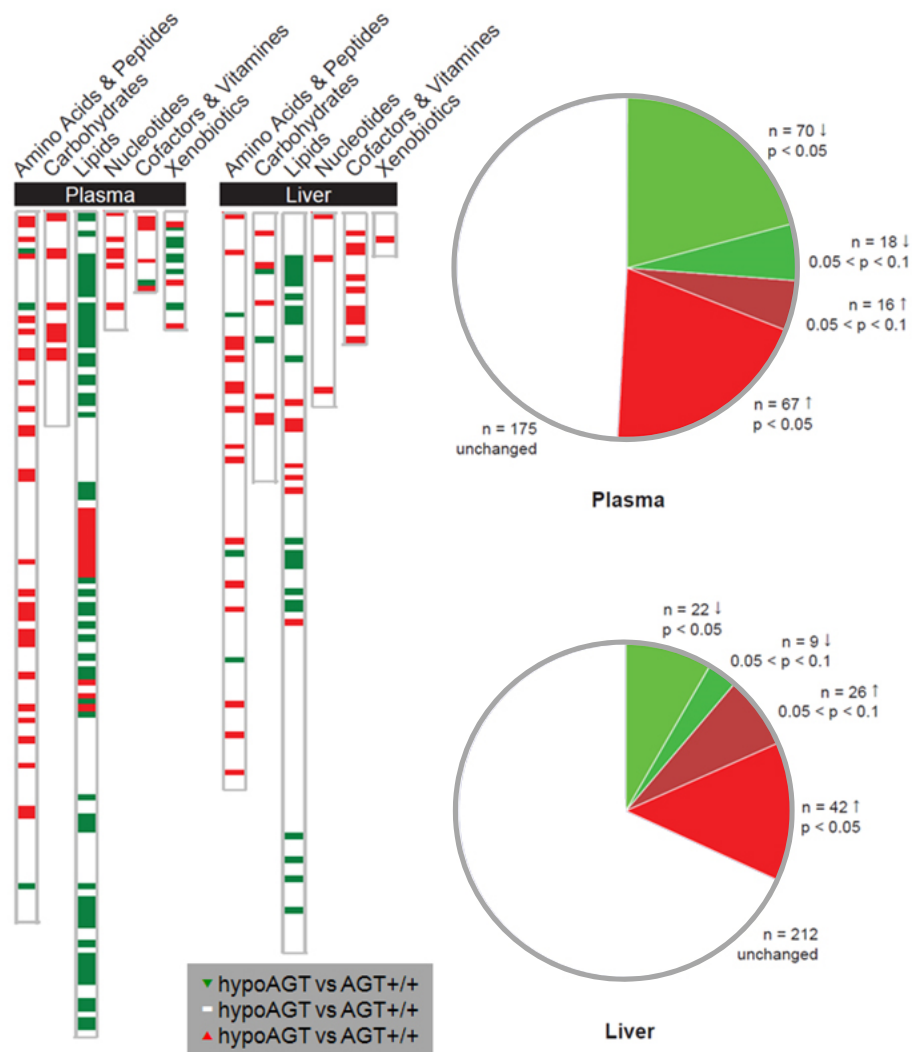


Figure 2.34 Global metabolite profiling in liver and plasma of hypoAGT mice. A

total of 311 biochemicals in liver and 336 in plasma were identified using unbiased metabolic profiling. Metabolites, represented by colored line, are grouped into six categories (left). The two pie charts break down the metabolites into up/down-regulated or unchanged with p value indicated. $n = 5/\text{group}$ for liver, $n = 9/\text{group}$ for plasma. Differences were determined using Welch's Two Sample t-test. $p \leq 0.05$ was taken as significant, $0.05 < p < 0.1$ identified biochemical approaching significance.

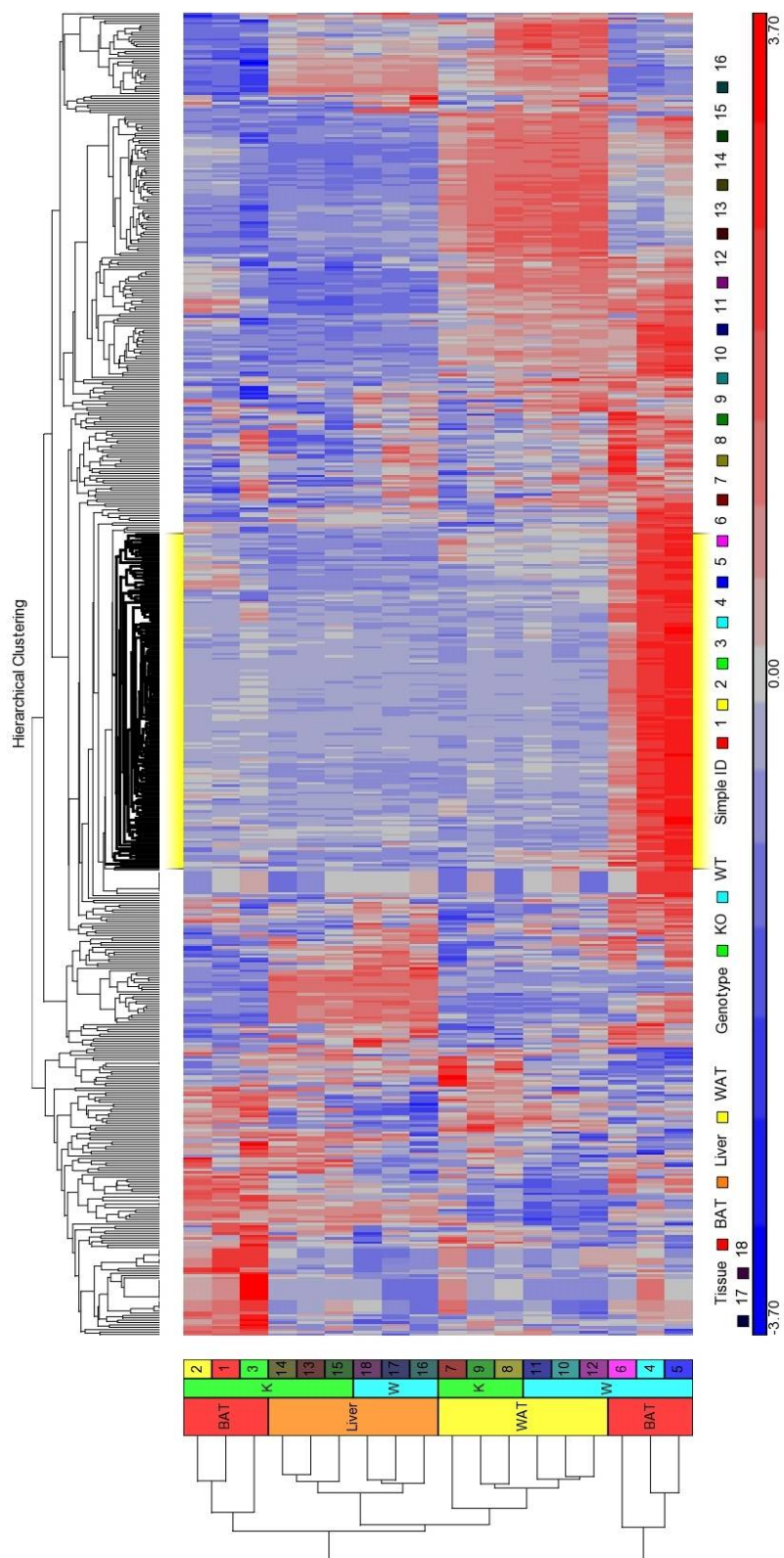


Figure 2.35 Clustered heat map of genes with 1.3 folds or larger change in expression of hepAGT^{-/-} mice. Red: upregulated, hepAGT^{-/-} vs hepAGT^{+/+}; Green: downregulated, hepAGT^{-/-} vs hepAGT^{+/+}. BAT, brown adipose tissue; WAT, white adipose tissue; W, hepAGT^{+/+}; K, hepAGT^{-/-}.

Table 2.1 Primers for gene expression profiling by qPCR.

Gene	Primer (Forward 5' - 3')	Primer (Reverse 5' - 3')	Product Size (bp)
<i>Agt</i>	CTGACCCAGTTCTTGCCAC	AACCTCTCATCGTTCCTTGG	147
<i>Actb</i>	GCCTTCCTTCTTGGGTATGG	GCACTGTGTTGGCATAGAGG	107
<i>Cpt1</i>	CGCACATTACAAGGACATGG	GAAGAGCCGAGTCATGGAAG	64
<i>Fasn</i>	TACCATGGCAACGTGACACT	GTCACACACCTGGGAGAGGT	93
<i>Lipc</i>	ACGTGGCTGCTCTTCTCCTA	AGGTGAACTTTGCTCCGAGA	64
<i>Pparg</i>	TTCAGAAAGTGCCTTGCTGTG	CCAACAGCTTCTCCTTCTCG	84
<i>Scd1</i>	TATGGATATCGCCCCTACGA	GGGAAGGTGTGGTGGTAGT	105
<i>Ucp1</i>	TCAGGATTGGCCTCTACGAC	TGCCACACCTCCAGTCATTA	110

Chapter Three: The Role of Cys18-Cys137 Disulfide Bridge in Angiotensinogen

This chapter is based on the manuscript titled “The role of angiotensinogen disulfide bridge”, submitted to Nature, with Congqing Wu as the first author. This project is supported by AHA Predoctoral Fellowship awarded to Congqing Wu.

Figures based on experiments conducted by others are listed here: figure 3.2, 3.3 from Yingchuan Xu.

Synopsis

A conserved structural feature of angiotensinogen is the disulfide bridge between Cys18 and Cys138 in humans, and Cys18 and Cys137 in mice. The formation of this disulfide bridge could trigger conformational changes in angiotensinogen, specifically the positioning of the N-terminus, which will facilitate renin cleavage of angiotensinogen between Leu10 and Val11 in the N-terminus. It was predicted that the redox-sensitive disulfide bridge might change the efficiency of angiotensinogen cleavage by renin bound to prorenin receptor to release angiotensin II, thus modulating angiotensin II-dependent functions. To directly test this prediction *in vivo*, we determined effects of the presence and absence of this disulfide bridge on angiotensin II concentrations and responses in mice expressing either native angiotensinogen or Cys18Ser, Cys137Ser mutated angiotensinogen in liver. Contrary to the prediction, disruption of Cys18-Cys137 disulfide bridge in angiotensinogen had no discernible effects on angiotensin II production and angiotensin II-dependent functions in mice.

Introduction

As the only precursor to all angiotensin peptides, angiotensinogen (AGT) is secreted from hepatocytes into the circulation as a mature protein of 452 amino acids (3, 107). It is well recognized that renin is the major enzyme that cleaves off the first 10 amino acids from the N-terminus of AGT to release angiotensin (Ang) I. Ang I is subsequently cleaved by angiotensin-converting enzyme (ACE) to form the major bioactive peptide of the renin-angiotensin system (RAS), AngII. Cleavage of AGT by renin is the rate-limiting step in producing AngII, implicating that the efficiency of AGT cleavage determines the rate of AngII production, and consequently influences AngII-related physiological and pathophysiological effects.

Since its discovery in 1939, plasma AGT has been viewed as a passive substrate reservoir for all angiotensin peptides. No regulatory role of AGT has been tested experimentally until its crystal structure was solved in 2010 (11). Zhou and colleagues resolved AGT structure to 2.1 Å resolution using a recombinant non-glycosylated form of the protein (11). It was predicted that AGT was secreted in an oxidized form containing a disulfide bridge between Cys18 and Cys138 in humans, and Cys18 and Cys137 in mice (3, 5, 11). It was also proposed that this disulfide bridge could constrain the N-terminus of AGT in a manner that facilitated its cleavage by renin (10, 11). In addition, the disulfide bridge formed in the secreted protein was labile, and its reduction by a proposed plasma thiol-reductase system led to decreased access to the renin cleavage site. Therefore, it was speculated that the reduced form of AGT was a less efficient substrate for renin. The regulatory role of the disulfide bridge in AGT was supported by a correlation of increased ratio of oxidized versus reduced forms of AGT in pregnant women with preeclampsia compared with normotensive pregnant women. Overall, this

model predicted that AngII-dependent responses could be regulated by the presence of a disulfide bridge between Cys18 and Cys138.

Adeno-associated virus (AAV) is nonpathogenic, with a single-stranded DNA genome. Its ability to infect both nondividing and dividing cells, long-term expression *in vivo*, and low immunogenicity makes AAV vectors one of the most promising viral vectors for gene therapy in humans (127). AAV2 is the first fully cloned and the most widely used AAV serotype. While AAV2 delivers persistent transgene expression, its expression levels are very low (128). This has led to development of vectors derived from novel AAV serotypes such as AAV 7, 8, and 9 (129, 130). Studies have demonstrated the importance of the serotype-specific capsid in transduction efficiency (131-133). Hybrid vectors like AAV2/8 (AAV2 rep gene fused with AAV8 cap gene) with tissue-specific promoters used in this study have been shown to direct robust and stable transgene expression in liver (130, 134).

In the present study, we investigated the functional consequences of disrupting the disulfide bridge in AGT in blood pressure and atherosclerosis, as AngII regulates blood pressure and promotes atherosclerosis (21, 50, 56, 83, 84, 135). We developed hepatocyte-specific AGT deficient mice (hepAGT^{-/-}) in which plasma AGT concentrations were severely depleted. AAV vectors were injected to replenish, in a hepatocyte-specific manner, either native AGT or mutated AGT (Cys18Ser, Cys137Ser) that were unable to form the disulfide bridge.

Methods

Ethics statement

All animal experiments reported in this part were performed with approval of the University of Kentucky Institutional Animal Care and Use Committee (University of Kentucky IACUC protocol number: 2006-0009).

Mouse housing conditions and diets

All mice were maintained in individually vented cages (maximally 5 mice per cage) in a barrier facility (14:10 hour light-dark cycles, ambient temperature of 22°C). Cage bedding was Teklad Sani-Chip bedding (Cat # 7090A, Harlan Teklad, Madison, WI). Mice were fed a normal rodent laboratory diet (Diet # 2918, Harlan Teklad, Madison, WI) and provided with drinking water ad libitum from a reverse osmosis system. Two weeks after AAV injections, all mice were fed a saturated fat-enriched diet (milk fat 21% wt/wt; Diet # TD.88137, Harlan Teklad, Madison, WI) for 12 weeks. This diet was developed in 1988 by collaboration between Harlan Teklad and Rockefeller University to mimic the nutrient composition of typical foods from western food chains (111). It is referred to as western diet.

Development of hepatocyte-specific AGT deficient mice

A targeting construct with loxP sites flanking exon 2 of AGT followed by a neo cassette was transfected into embryonic stem cells from a 129 mouse strain. After selection, positive cells were injected into blastocysts of C57BL/6 mice. The following breeding was maintained in a C57BL/6 background until homozygous AGT floxed mice were obtained, as previous described (34, 112). The breeding strategy to develop mice with hepatocyte-specific deficiency of AGT included 4 steps: (1) AGT floxed mice were bred

to FLPe mice (B6;SJL-Tg(ACTFLPe)9205Dym/J, Stock # 003800, N2 to C57BL/6 strain, The Jackson Laboratory, Bar Harbor, ME) to remove the neo cassette insertion in intron 2 of mouse AGT gene. (2) After removal of the neo cassette, these mice were bred to LDL receptor^{-/-} mice (B6.129S7-Ldlrtm1Her/J, Stock # 002207, N13 to C57BL/6 strain, The Jackson Laboratory) to generate *Agt^{ff} x Ldlr^{-/-}* mice. (3) Male mice expressing Cre recombinase under the control of a hepatocyte-specific albumin promoter (B6.Cg-Tg(Alb-cre)21Mgn/J, Stock # 003574, N7 to C57BL/6 strain, The Jackson laboratory) were bred to female *Ldlr^{-/-}* mice to generate male *Alb-cre^{1/0}* mice in the LDL receptor^{-/-} background. (4) *Alb-cre^{0/0} x Agt^{ff} x Ldlr^{-/-}* females were bred with *Alb-cre^{1/0} x Agt^{ff} x Ldlr^{-/-}* males to generate hepatocyte-specific AGT deficient mice hepAGT^{-/-}, and their wild type littermates hepAGT^{+/+}.

Production and injection of AAV vectors

AAV vectors (serotype 2/8) driven by a hepatocyte-specific thyroxine-binding globulin (TBG) promoter were produced by the Viral Vector Core at the University of Pennsylvania (Philadelphia, PA). These AAV vectors contained cDNA inserts encoding mouse native AGT or AGT with mutations at Cys18 and Cys137 (the two cysteines were replaced by two serines). AAV vector with null insertion (null AAV) was used as control.

All AAV vectors were diluted in PBS (1 x 10¹⁰ or 3 x 10¹⁰ genome copies/200 µl per mouse) and injected intraperitoneally into study mice.

Systolic blood pressure measurements

Systolic blood pressure was measured on conscious mice using a non-invasive tail-cuff system (Kent Scientific Corporation, Torrington, CT) following a standardized protocol described previously (119).

Measurement of plasma components

Blood samples were collected with EDTA (final concentration at 1.8 mg/ml) and centrifuged at 400 g for 20 minutes, 4 °C to separate plasma. Before termination, blood samples were collected using submandibular bleeding on conscious mice. At termination, blood samples were collected using right ventricular puncture after anesthesia (a mixture of ketamine 100 mg/kg and xylazine 10 mg/kg).

Plasma AGT concentrations were determined using an ELISA kit (Code # 27413, Immuno-Biological Laboratories Co., Ltd, Takasaki-Shi, Gunma, Japan) (55).

Plasma renin concentrations were measured by quantifying AngI generated in mouse plasma. In brief, plasma samples (8 µl) harvested with EDTA were incubated in an assay buffer (Na₂HPO₄ 0.1 M, EDTA 0.02 M, maleate buffer pH 6.5, phenylmethyl-sulfonyl fluoride 2 µl; total volume of 250 µl) with an excess of rat AGT at 37 °C for 30 minutes. Rat AGT was obtained through partial purification of nephrectomized rat plasma. This reaction was terminated by placing samples at 100 °C for 5 minutes. AngI generated in each sample was quantified by radioimmunoassay using a commercially available kit (Cat # 1553; DiaSorin, Stillwater, MN).

For plasma AngII concentrations, aprotinin (0.6 TIU per 1 ml of blood; Cat # RK-APRO, Phoenix Pharmaceuticals, Inc., CA) was added to blood samples before centrifugation. After extraction of plasma samples using Sep-Pak C18 classic cartridges (Cat # WAT051910; Waters Corp., Milford, MA), AngII concentrations were measured using radioimmunoassay. The antibody used for this assay was a rabbit anti-AngII antibody (Cat # T-4005; Bachem, Torrance, CA) as described previously (136).

Plasma total cholesterol concentrations were measured using an enzymatic kit (Cat # 439-17501; Wako Chemicals USA, Richmond, VA).

Western blotting of oxidized versus reduced forms of mouse AGT

To determine the abundance of oxidized versus reduced form of AGT in mouse plasma, plasma samples were incubated with methoxypolyethylene glycolmaleimide (mPEG; Product # 63187; Sigma-Aldrich, St. Louis, MO) as described by Zhou et al (11). Briefly, mouse plasma samples (5 μ l) were incubated with mPEG (10 μ l of 20 mM) in reaction buffer (5 μ l, 100 mM Tris-HCl with pH 8.0, 5 mM EDTA, and 0.15 M NaCl) at 37 °C for 3 hours. Subsequently, reducing loading buffer (Cat # 39000; Thermo Scientific, Rockford, IL) was added to each sample, and samples were heated at 98 °C for 5 minutes.

Proteins (0.1 μ l of plasma) were resolved by SDS-polyacrylamide gel electrophoresis, and transferred to PVDF membranes (Cat # IPVH09120; EMD Millipore, Billerica, MA). After blocking in fat-free milk buffer (5% wt/vol), membranes containing transferred proteins from mouse plasma were incubated with a chicken anti-mouse AGT antibody (1 μ g/ml; 1 hour at room temperature) developed by Aves Labs (Tigard, OR). The specificity of this antibody to mouse AGT was confirmed by the absence of an immunoreactive band in plasma of AGT deficient mice. The secondary antibody was HRP-conjugated rabbit anti-chicken IgY (Cat # 303-035-003; Jackson ImmunoResearch Laboratories, Inc., West Grove, PA) incubated with membranes at a concentration of 0.5 μ g/ml for 1 hour at room temperature. Immunoreactive bands were visualized by exposing membranes on a Kodak Image Station 4000R Pro after incubation with chemiluminescent substrate (Cat # 34080; Thermo Scientific, Rockford, IL).

Quantification of atherosclerosis

Atherosclerosis was quantified on the intima of the ascending region, aortic arch and 3 mm of the descending region using an *en face* method with ImagePro software as described previously (117, 118).

Statistical analysis

Data are represented as means \pm standard error of means (SEM). SigmaPlot version 12.0 (SYSTAT Software Inc., Chicago, IL) was used for statistical analyses. To compare multiple-group data, one way ANOVA was used for normally distributed variables and Kruskal-Wallis one way ANOVA on Ranks was used for non-normally distributed variables. Post-hoc analysis for these two analyses were Holm-Sidak method and Dunn's method, respectively, except for plasma renin concentrations in which post-hoc analysis used Tukey-Kramer adjustment. Plasma AGT concentrations (after square root transformation) were compared using two way repeated measures ANOVA and Holm-Sidak post-hoc method. $P < 0.05$ was considered statistically significant.

Results

AAV expression of native AGT raised plasma AGT concentrations in a dose-dependent manner

To determine the optimal dosage of AAV vector that replenishes plasma AGT in hepatocyte-specific AGT deficient mice (hepAGT^{-/-}) mice, we evaluated two doses of AGT AAV at 3×10^{10} (high dose) and 1×10^{10} (low dose) genome copies per mouse, respectively. AGT AAV was constructed with insertion of native mouse AGT gene. AAV with null insertion was included as control. AAV transgene expression was driven by hepatocyte-specific thyroxine-binding globulin (TBG) promoter.

While hepAGT^{+/+} mice were infected with no AAV (PBS injection) or null AAV, hepAGT^{-/-} mice were infected with low dose or high dose of AGT AAV, or null AAV, by intraperitoneal injection. Plasma samples were collected through submandibular

bleeding on week 2, 4, 8, and 16 after AAV injection. Plasma AGT concentrations in hepAGT^{-/-} mice receiving AGT AAV were elevated in a dose-dependent manner, and peaked between weeks 2 and 4, then declined modestly afterwards (Figure 3.1). HepAGT^{-/-} mice receiving high dose of AGT AAV vectors had plasma AGT concentrations comparable to that of hepAGT^{+/+} mice during the 16 weeks post AAV injection (Figure 3.1). On the basis of this observation, we administered AAV vectors at 3×10^{10} genome copies per mouse in the following studies.

AAV expression of native or mutated (C18S, C137S) AGT restored plasma AGT concentrations

To investigate functional consequences of disrupting the C18-C137 disulfide bridge, we compared native AGT and mutated (C18S, C137S) AGT in hepAGT^{-/-} mice via AAV expression of native or mutated (C18S, C137S) AGT. To achieve this, hepAGT^{-/-} mice were infected with null AAV, native AGT AAV, or mutated (C18S, C137S) AGT AAV. As a control, hepAGT^{+/+} mice were infected with null AAV.

To evaluate expression efficiency and stability of AAV vectors, we measured plasma AGT concentrations prior to AAV injection and 2, 6, 10, and 14 weeks after AAV injection. At baseline, all hepAGT^{-/-} mice lacking AGT expression in hepatocytes had barely detectable plasma AGT concentrations. The low plasma AGT concentrations remained unchanged in hepAGT^{-/-} mice receiving AAV vector containing the null insert (Figure 3.2). Plasma AGT concentrations in hepAGT^{-/-} mice receiving AAV vector expressing either wild-type or mutated AGT peaked 2 weeks post-injection and remained at concentrations comparable to hepAGT^{+/+} littermates from 6 to 14 weeks after AAV injections. There was no difference in plasma AGT concentrations among all groups at later intervals except for hepAGT^{-/-} administered AAV vector containing a null

insert (Figure 3.2).

Predominance of oxidized AGT in mouse plasma

To determine the ratio of oxidized AGT versus reduced AGT in mouse plasma, we developed western blotting using in-house chicken antibody against mouse AGT. Antibody specificity was demonstrated by a single distinctive band with molecular weight of ~50 kDa in hepAGT^{+/+} mouse plasma and absence of a discernible band in hepAGT^{-/-} mouse plasma (Figure 3.3A). Incubation of plasma with methoxypoly-ethylene glycol maleimide (mPEG) increased the molecular weight of AGT from hepAGT^{+/+} mouse plasma by 10 kDa (Figure 3.3A). This was consistent with mPEG interacting with the two cysteines at positions 300 and 316 on the non-renin interacting face, but being unable to interact with two cysteines at position 18 and 137 due to disulfide linkage. These findings demonstrated that oxidized AGT was predominant in mouse plasma.

To profile oxidized AGT and reduced AGT in mouse plasma replenished by AAV vectors, two weeks post AAV injection, plasma was collected from all groups and incubated with mPEG prior to Western blotting. A single band of AGT was detected in hepAGT^{+/+} mouse plasma that was shifted 10 kDa from native AGT. Western blotting of plasma AGT failed to detect any immunoreactive band in hepAGT^{-/-} mice administered AAV containing a null insert. In contrast, a 60 kDa immunoreactive band was clearly detected in each mouse repopulated with native AGT, demonstrating that AAV derived wild-type AGT was completely oxidized (Figure 3.3B). As expected, plasma in mice replenished with mutated (C18S, C137S) AGT showed a 60 kDa band due to interaction of mPEG with the remaining 2 cysteine residues, position 300 and 316 (Figure 3.3B). Overall, these data demonstrated that the experimental design enabled comparisons of AGT in forms that were either completely disulfide bridged or completely lacking the

disulfide bridge.

Replenishment of native versus mutated AGT had equivalent effects on plasma renin and AngII concentrations

Plasma renin concentrations were significantly increased (Figure 3.4) in hepAGT^{-/-} mice receiving null AAV vector due to diminished negative feedback (137), imposed by low plasma AngII concentrations (Figure 3.5), compared with hepAGT^{+/+} mice receiving null AAV vector (Figure 3.4). HepAGT^{-/-} mice replenished with native AGT showed no differences in plasma renin and AngII concentrations from hepAGT^{+/+} littermates. However, in contrast to the prediction of structural modeling (11), plasma renin and AngII concentrations in hepAGT^{-/-} mice administered mutated AGT AAV were not significantly different from those in hepAGT^{-/-} mice administered AAV expressing native AGT (Figure 3.4,3.5).

Replenishment of native versus mutated AGT had equivalent effects on systolic blood pressure and atherosclerosis

Consistent with low plasma AngII concentrations in hepAGT^{-/-} mice, administration of AAV containing a null vector did not change the low systolic blood pressure in hepAGT^{-/-} mice (Figure 3.6). Administration of AAV vectors containing either native or mutated AGT increased systolic blood pressure in hepAGT^{-/-} mice to levels indistinguishable from hepAGT^{+/+} littermates. However, systolic blood pressure was not significantly different between mice expressing native and mutated AGT (Figure 3.6).

LDL receptor^{-/-} mice develop profound hypercholesterolemia-induced atherosclerotic lesions in the aortic arch region after 12 weeks of western diet feeding (50, 56, 115). In this study, mice in these 4 groups all developed hypercholesterolemia (Figure 3.7).

HepAGT^{-/-} mice administered null AAV had significantly smaller lesions, compared with hepAGT^{+/+} littermates, as measured by percent lesion area in the aortic arch region. In contrast, hepAGT^{-/-} mice receiving either native or mutated AGT developed pronounced atherosclerotic lesions, and the percent lesion areas were not different between these two groups, as well as compared with hepAGT^{+/+} mice (Figure 3.8).

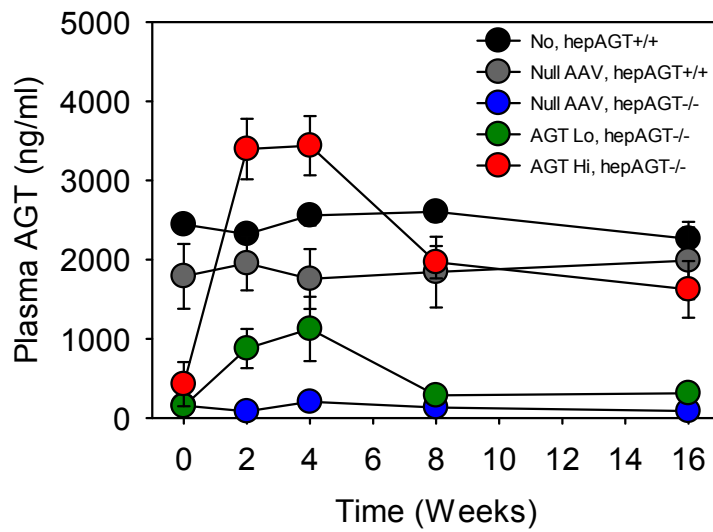


Figure 3.1 Plasma AGT concentrations were restored by AAV-mediated AGT expression at a dose-dependent manner. It was measured using an ELISA kit at week 0, 2, 4, 8, and 16 weeks after AAV injection. No, no AAV; Nu, null AAV; Lo, low dose of AGT AAV; Hi, high dose of AGT AAV. WT, hepAGT+/+; KO, hepAGT-/-. n = 4-6. Two way repeated measures ANOVA.

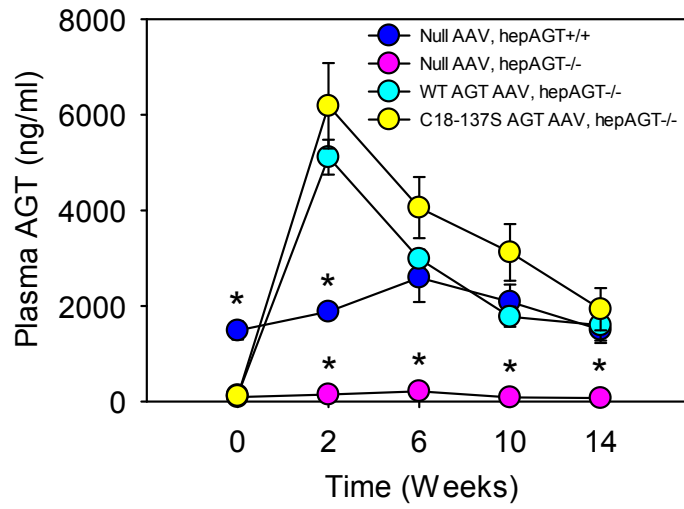
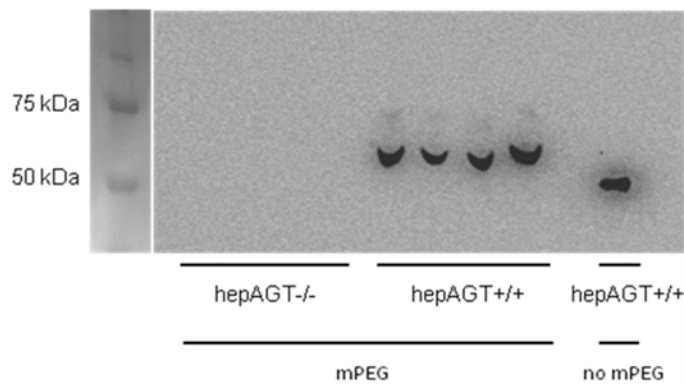


Figure 3.2 Plasma AGT concentrations were not different between hepAGT+/+ and hepAGT-/- receiving either WT AGT or C18-137 AGT AAV. It was measured using an ELISA kit at week 0, 2, 4, 8, and 16 weeks after AAV injection. n = 4-6. * p < 0.001 versus the other 3 groups at each time point. Two way repeated measures ANOVA.

A



B

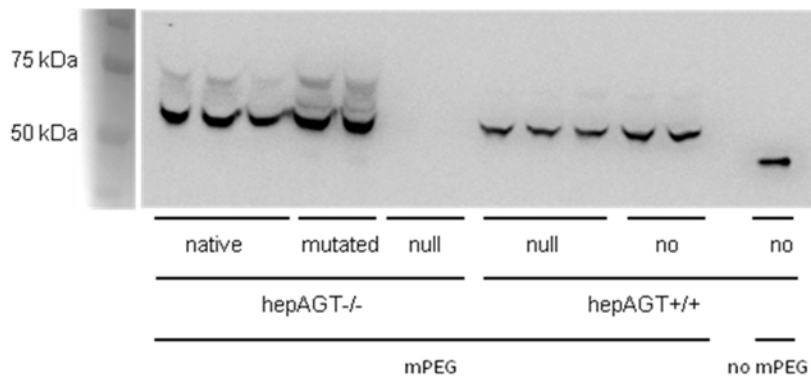


Figure 3.3 Only oxidized AGT was detected in mouse plasma. Oxidized AGT, at baseline (A) and 2 weeks post AAV injection (B), was detected by Western blotting. The AGT band showed a shift by 10 kDa due to addition of mPEG at two cysteins (position 18 and 137). Native represents mice receiving native AGT AAV; mutated represents mice receiving C18S, C137S mutated AGT AAV; null represents mice receiving null AAV; no represents mice receiving PBS.

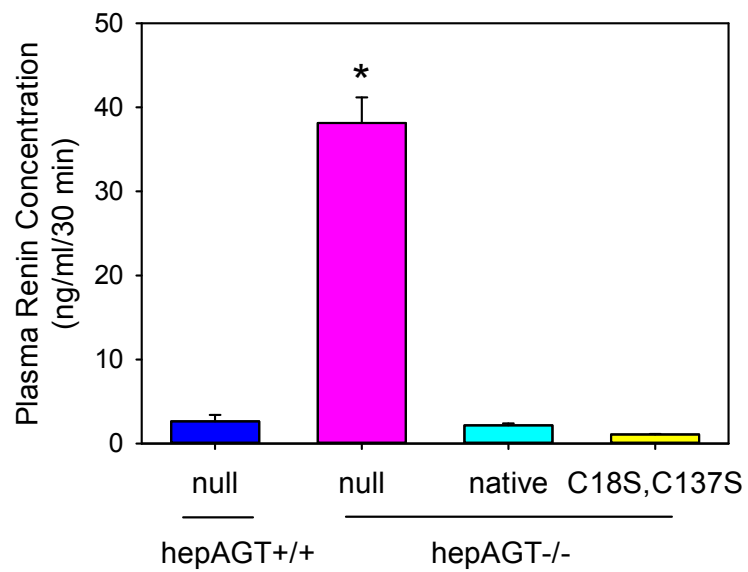


Figure 3.4 Plasma renin concentrations were not different between hepAGT-/- receiving native or C18-137S AGT AAV. It was measured at termination. n = 8-11. * p < 0.001 versus the other 3 groups, one way ANOVA. Null represents mice receiving null AAV; native represents mice receiving native AGT AAV; C18S, C137S represents mice receiving C18S, C137S mutated AGT AAV.

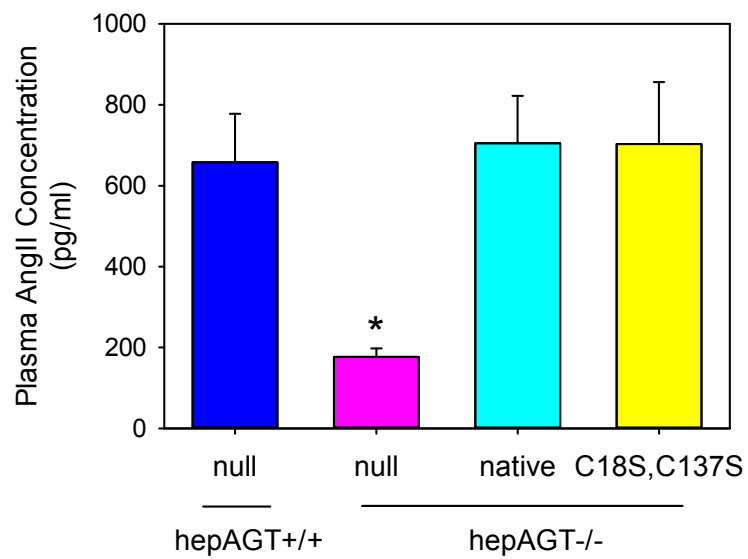


Figure 3.5 Plasma AngII concentrations were not different between hepAGT-/- receiving native or C18-137S AGT AAV. n = 8-11. * p = 0.002 versus the other 3 groups, one way ANOVA. Null represents mice receiving null AAV; native represents mice receiving native AGT AAV; C18S, C137S represents mice receiving C18S, C137S mutated AGT AAV.

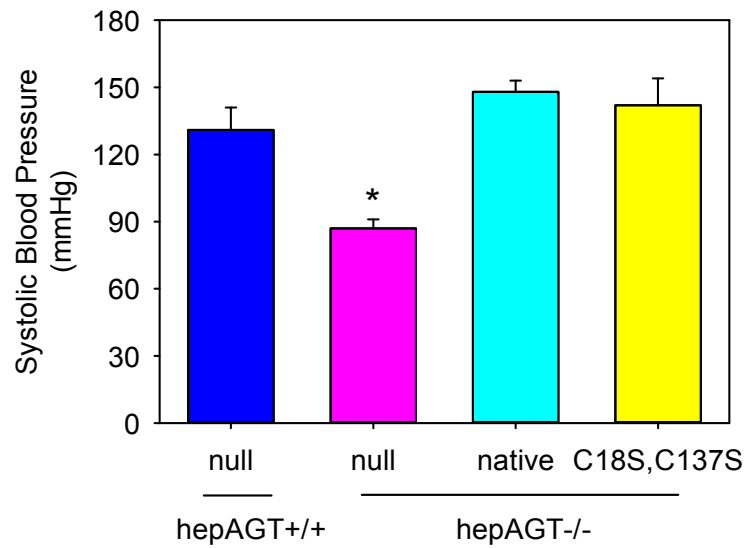


Figure 3.6 Systolic blood pressure was not different between hepAGT^{-/-} receiving native or C18-137S AGT AAV. It was measured using a non-invasive tail-cuff system 8 weeks after AAV injection. n = 4-6. * p < 0.01 versus the other 3 groups, one way ANOVA. Null represents mice receiving null AAV; native represents mice receiving native AGT AAV; C18S, C137S represents mice receiving C18S, C137S mutated AGT AAV.

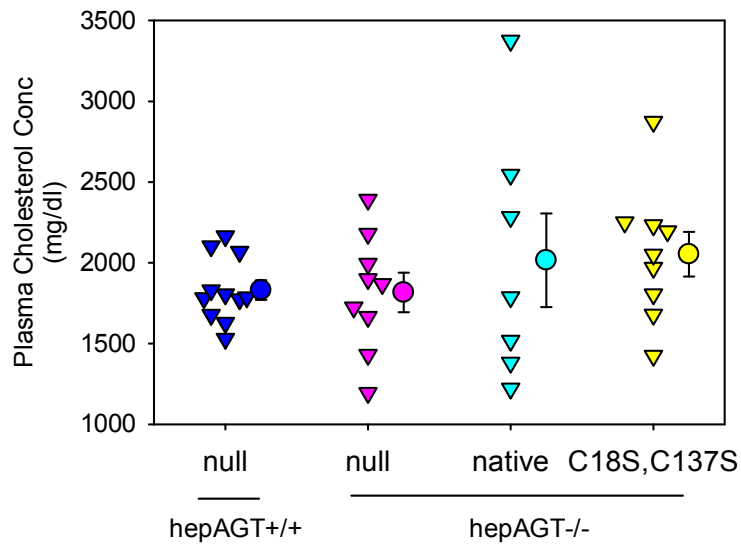


Figure 3.7 Plasma cholesterol concentrations were not different between hepAGT^{-/-} receiving native or C18-137S AGT AAV. It was measured at termination. n = 8-11. Triangles represent values of individual mice, circles represent means, and error bars are SEM. Null represents mice receiving null AAV; native represents mice receiving native AGT AAV; C18S, C137S represents mice receiving C18S, C137S mutated AGT AAV.

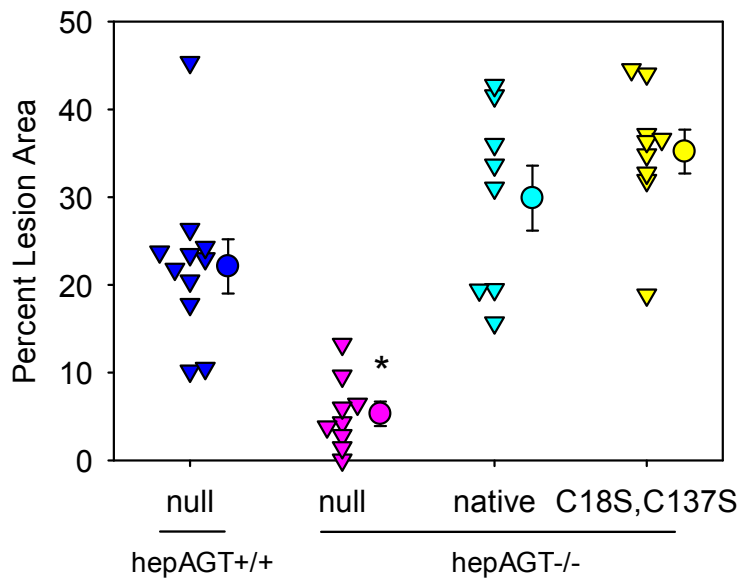


Figure 3.8 Atherosclerotic lesion areas were not different between hepAGT^{-/-} receiving native or C18-137S AGT AAV. It was measured on the intimal surface of the aortic arch region using an *en face* method. Triangles represent values of individual mice, circles represent means, and error bars are SEM. n = 8-11. * p < 0.001 versus the other 3 groups, one way ANOVA. Null represents mice receiving null AAV; native represents mice receiving native AGT AAV; C18S, C137S represents mice receiving C18S, C137S mutated AGT AAV.

Chapter Four: General Discussion

All experiments in the dissertation were designed to address the specific aims stated in Chapter One: **Aim 1**, to investigate the role of angiotensinogen (AGT) inhibition in atherosclerosis and obesity; **Aim 2**, to determine the contributes of systemic and local AGT to atherosclerosis and obesity; **Aim 3**, to analyze the structure-function relationship of Cys18-C138 linkage in AGT.

In Chapter Two, we developed two mouse models with genetic AGT inhibition, hypoAGT mice with global AGT reduction and hepAGT $-/-$ mice with hepatocyte-specific AGT deficiency. We also used antisense oligonucleotides (ASO) for pharmacological AGT inhibition. With these unique reagents, we demonstrated that whole body reduction of AGT (hypoAGT mice) virtually ablated hypercholesterolemia-induced atherosclerosis. To investigate the relative contributions of systemic versus local AGT to atherosclerosis, we performed bone marrow transplantation study and found minimal contributions of local AGT (leukocyte-derived), as the genotype of AGT in bone marrow donors had no effect on atherosclerosis in recipient *Ldlr* $^{-/-}$ mice. Using hepAGT $-/-$ mice, we revealed that hepatic AGT deficiency is responsible for the protection against atherosclerosis as hepAGT $-/-$ mice recapitulated the anti-atherosclerotic phenotypes in hypoAGT mice. As we routinely monitor the health of study mice by measuring body weight weekly, we observed AGT deficiency-induced resistance to diet-induced obesity in both hypoAGT mice and hepAGT $-/-$ mice. We concluded Chapter Two by demonstrating that AGT ASO in adult *Ldlr* $^{-/-}$ mice prevents and regresses diet-induced obesity.

In Chapter Three, we developed an *in vivo* system to examine the structure-function relation in AGT, specifically the role of the Cys18-Cys137 disulfide bridge of mouse

AGT, in AngII release and AngII-dependent pathophysiological effects. To achieve this, we engineered AGT with disrupted disulfide bridge by two cysteine substitutions with serine at position 18 and 137, respectively. Then, C18S, C137S mutated AGT was delivered by an AAV vector to repopulate plasma AGT in hepAGT^{-/-} mice. Essentially, we have an *in vivo* system in which plasma native AGT is replaced with mutated AGT. We demonstrated that mutated AGT lacking the disulfide bridge was equal to native AGT in releasing Ang II, normalizing blood pressure, and contributing to atherosclerosis. Apparently, our findings do not support the redox-sensitive disulfide bridge as a major regulatory mechanism of AGT cleavage by renin *in vivo*.

The role of angiotensinogen in atherosclerosis

Atherosclerosis is a chronic inflammatory disease that progresses through many complex biochemical and cellular events (81). There is a large body of evidence of abnormal cholesterol metabolism being a major determinant of lesion development. This is the main reason we bred all our study mice with LDL receptor deficient background, as LDL receptor is a major player in cholesterol metabolism and *Ldlr*^{-/-} mice have been widely used for atherosclerosis study. Our laboratory has demonstrated that hypercholesterolemia could exacerbate AngII-induced pathology such as abdominal aortic aneurysms. We did not find hypercholesterolemia changes plasma AGT concentrations. However, it is not clear whether hypercholesterolemia could change the ratio of intact AGT versus its cleaved form, des(AngI)-AGT.

Recently, substantial data from our laboratory and other groups has demonstrated a profound role of the RAS in experimental atherosclerosis (50, 84-86, 138). Although being an essential regulator of blood pressure and fluid homeostasis, the RAS promotes

atherosclerosis through neither of these effects (139, 140). In fact, as the major effector peptide of the RAS, AngII plays critical roles in many mechanisms of atherosclerosis, such as promoting adhesion molecules expression in endothelial cells, inducing oxidative stress in the intima, and promoting smooth muscle cell migration. In the classic RAS cascade, AGT is cleaved sequentially by renin and ACE to generate AngII, which functions mainly through AT1 receptors. However, there is accumulated evidence that other bioactive angiotensin peptides such as Ang1-7 generated through recently discovered RAS enzyme, ACE2, could antagonize AngII (141, 142). Despite the increasing complexity of the RAS, AGT remains the only substrate of this hormonal system, which makes AGT an ideal target to inhibit the RAS cascade as AGT inhibition could avoid the RAS complexity. As expected, we demonstrated that AGT inhibition, genetically or pharmacologically, virtually ablated atherosclerosis.

More clinically relevant, we demonstrated that weekly administration of AGT ASO was sufficient to prevent atherosclerosis in mice fed the western diet. Our pilot studies demonstrated that AGT ASO modestly prevented the progression of preexisting atherosclerosis, but failed to regress the pathology (data not shown). We need to explore further on the progression mechanism as the molecular and cellular events lead to initiation and progression would be divergent enough to require different therapeutics.

The role of AGT in obesity

Our consistent findings using multiple approaches confirmed that AGT inhibition not only prevented atherosclerosis, but also protected against diet-induced obesity. The anti-obesity features of AGT are unique because we did not observe body weight reductions with the 3 classic modes of RAS inhibitors. In an unbiased survey of literature on PubMed, we found a total of 83 original articles on pharmacological RAS inhibition in

mice with body weight data. Only 14 of them reported the effects of RAS inhibition on body weight gain. However, effects were either minimal, waxed and waned during the study, or accompanied by significant impact on food intake (143-156). The rest majority of published articles did not find any effects of the 3 classic modes of the RAS inhibition on body weight gain, which was consistent with our findings that these 3 modes showed dose-dependent effects on atherosclerosis, but none of them had significant impact on diet-induced body weight gain. Also, we are not aware of any literature evidence that suggests a link between the classic RAS inhibition and body weight loss in humans.

It has drawn our attention that global deletion of AGT, renin, or ACE resulted in lower body weight, compared with their wild type controls, respectively (92, 125, 126). However, interpretation of the lean phenotypes could be greatly confounded by their unhealthy conditions, as all these global knockout mouse models have low neonatal survival rate and severe kidney developmental and growth problems due to the critical role of the RAS in the fetal development (70, 71, 157, 158). The mechanisms underlying these lean phenotypes are divergent: it is the combination of decreased lipogenesis in white adipose tissue and increased locomotor activity for AGT (92), gastrointestinal loss of fat for renin (125), and increased metabolism in the liver for ACE (126). It is reasonable to think RAS inhibition should impact body weight gain through similar mechanisms regardless of the target. In contrast, pharmacological and genetic approaches used in our study overcame these developmental issues. On the basis of these consistent phenotypic data generated from multiple mouse models to manipulate AGT, we conclude that resistance to diet-induced obesity is specific to AGT inhibition, which is not related to development impairment as shown in AGT, renin, or ACE knockout mice. An intriguing question remains whether these effects of AGT inhibition are RAS-independent. In a pilot study, we used AAV vectors to deliver des(AngI)-AGT or

renin-resistant AGT into hepAGT^{-/-} mice by AAV. We found that renin-resistant AGT, but not des(AngI)-AGT, rescued the lean phenotype in hepAGT^{-/-} mice (data not shown).

We are validating whether renin-resistant AGT is truly resistant to renin cleavage.

Lean phenotypes in AGT inhibition were not attributed to decreased caloric intake or intestinal fat absorption, but increased energy expenditure as uniformly shown by high oxygen consumption and carbon dioxide production. The question is which tissues are responsible for the increased energy expenditure. Global metabolite profiling revealed AGT inhibition decreased lipid metabolites in liver. Combined with unchanged gene expression in lipid catabolism, it is unlikely that increased energy expenditure occurs in liver. Global gene profiling showed that hepatocyte-specific deficiency of AGT had most extensive impact on gene expression in brown adipose tissue, compared with liver and white adipose tissue. Together with AGT deficiency-induced up-regulation of *Ucp1* gene expression in brown adipose tissues, this points to brown adipose tissue as the candidates responsible for the lean phenotype. Increased metabolism in brown adipose tissue could easily explain the fact that AGT ASO not only prevented, but also regressed obesity, while the common mechanism for obesity prevention such as inhibiting adipogenesis could not explain obesity regression.

Adipose tissue is best known for fat storage, as seen in white adipose tissue. It can also use energy for heat production through specialized adipocyte, in brown adipose tissue. Abundant UCP1 in mitochondria is the hallmark of brown adipocytes, responsible for metabolism of thermogenesis instead of ATP synthesis. The capacity of brown adipocyte to counteract metabolic diseases, including obesity and type 2 diabetes has drawn intense interest (159). In humans, it was accepted for a long time that adults have too little brown fat to impact body weight (159). However, progress in imaging revealed

substantial presence of UCP1 positive adipocytes in adults. In addition, obese subjects had lower mass and activity in those adipocytes (160-162). Therefore, brown adipose tissue is of great therapeutic potential against obesity. Inhibition of AGT by ASO regressed established obesity in mice fed the western diet, possibly by promoting brown adipocyte activity.

Systemic AGT versus local AGT

The principal sources for AGT, renin, and ACE are liver, kidneys, and lungs, respectively. They are considered systemic. In the past decades, there is a growing appreciation of tissue (local) RAS in many physiological functions. Classical components of the RAS are present in atherosclerotic lesions (50, 85, 115, 163-167). Our laboratory has reported that macrophage derived renin or ACE promotes atherosclerosis (50, 115), suggesting a role of local RAS in atherosclerosis. Our bone marrow transplantation study clearly demonstrated that macrophage AGT had no effect on atherosclerosis. However, it does not necessarily contradict our previous report on the importance of local RAS (50, 115), as hepatocyte-derived AGT is secreted into circulation and readily taken up by tissues to generate AngII locally. Recently, hepatocyte-derived AGT has been showed to be the primary source of renal AngII (36). Similarly, we found hepatocyte-specific AGT deficiency was responsible for atherosclerosis prevention. Given that many RAS inhibitory drugs are more efficient when they can inhibit tissue RAS, we think it is appealing that pharmacological inhibition of AGT could inhibit both systemic and tissue RAS.

Besides hepatocytes, AGT is present in many other cell types. Adipocytes are an abundant source for AGT (34, 168). It is possible the low but detectable plasma AGT

concentrations in hepAGT $-/-$ mice was due to presence of AGT in adipocytes (34). However, adipocyte-specific AGT deficiency did not affect diet-induced obesity (34). AGT is also expressed in kidneys. However, a recent study demonstrated that AGT derived from liver, rather than kidneys, is responsible for normal renal function as the primary source of renal AngII (36). We have detected AGT in macrophages (50), and macrophage infiltration plays important role in both atherosclerosis and obesity. However, our data excluded macrophage AGT as a possible contributor to either atherosclerosis or body weight gain. Therefore, hepatic AGT, not tissue AGT, is the substrate for local RAS in atherosclerosis and obesity.

The role of Cys18-Cys137 disulfide bridge

The elegant work by Zhou and colleagues (11) has provided the crystal structure of AGT. From this structure, a novel proposal was formulated that disulfide bridge between Cys18 and Cys138 in human AGT could regulate AngI release at a pericellular level to modulate blood pressure. It was used in the interpretation that an 8% difference in the percentage of oxidized AGT in plasma (synonymous with increased percentage of disulfide bridging in AGT) was the basis for increased blood pressure in women with preeclampsia (11). Despite being provocative, it did not establish a causal relationship between the increase of disulfide bridging and the rise of blood pressure. Given the vast impact of blood pressure regulation by the RAS to public health, there is a need to validate the functional significance of the disulfide bridging in AGT.

In an *in vivo* system that was developed to determine structure-function relationship for AGT, we demonstrated that mutated AGT lacking the disulfide bridge was not different from exclusively disulfide bridged AGT in generating Ang II, recovering blood pressure,

and contributing to atherosclerosis. Although redox status of AGT may influence the interaction at the precision that can be obtained *in vitro*, our findings do not support the redox-sensitive disulfide bridge as a major regulatory mechanism of AGT cleavage by renin *in vivo*.

A critical question remains whether mouse is a valid model to test this disulfide bridge theory based on *in vitro* data from human AGT. I break down my answer to the question into three parts:

First, I discuss the structural similarity in AGT between humans and mice. In their structural analysis, Zhou and colleagues included recombinant AGT from mouse, rat, and human. The crystal structures of mouse AGT, solved to highest resolution at 2.1 Å, showed that AGT cleavage site was inaccessibly buried in its N-terminal tail. The general features of mouse AGT are preserved in the 3.15 Å rat and 3.3 Å human structure. Moreover, human AGT contains four cysteines, but those forming the Cys18-Cys138 linkage are the only two conserved in all species. Therefore, the focus of both the study of Zhou *et al* (11) and that of our own study, is on a conserved structure present in both human and mouse AGT.

Second, human plasma but not mouse plasma contains equilibrated oxidized and reduced AGT, as oxidized AGT can be reduced by interaction with proposed thiol-reductant systems in human plasma (11). Does that make our mouse studies irrelevant to the disulfide bridge theory? This theory, arising largely from structural analysis of AGT supported solely by *in vitro* analysis of the renin-AGT reaction, is based on two assumptions: 1. The presence of the C18-C138 disulfide bridge of AGT facilitates AngI release; 2. The ratio of reduced-to-oxidized (i.e. absence versus presence of disulfide

bridge) AGT can be regulated to change blood pressure under certain conditions, such as preeclampsia. To directly test these assumptions, we engineered mice with AGT that represented either extreme, namely disulfide bridge versus unbridged ratios being 0:100 or 100:0 (i.e complete absence versus complete presence of disulfide bridge).

Therefore, this approach provided an optimal condition for defining the contribution of the disulfide bridge within AGT to blood pressure responses, and other indexes of AGT-renin reaction such as atherosclerosis.

Finally, the role of the disulfide bridge in regulating AGT cleavage is only relevant in tissues (local) where prorenin receptors are present, while hepatic AGT, secreted into circulation, is considered systemic. The study by Nguyen *et al* (169) is cited by Zhou *et al* (11), in reference to a role for the prorenin receptors as a regulator of the interaction between AGT and renin. It is worth noting that Nguyen *et al* (169) concluded that only 1% of soluble renin binds to prorenin receptors. This study and follow up studies (170, 171) have indicated that prorenin receptors have marginal effects *in vivo* on AngII release and AngII-mediated effects. The K_d of prorenin receptors for renin has been determined at 5-20 nmol/l by several groups (169-171). Zhou *et al* (11) was able to demonstrate the presence of prorenin receptors lowered K_m for the interaction of oxidized AGT with renin at 0.1nM. Although renin concentrations in plasma are in the picomolar range, renin concentrations in tissues may be 100-fold greater (169). The *in vitro* data obtained by Zhou *et al* encouraged us to test their proposal *in vivo*. In fact, mice express prorenin receptors in several tissues, including renal tissue as proposed by Zhou *et al* (11). A recent study has provided convincing evidence that liver-derived AGT (but not renal AGT) is the primary source of renal production of AngII that regulates blood pressure (36). Therefore, administration of AAV with liver-specific promoter driven AGT expression of disulfide-bridged or unbridged forms to mice with liver-specific AGT

deficiency would deliver AGT substrate to kidney. Any role of prorenin receptors to facilitate the renin/AGT reaction in modulating blood pressure would be operative in our *in vivo* study. The effect of AGT on atherosclerosis is also likely to be due to its cleavage at a cellular level since renin in tissues determines lesion development as demonstrated in our previous study (50). Taken together, we consider that two of our major end points, blood pressure and atherosclerosis, are regulated by AGT cleavage at a cellular level within tissues, rather than being a systemic effect.

Taken together, our *in vivo* system, utilizing hepAGT^{-/-} mice and AAV vectors delivering engineered AGT, is a valid model to pull out “refinements” related to redox status for AGT. However, our data do not support an important role of a redox mediated disulfide bridge for regulating the *in vivo* effects of AGT.

Conclusions

We developed a host of unique reagents and *in vivo* systems to explore the effects of AGT inhibition on atherosclerosis and obesity, and the structure-function relationship of the Cys18-Cys137 disulfide bridge in AGT. We found AGT deficiency prevented atherosclerosis and obesity, and hepatic AGT was responsible for these effects. We revealed the therapeutic potentials of AGT inhibition by demonstrating that weekly administration of AGT ASO not only prevented but also regressed obesity. Now we are exploring the mechanisms of AGT inhibition induced lean phenotype. We are excited by a particular preliminary data suggesting global AGT deficiency (hypoAGT) may delay the release of triglycerides from enterocytes, which has the potential to affect lipid metabolism in metabolically active tissues like liver and brown adipose tissue. We will be further examining the data before we could establish a molecular link between AGT and

lipid metabolism, thereby facilitating the development of AGT inhibition as therapeutics against obesity.

References

1. Ohkubo H, *et al.* (1983) Cloning and sequence analysis of cDNA for rat angiotensinogen. *Proceedings of the National Academy of Sciences of the United States of America* 80(8):2196-2200.
2. Gaillard I, Clauser E, & Corvol P (1989) Structure of human angiotensinogen gene. *DNA* 8(2):87-99.
3. Clouston WM, Evans BA, Haralambidis J, & Richards RI (1988) Molecular cloning of the mouse angiotensinogen gene. *Genomics* 2(3):240-248.
4. Mori M, *et al.* (1989) Restriction fragment length polymorphisms of the angiotensinogen gene in inbred rat strains and mapping of the gene on chromosome 19q. *Cytogenet Cell Genet* 50(1):42-45.
5. Clouston WM, Fournier RE, & Richards RI (1989) The angiotensinogen gene is located on mouse chromosome 8. *FEBS Lett* 255(2):419-422.
6. Fukamizu A, *et al.* (1990) Structure and expression of the human angiotensinogen gene. Identification of a unique and highly active promoter. *The Journal of biological chemistry* 265(13):7576-7582.
7. Isa MN, *et al.* (1990) Assignment of the human angiotensinogen gene to chromosome 1q42-q43 by nonisotopic in situ hybridization [corrected]. *Genomics* 8(3):598-600.
8. Takei Y, Joss JM, Kloas W, & Rankin JC (2004) Identification of angiotensin I in several vertebrate species: its structural and functional evolution. *Gen Comp Endocrinol* 135(3):286-292.

9. Gimenez-Roqueplo AP, Celerier J, Lucarelli G, Corvol P, & Jeunemaitre X (1998) Role of N-glycosylation in human angiotensinogen. *The Journal of biological chemistry* 273(33):21232-21238.
10. Streatfeild-James RM, *et al.* (1998) Angiotensinogen cleavage by renin: importance of a structurally constrained N-terminus. *FEBS Lett* 436(2):267-270.
11. Zhou A, *et al.* (2010) A redox switch in angiotensinogen modulates angiotensin release. *Nature* 468(7320):108-111.
12. Printz MP, Printz JM, & Dworschack RT (1977) Human angiotensinogen. Purification partial characterization, and a comparison with animal prohormones. *The Journal of biological chemistry* 252(5):1654-1662.
13. Hatae T, Takimoto E, Murakami K, & Fukamizu A (1994) Comparative studies on species-specific reactivity between renin and angiotensinogen. *Mol Cell Biochem* 131(1):43-47.
14. Celerier J, Cruz A, Lamande N, Gasc JM, & Corvol P (2002) Angiotensinogen and its cleaved derivatives inhibit angiogenesis. *Hypertension* 39(2):224-228.
15. Vincent F, *et al.* (2009) Angiotensinogen delays angiogenesis and tumor growth of hepatocarcinoma in transgenic mice. *Cancer Res* 69(7):2853-2860.
16. Nibu Y, Takahashi S, Tanimoto K, Murakami K, & Fukamizu A (1994) Identification of cell type-dependent enhancer core element located in the 3'-downstream region of the human angiotensinogen gene. *The Journal of biological chemistry* 269(46):28598-28605.

17. Klett C, *et al.* (1988) Angiotensin II controls angiotensinogen secretion at a pretranslational level. *J Hypertens Suppl* 6(4):S442-445.
18. Nakamura A, *et al.* (1990) Regulation of liver angiotensinogen and kidney renin mRNA levels by angiotensin II. *The American journal of physiology* 258(1 Pt 1):E1-6.
19. Jamaluddin M, *et al.* (2000) Angiotensin II induces nuclear factor (NF)-kappaB1 isoforms to bind the angiotensinogen gene acute-phase response element: a stimulus-specific pathway for NF-kappaB activation. *Mol Endocrinol* 14(1):99-113.
20. Kobori H, *et al.* (2007) Kidney-specific enhancement of ANG II stimulates endogenous intrarenal angiotensinogen in gene-targeted mice. *Am J Physiol Renal Physiol* 293(3):F938-945.
21. Gonzalez-Villalobos RA, *et al.* (2008) Intrarenal angiotensin II and angiotensinogen augmentation in chronic angiotensin II-infused mice. *Am J Physiol Renal Physiol* 295(3):F772-779.
22. Brasier AR, Jamaluddin M, Han Y, Patterson C, & Runge MS (2000) Angiotensin II induces gene transcription through cell-type-dependent effects on the nuclear factor-kappaB (NF-kappaB) transcription factor. *Mol Cell Biochem* 212(1-2):155-169.
23. Jain S, Li Y, Patil S, & Kumar A (2007) HNF-1alpha plays an important role in IL-6-induced expression of the human angiotensinogen gene. *Am J Physiol Cell Physiol* 293(1):C401-410.

24. Campbell DJ & Habener JF (1986) Angiotensinogen gene is expressed and differentially regulated in multiple tissues of the rat. *The Journal of clinical investigation* 78(1):31-39.
25. Deschepper CF (1994) Angiotensinogen: hormonal regulation and relative importance in the generation of angiotensin II. *Kidney international* 46(6):1561-1563.
26. Lynch KR & Peach MJ (1991) Molecular biology of angiotensinogen. *Hypertension* 17(3):263-269.
27. Cassis LA, Lynch KR, & Peach MJ (1988) Localization of angiotensinogen messenger RNA in rat aorta. *Circulation research* 62(6):1259-1262.
28. Cassis LA, Saye J, & Peach MJ (1988) Location and regulation of rat angiotensinogen messenger RNA. *Hypertension* 11(6 Pt 2):591-596.
29. Saye JA, Cassis LA, Sturgill TW, Lynch KR, & Peach MJ (1989) Angiotensinogen gene expression in 3T3-L1 cells. *The American journal of physiology* 256(2 Pt 1):C448-451.
30. Phillips MI, Speakman EA, & Kimura B (1993) Levels of angiotensin and molecular biology of the tissue renin angiotensin systems. *Regul Pept* 43(1-2):1-20.
31. Gomez RA, et al. (1988) Fetal expression of the angiotensinogen gene. *Endocrinology* 123(5):2298-2302.

32. Satou R, *et al.* (2008) Costimulation with angiotensin II and interleukin 6 augments angiotensinogen expression in cultured human renal proximal tubular cells. *Am J Physiol Renal Physiol* 295(1):F283-289.
33. Stornetta RL, Hawelu-Johnson CL, Guyenet PG, & Lynch KR (1988) Astrocytes synthesize angiotensinogen in brain. *Science* 242(4884):1444-1446.
34. Yiannikouris F, *et al.* (2012) Adipocyte-specific deficiency of angiotensinogen decreases plasma angiotensinogen concentration and systolic blood pressure in mice. *Am J Physiol Regul Integr Comp Physiol* 302(2):R244-251.
35. Stec DE, Davisson RL, Haskell RE, Davidson BL, & Sigmund CD (1999) Efficient liver-specific deletion of a floxed human angiotensinogen transgene by adenoviral delivery of Cre recombinase in vivo. *The Journal of biological chemistry* 274(30):21285-21290.
36. Matsusaka T, *et al.* (2012) Liver angiotensinogen is the primary source of renal angiotensin II. *J Am Soc Nephrol* 23(7):1181-1189.
37. Campbell DJ, *et al.* (1984) Characterization of precursor and secreted forms of rat angiotensinogen. *Endocrinology* 114(3):776-785.
38. Campbell DJ (1987) Circulating and tissue angiotensin systems. *The Journal of clinical investigation* 79(1):1-6.
39. Dzau VJ (1989) Multiple pathways of angiotensin production in the blood vessel wall: evidence, possibilities and hypotheses. *J Hypertens* 7(12):933-936.
40. Belova LA (2000) Angiotensin II-generating enzymes. *Biochemistry (Mosc)* 65(12):1337-1345.

41. Bouhnik J, *et al.* (1981) Rat angiotensinogen and des(angiotensin I)angiotensinogen: purification, characterization, and partial sequencing. *Biochemistry* 20(24):7010-7015.
42. Azizi M, Webb R, Nussberger J, & Hollenberg NK (2006) Renin inhibition with aliskiren: where are we now, and where are we going? *J Hypertens* 24(2):243-256.
43. Beaty O, 3rd, Sloop CH, Schmid HE, Jr., & Buckalew VM, Jr. (1976) Renin response and angiotensinogen control during graded hemorrhage and shock in the dog. *The American journal of physiology* 231(4):1300-1307.
44. Eggena P & Barrett JD (1988) Renin substrate release in response to perturbations of renin-angiotensin system. *The American journal of physiology* 254(4 Pt 1):E389-393.
45. Danser AH (2003) Local renin-angiotensin systems: the unanswered questions. *Int J Biochem Cell Biol* 35(6):759-768.
46. Katz SA, Opsahl JA, Lunzer MM, Forbis LM, & Hirsch AT (1997) Effect of bilateral nephrectomy on active renin, angiotensinogen, and renin glycoforms in plasma and myocardium. *Hypertension* 30(2 Pt 1):259-266.
47. Karlsson C, *et al.* (1998) Human adipose tissue expresses angiotensinogen and enzymes required for its conversion to angiotensin II. *J Clin Endocrinol Metab* 83(11):3925-3929.
48. Okamura A, *et al.* (1999) Upregulation of renin-angiotensin system during differentiation of monocytes to macrophages. *J Hypertens* 17(4):537-545.

49. Sun Y, Zhang J, Zhang JQ, & Weber KT (2001) Renin expression at sites of repair in the infarcted rat heart. *J Mol Cell Cardiol* 33(5):995-1003.
50. Lu H, et al. (2008) Renin inhibition reduces hypercholesterolemia-induced atherosclerosis in mice. *The Journal of clinical investigation* 118(3):984-993.
51. Arakawa K, Yuki M, & Ikeda M (1980) Chemical identity of tryptensin with angiotensin. *Biochem J* 187(3):647-653.
52. Katz SA, Opsahl JA, & Forbis LM (2001) Myocardial enzymatic activity of renin and cathepsin D before and after bilateral nephrectomy. *Basic Res Cardiol* 96(6):659-668.
53. Katsurada A, et al. (2007) Novel sandwich ELISA for human angiotensinogen. *Am J Physiol Renal Physiol* 293(3):F956-960.
54. Cumin F, Le-Nguyen D, Castro B, Menard J, & Corvol P (1987) Comparative enzymatic studies of human renin acting on pure natural or synthetic substrates. *Biochim Biophys Acta* 913(1):10-19.
55. Kobori H, et al. (2008) Determination of plasma and urinary angiotensinogen levels in rodents by newly developed ELISA. *Am J Physiol Renal Physiol* 294(5):F1257-1263.
56. Lu H, et al. (2012) Comparative effects of different modes of renin angiotensin system inhibition on hypercholesterolaemia-induced atherosclerosis. *British journal of pharmacology* 165(6):2000-2008.

57. Lewicki JA, Printz JM, & Printz MP (1983) Clearance of rabbit plasma angiotensinogen and relationship to CSF angiotensinogen. *The American journal of physiology* 244(4):H577-585.
58. Hilgenfeldt U (1988) Half-life of rat angiotensinogen: influence of nephrectomy and lipopolysaccharide stimulation. *Mol Cell Endocrinol* 56(1-2):91-98.
59. Yayama K, *et al.* (1995) Role of the kidney in the plasma clearance of angiotensinogen in the rat: plasma clearance and tissue distribution of 125I-angiotensinogen. *Life Sci* 57(19):1791-1801.
60. Daugherty A, Thorpe SR, Lange LG, Sobel BE, & Schonfeld G (1985) Loci of catabolism of beta-very low density lipoprotein in vivo delineated with a residualizing label, 125I-dilactitol tyramine. *The Journal of biological chemistry* 260(27):14564-14570.
61. Ohkubo H, *et al.* (1990) Generation of transgenic mice with elevated blood pressure by introduction of the rat renin and angiotensinogen genes. *Proceedings of the National Academy of Sciences of the United States of America* 87(13):5153-5157.
62. Kimura S, *et al.* (1992) High blood pressure in transgenic mice carrying the rat angiotensinogen gene. *The EMBO journal* 11(3):821-827.
63. Takahashi S, *et al.* (1991) Expression of the human angiotensinogen gene in transgenic mice and transfected cells. *Biochem Biophys Res Commun* 180(2):1103-1109.

64. Fukamizu A, *et al.* (1993) Chimeric renin-angiotensin system demonstrates sustained increase in blood pressure of transgenic mice carrying both human renin and human angiotensinogen genes. *The Journal of biological chemistry* 268(16):11617-11621.
65. Tanimoto K, *et al.* (1994) Angiotensinogen-deficient mice with hypotension. *The Journal of biological chemistry* 269(50):31334-31337.
66. Kim HS, *et al.* (1995) Genetic control of blood pressure and the angiotensinogen locus. *Proceedings of the National Academy of Sciences of the United States of America* 92(7):2735-2739.
67. Kai T, Kino H, & Ishikawa K (1998) Role of the renin-angiotensin system in cardiac hypertrophy and renal glomerular sclerosis in transgenic hypertensive mice carrying both human renin and angiotensinogen genes. *Hypertens Res* 21(1):39-46.
68. Nagata M, *et al.* (1996) Nephrogenesis and renovascular development in angiotensinogen-deficient mice. *Lab Invest* 75(5):745-753.
69. Walther T, *et al.* (2004) Angiotensin deficiency in mice leads to dilated cardiomyopathy. *Eur J Pharmacol* 493(1-3):161-165.
70. Yanai K, *et al.* (2000) Renin-dependent cardiovascular functions and renin-independent blood-brain barrier functions revealed by renin-deficient mice. *The Journal of biological chemistry* 275(1):5-8.
71. Kregge JH, *et al.* (1995) Male-female differences in fertility and blood pressure in ACE-deficient mice. *Nature* 375(6527):146-148.

72. Oliverio MI, *et al.* (1998) Reduced growth, abnormal kidney structure, and type 2 (AT2) angiotensin receptor-mediated blood pressure regulation in mice lacking both AT1A and AT1B receptors for angiotensin II. *Proceedings of the National Academy of Sciences of the United States of America* 95(26):15496-15501.
73. Tsuchida S, *et al.* (1998) Murine double nullizygotes of the angiotensin type 1A and 1B receptor genes duplicate severe abnormal phenotypes of angiotensinogen nullizygotes. *The Journal of clinical investigation* 101(4):755-760.
74. Lochard N, Silversides DW, van Kats JP, Mercure C, & Reudelhuber TL (2003) Brain-specific restoration of angiotensin II corrects renal defects seen in angiotensinogen-deficient mice. *The Journal of biological chemistry* 278(4):2184-2189.
75. Ishida J, *et al.* (1998) Rescue of angiotensinogen-knockout mice. *Biochem Biophys Res Commun* 252(3):610-616.
76. Kang N, *et al.* (2002) Reduced hypertension-induced end-organ damage in mice lacking cardiac and renal angiotensinogen synthesis. *J Mol Med (Berl)* 80(6):359-366.
77. Davisson RL, *et al.* (1997) Complementation of reduced survival, hypotension, and renal abnormalities in angiotensinogen-deficient mice by the human renin and human angiotensinogen genes. *The Journal of clinical investigation* 99(6):1258-1264.

78. Davisson RL, Ding Y, Stec DE, Catterall JF, & Sigmund CD (1999) Novel mechanism of hypertension revealed by cell-specific targeting of human angiotensinogen in transgenic mice. *Physiol Genomics* 1(1):3-9.
79. Massiera F, *et al.* (2001) Adipose angiotensinogen is involved in adipose tissue growth and blood pressure regulation. *FASEB J* 15(14):2727-2729.
80. Ding Y, Stec DE, & Sigmund CD (2001) Genetic evidence that lethality in angiotensinogen-deficient mice is due to loss of systemic but not renal angiotensinogen. *The Journal of biological chemistry* 276(10):7431-7436.
81. Rader DJ & Daugherty A (2008) Translating molecular discoveries into new therapies for atherosclerosis. *Nature* 451(7181):904-913.
82. Hillaert MA, *et al.* (2011) Measuring and targeting aldosterone and renin in atherosclerosis-a review of clinical data. *Am Heart J* 162(4):585-596.
83. Daugherty A, Manning MW, & Cassis LA (2000) Angiotensin II promotes atherosclerotic lesions and aneurysms in apolipoprotein E-deficient mice. *The Journal of clinical investigation* 105(11):1605-1612.
84. Weiss D, Kools JJ, & Taylor WR (2001) Angiotensin II-induced hypertension accelerates the development of atherosclerosis in apoE-deficient mice. *Circulation* 103(3):448-454.
85. Daugherty A, Rateri DL, Lu H, Inagami T, & Cassis LA (2004) Hypercholesterolemia stimulates angiotensin peptide synthesis and contributes to atherosclerosis through the AT1A receptor. *Circulation* 110(25):3849-3857.

86. Wassmann S, *et al.* (2004) Inhibition of diet-induced atherosclerosis and endothelial dysfunction in apolipoprotein E/angiotensin II type 1A receptor double-knockout mice. *Circulation* 110(19):3062-3067.
87. Weiss D & Taylor WR (2008) Deoxycorticosterone acetate salt hypertension in apolipoprotein E-/- mice results in accelerated atherosclerosis: the role of angiotensin II. *Hypertension* 51(2):218-224.
88. Sugiyama F, *et al.* (1997) Acceleration of atherosclerotic lesions in transgenic mice with hypertension by the activated renin-angiotensin system. *Lab Invest* 76(6):835-842.
89. Jones BH, Standridge MK, Taylor JW, & Moustaid N (1997) Angiotensinogen gene expression in adipose tissue: analysis of obese models and hormonal and nutritional control. *The American journal of physiology* 273(1 Pt 2):R236-242.
90. Rahmouni K, Mark AL, Haynes WG, & Sigmund CD (2004) Adipose depot-specific modulation of angiotensinogen gene expression in diet-induced obesity. *Am J Physiol Endocrinol Metab* 286(6):E891-895.
91. Boustany CM, *et al.* (2004) Activation of the systemic and adipose renin-angiotensin system in rats with diet-induced obesity and hypertension. *Am J Physiol Regul Integr Comp Physiol* 287(4):R943-949.
92. Massiera F, *et al.* (2001) Angiotensinogen-deficient mice exhibit impairment of diet-induced weight gain with alteration in adipose tissue development and increased locomotor activity. *Endocrinology* 142(12):5220-5225.

93. Kim S, *et al.* (2002) Effects of high-fat diet, angiotensinogen (agt) gene inactivation, and targeted expression to adipose tissue on lipid metabolism and renal gene expression. *Horm Metab Res* 34(11-12):721-725.
94. Kai T, Sugimura K, Shimada S, Kurooka A, & Ishikawa K (1999) Renin-angiotensin system stimulates cardiac and renal disorders in Tsukuba hypertensive mice. *Clin Exp Pharmacol Physiol* 26(3):206-211.
95. Jeunemaitre X, *et al.* (1992) Molecular basis of human hypertension: role of angiotensinogen. *Cell* 71(1):169-180.
96. Sethi AA, *et al.* (2003) Angiotensinogen single nucleotide polymorphisms, elevated blood pressure, and risk of cardiovascular disease. *Hypertension* 41(6):1202-1211.
97. Katsuya T, *et al.* (1995) Association of angiotensinogen gene T235 variant with increased risk of coronary heart disease. *Lancet* 345(8965):1600-1603.
98. Jeunemaitre X, *et al.* (1997) Genetic polymorphisms of the renin-angiotensin system and angiographic extent and severity of coronary artery disease: the CORGENE study. *Hum Genet* 99(1):66-73.
99. Rodriguez-Perez JC, *et al.* (2001) Association of angiotensinogen M235T and A(-6)G gene polymorphisms with coronary heart disease with independence of essential hypertension: the PROCAGENE study. Prospective Cardiac Gene. *J Am Coll Cardiol* 37(6):1536-1542.
100. Zafarmand MH, van der Schouw YT, Grobbee DE, de Leeuw PW, & Bots ML (2008) The M235T polymorphism in the AGT gene and CHD risk: evidence of a

Hardy-Weinberg equilibrium violation and publication bias in a meta-analysis.

PLoS One 3(6):e2533.

101. Gardemann A, *et al.* (1999) Angiotensinogen T174M and M235T gene polymorphisms are associated with the extent of coronary atherosclerosis. *Atherosclerosis* 145(2):309-314.
102. Tsai CT, *et al.* (2007) Renin-angiotensin system gene polymorphisms and coronary artery disease in a large angiographic cohort: detection of high order gene-gene interaction. *Atherosclerosis* 195(1):172-180.
103. Prat-Larquemin L, *et al.* (2004) Adipose angiotensinogen secretion, blood pressure, and AGT M235T polymorphism in obese patients. *Obes Res* 12(3):556-561.
104. Takakura Y, *et al.* (2006) Angiotensinogen gene polymorphism (Met235Thr) influences visceral obesity and insulin resistance in obese Japanese women. *Metabolism* 55(6):819-824.
105. Procopciuc LM, *et al.* (2010) Renin angiotensin system polymorphisms in patients with metabolic syndrome (MetS). *Eur J Intern Med* 21(5):414-418.
106. Cooper R, *et al.* (1997) ACE, angiotensinogen and obesity: a potential pathway leading to hypertension. *J Hum Hypertens* 11(2):107-111.
107. Wu C, Lu H, Cassis LA, & Daugherty A (2011) Molecular and Pathophysiological Features of Angiotensinogen: A Mini Review. *North American journal of medicine & science* 4(4):183-190.

108. Yusuf S, *et al.* (2000) Effects of an angiotensin-converting-enzyme inhibitor, ramipril, on cardiovascular events in high-risk patients. The Heart Outcomes Prevention Evaluation Study Investigators. *N Engl J Med* 342(3):145-153.
109. Yusuf S, *et al.* (2008) Telmisartan, ramipril, or both in patients at high risk for vascular events. *N Engl J Med* 358(15):1547-1559.
110. Hirst JA, *et al.* (2012) The impact of renin-angiotensin-aldosterone system inhibitors on Type 1 and Type 2 diabetic patients with and without early diabetic nephropathy. *Kidney international* 81(7):674-683.
111. Plump AS, *et al.* (1992) Severe hypercholesterolemia and atherosclerosis in apolipoprotein E-deficient mice created by homologous recombination in ES cells. *Cell* 71(2):343-353.
112. Yiannikouris F, *et al.* (2012) Adipocyte deficiency of angiotensinogen prevents obesity-induced hypertension in male mice. *Hypertension* 60(6):1524-1530.
113. Daugherty A & Cassis L (1999) Chronic angiotensin II infusion promotes atherogenesis in low density lipoprotein receptor -/- mice. *Ann N Y Acad Sci* 892:108-118.
114. Daugherty A, Manning MW, & Cassis LA (2001) Antagonism of AT2 receptors augments angiotensin II-induced abdominal aortic aneurysms and atherosclerosis. *British journal of pharmacology* 134(4):865-870.
115. Chen X, *et al.* (2013) Contributions of leukocyte angiotensin-converting enzyme to development of atherosclerosis. *Arterioscler Thromb Vasc Biol* 33(9):2075-2080.

116. Cassis LA, Rateri DL, Lu H, & Daugherty A (2007) Bone marrow transplantation reveals that recipient AT1a receptors are required to initiate angiotensin II-induced atherosclerosis and aneurysms. *Arterioscler Thromb Vasc Biol* 27(2):380-386.
117. Daugherty A & Whitman SC (2003) Quantification of atherosclerosis in mice. *Methods Mol Biol* 209:293-309.
118. Daugherty A & Rateri DL (2005) Development of experimental designs for atherosclerosis studies in mice. *Methods* 36(2):129-138.
119. Daugherty A, Rateri D, Hong L, & Balakrishnan A (2009) Measuring blood pressure in mice using volume pressure recording, a tail-cuff method. *J Vis Exp* (27).
120. Jandacek RJ & Webb MR (1978) Physical properties of pure sucrose octaesters. *Chemistry and Physics of Lipids* 22(2):163-176.
121. Miller KW, *et al.* (1995) Disposition of ingested olestra in the Fischer 344 rat. *Fundam Appl Toxicol* 24(2):229-237.
122. Daher GC, *et al.* (1997) Olestra ingestion and dietary fat absorption in humans. *J Nutr* 127(8 Suppl):1694S-1698S.
123. Jandacek RJ, Heubi JE, & Tso P (2004) A novel, noninvasive method for the measurement of intestinal fat absorption. *Gastroenterology* 127(1):139-144.
124. Gomez RA, *et al.* (1993) Leukocytes synthesize angiotensinogen. *Hypertension* 21(4):470-475.

125. Jayasooriya AP, *et al.* (2008) Mice lacking angiotensin-converting enzyme have increased energy expenditure, with reduced fat mass and improved glucose clearance. *Proceedings of the National Academy of Sciences of the United States of America* 105(18):6531-6536.
126. Takahashi N, *et al.* (2007) Increased energy expenditure, dietary fat wasting, and resistance to diet-induced obesity in mice lacking renin. *Cell metabolism* 6(6):506-512.
127. Daya S & Berns KI (2008) Gene therapy using adeno-associated virus vectors. *Clin Microbiol Rev* 21(4):583-593.
128. Kotin RM (1994) Prospects for the use of adeno-associated virus as a vector for human gene therapy. *Human gene therapy* 5(7):793-801.
129. Sanlioglu S, Monick MM, Luleci G, Hunninghake GW, & Engelhardt JF (2001) Rate limiting steps of AAV transduction and implications for human gene therapy. *Curr Gene Ther* 1(2):137-147.
130. Gao G, Vandenberghe LH, & Wilson JM (2005) New recombinant serotypes of AAV vectors. *Curr Gene Ther* 5(3):285-297.
131. Auricchio A, *et al.* (2002) Noninvasive gene transfer to the lung for systemic delivery of therapeutic proteins. *The Journal of clinical investigation* 110(4):499-504.
132. Auricchio A, *et al.* (2001) Exchange of surface proteins impacts on viral vector cellular specificity and transduction characteristics: the retina as a model. *Hum Mol Genet* 10(26):3075-3081.

133. Rabinowitz JE, *et al.* (2002) Cross-packaging of a single adeno-associated virus (AAV) type 2 vector genome into multiple AAV serotypes enables transduction with broad specificity. *J Virol* 76(2):791-801.
134. Kitajima K, *et al.* (2006) Complete prevention of atherosclerosis in apoE-deficient mice by hepatic human apoE gene transfer with adeno-associated virus serotypes 7 and 8. *Arterioscler Thromb Vasc Biol* 26(8):1852-1857.
135. Gurley SB, *et al.* (2011) AT1A angiotensin receptors in the renal proximal tubule regulate blood pressure. *Cell metabolism* 13(4):469-475.
136. Cassis LA, Huang J, Gong MC, & Daugherty A (2004) Role of metabolism and receptor responsiveness in the attenuated responses to Angiotensin II in mice compared to rats. *Regul Pept* 117(2):107-116.
137. Herrmann HC & Dzau VJ (1983) The feedback regulation of angiotensinogen production by components of the renin-angiotensin system. *Circulation research* 52(3):328-334.
138. Hayek T, *et al.* (2003) Tissue angiotensin-converting-enzyme (ACE) deficiency leads to a reduction in oxidative stress and in atherosclerosis: studies in ACE-knockout mice type 2. *Arterioscler Thromb Vasc Biol* 23(11):2090-2096.
139. Daugherty A, Poduri A, Chen X, Lu H, & Cassis LA (2010) Genetic variants of the Renin Angiotensin system: effects on atherosclerosis in experimental models and humans. *Curr Atheroscler Rep* 12(3):167-173.
140. Lu H, Cassis LA, & Daugherty A (2007) Atherosclerosis and arterial blood pressure in mice. *Curr Drug Targets* 8(11):1181-1189.

141. Donoghue M, *et al.* (2000) A novel angiotensin-converting enzyme-related carboxypeptidase (ACE2) converts angiotensin I to angiotensin 1-9. *Circulation research* 87(5):E1-9.
142. Thatcher SE, Gupte M, Hatch N, & Cassis LA (2012) Deficiency of ACE2 in Bone-Marrow-Derived Cells Increases Expression of TNF-alpha in Adipose Stromal Cells and Augments Glucose Intolerance in Obese C57BL/6 Mice. *Int J Hypertens* 2012:762094.
143. Iwai M, *et al.* (2010) Direct renin inhibition improved insulin resistance and adipose tissue dysfunction in type 2 diabetic KK-A(y) mice. *J Hypertens* 28(7):1471-1481.
144. Stucchi P, Cano V, Ruiz-Gayo M, & Fernandez-Alfonso MS (2009) Aliskiren reduces body-weight gain, adiposity and plasma leptin during diet-induced obesity. *British journal of pharmacology* 158(3):771-778.
145. Ortlepp JR, *et al.* (2002) Inhibition of the renin-angiotensin system ameliorates genetically determined hyperinsulinemia. *Eur J Pharmacol* 436(1-2):145-150.
146. Weisinger RS, *et al.* (2009) Angiotensin converting enzyme inhibition lowers body weight and improves glucose tolerance in C57BL/6J mice maintained on a high fat diet. *Physiol Behav* 98(1-2):192-197.
147. Abd Alla J, *et al.* (2010) Angiotensin-converting enzyme inhibition down-regulates the pro-atherogenic chemokine receptor 9 (CCR9)-chemokine ligand 25 (CCL25) axis. *The Journal of biological chemistry* 285(30):23496-23505.

148. Frantz ED, Crespo-Mascarenhas C, Barreto-Vianna AR, Aguila MB, & Mandarim-de-Lacerda CA (2013) Renin-angiotensin system blockers protect pancreatic islets against diet-induced obesity and insulin resistance in mice. *PLoS One* 8(7):e67192.
149. Ma LJ, *et al.* (2004) Prevention of obesity and insulin resistance in mice lacking plasminogen activator inhibitor 1. *Diabetes* 53(2):336-346.
150. Nakagami H, *et al.* (2008) Differential response of vascular hepatocyte growth factor concentration and lipid accumulation between telmisartan and losartan in ApoE-deficient mice. *Mol Med Rep* 1(5):657-661.
151. Fujisaka S, *et al.* (2011) Telmisartan improves insulin resistance and modulates adipose tissue macrophage polarization in high-fat-fed mice. *Endocrinology* 152(5):1789-1799.
152. Schupp M, *et al.* (2005) Molecular characterization of new selective peroxisome proliferator-activated receptor gamma modulators with angiotensin receptor blocking activity. *Diabetes* 54(12):3442-3452.
153. Araki K, *et al.* (2006) Telmisartan prevents obesity and increases the expression of uncoupling protein 1 in diet-induced obese mice. *Hypertension* 48(1):51-57.
154. Souza-Mello V, *et al.* (2010) Comparative effects of telmisartan, sitagliptin and metformin alone or in combination on obesity, insulin resistance, and liver and pancreas remodelling in C57BL/6 mice fed on a very high-fat diet. *Clin Sci (Lond)* 119(6):239-250.

155. He H, *et al.* (2010) Telmisartan prevents weight gain and obesity through activation of peroxisome proliferator-activated receptor-delta-dependent pathways. *Hypertension* 55(4):869-879.
156. Nagata T, *et al.* (2013) Tofogliflozin, a novel sodium-glucose co-transporter 2 inhibitor, improves renal and pancreatic function in db/db mice. *British journal of pharmacology* 170(3):519-531.
157. Niimura F, *et al.* (1995) Gene targeting in mice reveals a requirement for angiotensin in the development and maintenance of kidney morphology and growth factor regulation. *The Journal of clinical investigation* 96(6):2947-2954.
158. Taniguchi K, *et al.* (1998) Pathologic characterization of hypotensive C57BL/6J-agt: angiotensinogen-deficient C57BL/6J mice. *Int J Mol Med* 1(3):583-587.
159. Harms M & Seale P (2013) Brown and beige fat: development, function and therapeutic potential. *Nat Med* 19(10):1252-1263.
160. Cypess AM, *et al.* (2009) Identification and importance of brown adipose tissue in adult humans. *N Engl J Med* 360(15):1509-1517.
161. Nedergaard J, Bengtsson T, & Cannon B (2007) Unexpected evidence for active brown adipose tissue in adult humans. *Am J Physiol Endocrinol Metab* 293(2):E444-452.
162. Saito M, *et al.* (2009) High incidence of metabolically active brown adipose tissue in healthy adult humans: effects of cold exposure and adiposity. *Diabetes* 58(7):1526-1531.

163. Diet F, *et al.* (1996) Increased accumulation of tissue ACE in human atherosclerotic coronary artery disease. *Circulation* 94(11):2756-2767.
164. Ohishi M, *et al.* (1997) Enhanced expression of angiotensin-converting enzyme is associated with progression of coronary atherosclerosis in humans. *J Hypertens* 15(11):1295-1302.
165. Fukuhara M, *et al.* (2000) Angiotensin-converting enzyme expression in human carotid artery atherosclerosis. *Hypertension* 35(1 Pt 2):353-359.
166. Potter DD, Sobey CG, Tompkins PK, Rossen JD, & Heistad DD (1998) Evidence that macrophages in atherosclerotic lesions contain angiotensin II. *Circulation* 98(8):800-807.
167. Schieffer B, *et al.* (2000) Expression of angiotensin II and interleukin 6 in human coronary atherosclerotic plaques: potential implications for inflammation and plaque instability. *Circulation* 101(12):1372-1378.
168. Lu H, Boustany-Kari CM, Daugherty A, & Cassis LA (2007) Angiotensin II increases adipose angiotensinogen expression. *Am J Physiol Endocrinol Metab* 292(5):E1280-1287.
169. Nguyen G, *et al.* (2002) Pivotal role of the renin/prorenin receptor in angiotensin II production and cellular responses to renin. *The Journal of clinical investigation* 109(11):1417-1427.
170. Nabi AH, *et al.* (2006) Binding properties of rat prorenin and renin to the recombinant rat renin/prorenin receptor prepared by a baculovirus expression system. *Int J Mol Med* 18(3):483-488.

171. Batenburg WW, *et al.* (2007) Prorenin is the endogenous agonist of the (pro)renin receptor. Binding kinetics of renin and prorenin in rat vascular smooth muscle cells overexpressing the human (pro)renin receptor. *J Hypertens* 25(12):2441-2453.

Vita

Name: Congqing Wu

Place of Birth: China

EDUCATION

2002 - 2005, M.S., Biochemistry and Molecular Biology,

Institute: National Key Laboratory of Crop Genetic Improvement, Huazhong Agricultural University, China

Mentor: Lizhong Xiong, Ph.D.

1998 – 2002, B.S., Horticulture

Institute: National Center of Vegetable Improvement, Huazhong Agricultural University, China

Mentor: Zhibiao Ye, Ph.D.

TRAINING

2008, Scientist Associate

Institute: Department of Plant Pathology, University of Kentucky College of Agriculture

PI: Mark Farman, Ph.D.

PUBLICATIONS

1. Hong Lu, **Congqing Wu**, Deborah A. Howatt, Anju Balakrishnan, Richard Charnigo, Lisa A. Cassis, Alan Daugherty. Differential effects of dietary sodium intake on blood pressure and atherosclerosis in hypercholesterolemic mice. *Journal of Nutritional Biochemistry*, 2013; 24(1):49-53.

2. Hong Lu, Anju Balakrishnan, Deborah A. Howatt, **Congqing Wu**, Richard Charnigo, Gene Liao, Lisa A. Cassis, Alan Daugherty. Comparative effects of different modes of renin angiotensin system inhibition on hypercholesterolemia-induced atherosclerosis. *British Journal of Pharmacology*, 2012; 165:2000-2008.
3. **Congqing Wu**, Hong Lu, Lisa A. Cassis, Alan Daugherty. Molecular and pathophysiological features of angiotensinogen: A Mini Review. *North American Journal of Medicine and Science*, 2011; 4(4):183-190.
4. **Congqing Wu**, Honghong Hu, Ya Zeng, Dacheng Liang, Kabin Xie, Jianwei Zhang, Zhaohui Chu, Lizhong Xiong. Identification of novel stress-responsive transcription factor genes in rice by cDNA array analysis. *Journal of Integrative Plant Biology*, 2006; 48(10):1216-1224.
5. Kabin Xie, **Congqing Wu**, Lizhong Xiong. Genomic organization, differential expression and interaction of SPL transcription factors and microRNA156 in rice. *Plant Physiology*, 2006; 142:280-293.

Fellowship:

2012-2014 AHA Predoctoral Fellowship